REPUBLIC OF IRAQ

MINISTRY OF HIGHER EDUCATION AND SCIENTIFIC RESEARCH

AL-FURAT AL-AWSAT TECHNICAL UNIVERSITY

TECHNICAL ENGINEERING COLLEGE- NAJAF

Design of Substrate Integrated Waveguide Antennas for Wireless Communication Systems

A THESIS

SUBMITTED TO THE COUNCIL OF COMMUNICATION TECHNIQUES ENGINEERING DEPARTMENT IN PARTIAL FULFILLMENT OF THE REQUIREMENTS FOR THE TECHNICAL MASTER DEGREE IN COMMUNICATION ENGINEERING

BY

Rand Muwafaq Hadi

(B. Sc Communication techniques Eng.)

Supervised by

Assist. Prof. Dr. Faris Mohammed Ali

September/2020

بسم الله الرحمن الرحيم

﴿يَرْفَعِ اللَّهُ الَّذِينَ آمَنُوا مِنكُمْ وَالَّذِينَ أُوتُوا

الْعِلْمَ دَرَجَاتٍ﴾

صَدَقَ اللَّهُ الْعَلِيُّ الْعَظِيمُ

الآية (11) من سورة المجادلة

DEDICATION

To the greatest person that Allah has ever created, Prophet **Mohammad peace** is on him.

To the best person that Allah has ever created after His Prophet, **Imam Ali** peace be upon him.

To those who have all the credit on me, to those who were the cause of my existence, to my beloved **parent**.

To my **brothers**, my **husband,** my little **daughter** and my **friends**...

To all who supported and encouraged me to achieve my success.

Acknowledgement

Supervisor Certification

I certify that this thesis titled **" Design of Substrate Integrated Waveguide Antennas for Wireless Communication systems "** which is being submitted by **Rand Muwafaq Hadi** was prepared under my supervision at the Communication Techniques Engineering Department, Engineering Technical College-Najaf, AL-Furat Al-Awsat Technical University, as a partial fulfillment of the requirements for master degree in communication engineering.

Signature:
Name: **Assist. Prof. Dr. Faris Mohammed Ali**
(Supervisor)
Date: /   / 2020

In view of the available recommendation, I forward this thesis for debate by the examining committee.

Signature:
Name: **Dr. Salim M. Wadi**
    (Head of Comm. Tech. Eng.   Dept.)
Date: /   / 2020

Committee Report

We certify that we have read this thesis titled **" Design of Substrate Integrated Waveguide Antennas for Wireless Communication Systems"** which is being submitted by **Rand Muwafaq Hadi** and as Examining Committee, examined the student in its contents. In our opinion, the thesis is adequate for award of degree of Master in communication engineering.

Signature:
Name: **Assist. Prof. Dr. Faris .M. Ali**
       (Supervisor)
Date: /   / 2020

Signature: **Dr. Hussam Noman Mohammed Ali**	Signature: **Assist. Prof. Dr. Ali J. Salim**
Name:	Name:
(Member)	(Member)
Date: / / 2020	Date: / / 2020

Signature:

Name: **Assist. Prof. Dr. Ahmed Ghanim Wadday**

     (Chairman)

Date: /   / 2020

Approval of the Engineering Technical College- Najaf

Signature:
Name: **Assist. Prof. Dr. Hassanein Ghani Al-Husseini**
Dean of Engineering Technical College- Najaf
Date: /   / 2020

Abstract

This thesis presents five different antennas using the SIW technique and each individual proposed antenna has features allowing it to work in different applications. All proposed antennas are simulated using the FR4 substrate with a dielectric constant of 4.3, a thickness of 1.5mm, and a tangent loss of 0.02 and one design used Roger substrate with a dielectric constant of 2.2, a thickness of 1.5mm, and a tangent loss of 0.0009 . The adopted substrate is used because it is widely available in markets and affordable. All antennas are excited using either the microstrip or the Coplanar Waveguide CPW where the transition junctions are required to transfer from the Transverse Electromagnetic Mode TEM into Transverse Electrical TE modes which are the fundamental modes in Rectangular waveguides. The proposed antennas are evaluated using the computer simulation technology CST program.

The first proposed design is a square SIW cavity with two-curved slots having different lengths to make the design working at dual frequency bands. The first band is obtained at a resonant frequency of 11.34GHz with a bandwidth of 502MHz gain of 6.28dB, while the 18.42GHz is the resonant frequency of the second band with a bandwidth of 4.48GHz and a gain of 3.9dB.

Next, a square slot surrounded by rows of vias working as a SIW cavity is presented. This design also have dual bands at central frequencies at 12.47GHz and 17.82GHz with maximum gain about 4.89 dB with bandwidth about 805.7MHz and 921.8 MHz for the dual bands.

The third design is different from other previous works because it has both active and parasitic elements and use Roger dielectric material as a substrate.

Single band is obtained in this design working at frequencies of 18.3GHz. Gain 7.8dB and total efficiency 98%.

Eventually, two other designs are introduced where the first design is a rectangular patch antenna shielded by two rows of vias and the second one is a rectangular SIW which is open-ended. two concentric circular slots are carved from the top wall of the SIW. Both designs have wide bandwidth with high gains.

Contents

Nomenclatures (Symbols)

Symbol	Meaning
β	Phase constant
a_{eq}	Equivalent width
$asiw$	Width between two rows of vias
c	Speed of light (3×10^8) m/sec
D	Directivity
d	Diameter of via holes
Dc	Diameter of circular slot
D_O	Maximum directivity
d_{shift}	Dimension of feed shift
dy	Driven element
e_c	Conduction efficiency
ed	Dielectric efficiency
e_o	Total efficiency
e_r	Radiation efficiency
f_c	Center frequency
f_H	Highest frequency
f_L	Lowest frequency
f_r	Resonant frequency
G	Gain
g	Gap between element
h	Substrate height
K	Free space wave number
L	Substrate length
LFL	Length of feed line
Lg	Ground length
Lms	Microstrip length
LS	Length of slot
$Ls1$	Length of slot1
$Ls2$	Length of slot2
$Ltap$	Taper's length
η	Intrinsic impedance of the medium
p	Space between two via holes
P_{in}	Total input power

P_{rad}	Total power radiation
Rc	Radius circular
R_s	Surface resistance of the conductors
S	Distance between slots
S_{11}	Reflection coefficient
t	Thickness of ground & thickness of patch
$\tan \delta$	Tangent loss
W	Substrate width
W_c	Width of circular slot
WFL	Width of feed line
Wg	Ground width
Wms	Space between slot
Wms	Microstrip Width
WS	Width of slot
$Wtap$	Taper 's width
ΔL	The extended increase of patch length
λ_g	The guided wavelength
λ_o	Free-space wavelength
μ_o	Permeability of free space
σ	Conductivity of the metal
$\mathcal{E}_{eff}$	Effective dielectric constant
ϵ_r	Relative dielectric constant of substrate

List of Abbreviations

Abbreviation	Meaning
APESIWA	Active-Parasitic Element Substrate Integrated waveguide Antenna.
BT	Bluetooth
BW	Bandwidth
CPA	Circular Patch Antenna
CPW	Coplanar Waveguide
CSAWSIW	Curved Slot Antenna Without SIW
CSIWA	Circular SIW Antenna
CSSIWA	Curved Slot SIW Antenna
CST	Computer Simulation Technology
dB	DC Bell
DCSA	Dual Circular Slots Antenna
DCSSIWA	Slots SIW Antenna
FR4	Flame Resistant
GHz	Gigahertz
PAWOF	Patch Antenna With Offset Feeding
PEC	Perfect Electric Conductor
RW	Rectangular Waveguide
SIIDG	Substrate Integrated Image Dielectric Guide
SIIG	Substrate Integrated Insular Guide
SIINDG	Substrate Integrated Inset Dielectric Guide
SINRD	Substrate Integrated Non-Radiative Dielectric
SIRW	Substrate Integrated Ridge Waveguide
SISW	Substrate Integrated Slab Waveguide
SIW	Substrate Integrated Waveguide
SIW-PAOF	SIW Patch Antenna With Offset Feeding
TEM	Transverse Electric Magnetic
Wi-Fi	Wireless Fidelity

List of Figures

List of Tables

List of Publications

Paper No.	Paper Title	Paper Status
Paper 1	Design of SIW wideband curved slot antenna for Radar and Satellite Applications . Al-Furat Journal of Innovation in Electronic and Computer Engineering, 1(01).	Online
Paper 2	Dual Bands Microstrip Substrate Integrated Waveguide (SIW) Antenna for K-band Applications, Technology Reports of Kansai University, Volume 62, Issue 04, April, 2020.	Online
Paper 3	Low profile Substrate Integrated Waveguide(SIW) wideband antenna for Ku-band Applications, TELKOMNIKA (Telecommunication Computing Electronics and Control. SJR 2018: 0.283 (Q2) ,Cite Score 2018 : 1.09, SNIP 2018: 0.730	Accepted

Chapter One
Introduction
and
Literature Survey

CHAPTER ONE

INTRODUCTION AND LITERATURE SURVEY

1.1 Introduction

In the past decades, wireless communication systems witnessed considerable expansions. The backbone and driving force beyond the latest developments in wireless communication technology appeared due to the antenna.

All devices that transmit information across a free space need to switch their signals from the device to free space in the form of electromagnetic waves, otherwise, they need to use an antenna. The antenna has an essential role in the successful design of any wireless instrument because its features has a high effect on the wireless systems [1][2].

Wireless and satellite communications have rapidly developed in the past decades. Today the world depends on wireless links in the communication. Recently, one of the principal interests in the information and communication field is the development of wireless local area network WLAN. Thus, the current trend is to develop minimal weight, low cost, low profile antennas in communication systems to be capable of maintaining high performance over a wide spectrum of frequencies [3].

Wireless communication has become more popular recently due to the fast revolution in wireless technology. This revolution is due to an increase in customers [4]. With all this revaluation in communications, there is a real need to replace the traditional waveguides see Fig (1.1), because of a waveguide's physical structure is huge, and it requires complicated transitions to interface with planar circuitry.
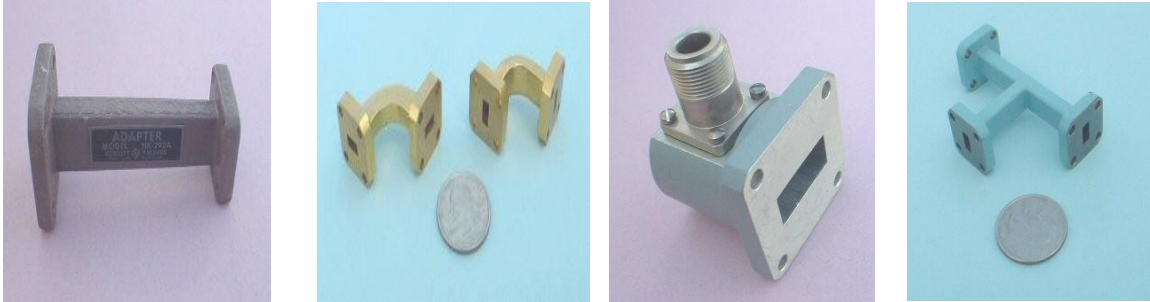
(a) Rectangular waveguide	(b) Waveguide to coax adapter	(c) Waveguide bends	(d) E-tee

Fig. (1.1): traditional waveguide types.

The transitions required to integrate rectangular waveguides with the planar circuitry are costly and bulky. The Substrate Integrated Waveguides (SIWs) are relatively new forms of planar transmission line incorporating the waveguide into a flat circuit like a printed circuit board or a ceramic that is co-fired with low temperature.

SIW provides the advantages of the rectangular waveguides, such as high power handling, high Q-factor, and low losses in flat circuitry. It also provides the advantages of low profile, lightweight, high selectivity, smooth or curved surface conformity and fast integration with flat circuits (Deslandes and Wu, 2006). SIWs are used for wireless communications and radar systems needing a narrow beam or formed beam. These developments lead to the hugging of mobile and wireless traffic volume, predicted to increase over a thousand times over the next years [5,6].

In this thesis, used CST program to design five SIW antennas that work in wireless applications with reasonable directivity and gain with enhanced bandwidth. In all of the presented SIW antennas, the substrate layer (middle layer) utilized are made from the FR4 with a relative dielectric constant of $\epsilon r= 4.3$ and there is one design used Roger dielectric martial

with $\epsilon r = 2.2$. With different slot shapes etched on one top of the conducting material and sizes.

1.2   Aim of the work

The major aim of this work is to design antennas based on SIW technology in wireless communication systems. This aim can be accomplished through the following objectives:

1. Design of the SIW antenna and etching slots with different shapes in a square (or rectangular) patch with specific dimensions according to the required operating frequency. Also, the offset feeding on one of the designs can be used.

2. Applying the fundamentals of a well- known antenna named Yagi-Uda antenna in the design of a microstrip antenna with SIW technology to get high directivity and high gain.

3. Suggesting different parameters for each design and testing each one to determine the role that each parameter may play in the behavior of the antenna, and then evaluating the obtained results.

1.3   Literature Survey

Many papers that have been published deal with the design of antennas based on the technique of SIW. SIW technique is more attractive in antennas design for wireless communication systems.

this literature survey presents previous work in the case of the SIW antenna. These references will be in terms of the used substrate and the shape of the used antenna. Then, review the results obtained from the references.

•**In 2008, G. Q. Luo et al [7]** presented an antenna including backed cavity and feeding element that is completely constructed at a single substrate by using substrate integrated waveguide technique and grounded coplanar waveguide. The center frequency at 10 GHz with 1.7% fractal bandwidth which has a gain of about 5.4 dBi. Substrate thickness h is 0.5 mm.

•**In 2010, Mohamed H. Awida et al [8]** presented SIW cavity-backed antenna, print patch on a substrate using PCB process, to operate at Ku-band range with center frequency about 12.5 GHz which has a gain of about 8 dBi with a substrate thickness h is 1.575 mm. It is selected to achieve larger than 9% fractional bandwidth.

•**In 2011, D. Y. Kim et al [9]** presented antenna with two circular-polarized with circular patch antennas which have a cavity-backed resonator based on SIW with two different feeding transitions. Center frequency is 10GHz, bandwidth is 2.06 GHz (14.42 %) and maximum gain is about 7.79 dBi. The results indicate that the microstrip-to-SIW transition case is better feeding than the coax-to-SIW transition.

•**In 2012, G. Q. Luo et al [10]** presented an antenna including backed cavity and feeding element that is completely constructed at a single substrate by using SIW and grounded coplanar waveguide with center frequencies at 9.84 GHz and10.27 GHz with 6.3% fractional bandwidth which has a gain of about 6 dBi.

•**In 2012, A. Elboushi and A. Sebak [11]** offered an antenna which consists of a circular patch radiator used to feed a surface mounted circular SIW. This antenna resonates at 30.5 GHz with a return loss equal -37 dB. The gain enhancement of this antenna is 3.5 dBi and fractional bandwidth

8.6% substrate using two layers ε_{r1} =10.2, h_1=0.635mm and ε_{r2} =2.33, h_2 = 0.7874mm.

• **In 2013, S. Moitra et al [12]** introduced an antenna with multi slots at the upper ; they studied the effect of increment number of slots. The return loss of the two slots antenna structure has been found to resonate at 15.75 GHz is -15 dB. The two-slot structure has been modified into four slot structure and the antenna has been found to resonate at 16.16 GHz with a return loss of -16 dB. The four slot structure has been modified to six slot structure to obtain a resonance frequency equal to 15.5 GHz with a return loss of -16 dB. The gain of two slots, four slots, and six slots are 3.7dBi, 5.7 dBi, and 6.3 dBi respectively.

• **In 2014, S. Mukherjee et al [13]** presented bow-tie slot antenna. The slot is etched at the upper metallic plate and the four sidewalls of a cavity are formed by four rows of metallic vias. The antenna is fabricated by standard PCB technology. The first and second resonances are at 9.98 GHz and 10.6 GHz respectively. The bandwidth of the proposed antenna is 1.03 GHz (9.43%) which gain of 3.7 dBi.

• **In 2014, H. Dashti and M. H. Neshati [14]** presented an antenna resonated at 8.3GHz fed by half mode SIW cavity. This antenna consists of half mode circular SIW cavity. It offers a gain of 7.5 dBi with impedance bandwidth of 9.6% and radiation efficiency is around 95%.

• **In 2015, C. Zhang et al [15]** introduced a new type of leaky, N-shaped, circular polarization antenna cut on the top of the integrated waveguide (SIW). The antenna resonates at 8.2GHZ frequency 8.93 dB.

• **In 2016, K Nouri et al [16]** proposed an antenna which consist of multi slots at the upper layer and via holes. This antenna is constructed into one

substrate with a thickness h of 0.508 mm and dielectric constant ε_r of (2.2).The return loss of these three bands are 20 dB for 25.4 GHz, lower than 15 dB for 29 GHz and lower than 15 dB for frequency 35 GHz.

- **In 2016, O.Caytan et al.[17]** proposed the first wideband semi-mode (HM) SIW slot antenna on a cork substrate. The impedance bandwidth is 1.30 GHz (23.7 %), and the front-to-back ratio is 15.0 dB with a maximum gain about 4.3 dBi at resonant frequency 5.50 GHz.

- **In 2017, P.chaurasia et al [18]** introduced an antenna with seven slot at the upper layer and via holes. The antenna resonates at 11.8 GHz with gain of 4.29 dBi and return loss is -17.74 dB, bandwidth (342.7) MHz which is about (2.9 %).

- **In 2017, Hanumanthappa et al[19]** proposed an antenna with SIW technology to multiband monopole for WLAN/WIMAX applications. The antenna resonant frequencies are 2.2, 3.8, and 5.8 and the impedance bandwidths are 0.2GHz, 0.33GHz, and 0.35GHz, respectively. This covers all WLAN and WIMAX groups. Thus, the gains are 1.2, 1.5 and 2.3, respectively.

- **In 2018, H. A. Ali et al [20]** introduced cavity-backed antenna. It consists of two stacked SIW cavities, linked by a slot. The design is implemented by using two identical dielectric layers with thickness h. The antenna with two stacked cavities resonate at 4 GHz, with a bandwidth 120 MHz and gain about 3.24 dBi.

- **In 2018, A. Kumar et al [21]** designed antenna with cavity-backed for Ku-band applications. The presented antenna uses a modified triangular-ring-slot etched on one top of the metallic. It is fabricated by using PCB (printed

circuit board) process. The antenna bandwidth 2 GHz is about (13.53%) ranging from (14.43-16.49) GHz, with gain about 4dBi.

- **In 2018, H. Amer et al[22]** presented a planar slot low profile antenna design by using the SIW technique and GCPW design. The entire antenna, including backed cavity and feeding portion, is entirely constructed on single-substrate.
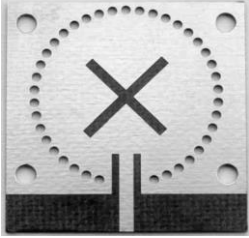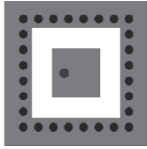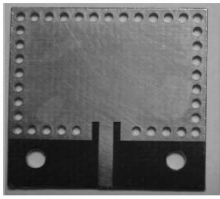
  A SIW antenna is presented with a 6.35 dB gain and 7.3 dB directivity. The reflection coefficient (S11) at 10.2 GHz is -37.23 dB with a bandwidth of 345 MHz (3.38%).
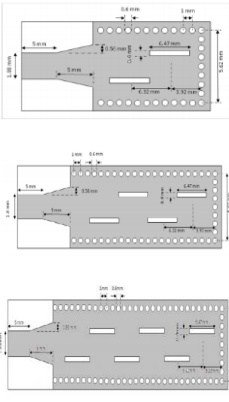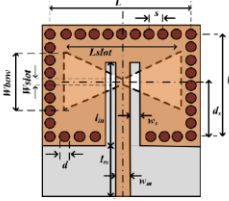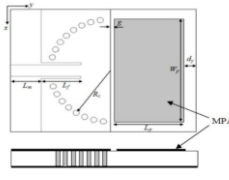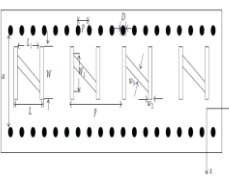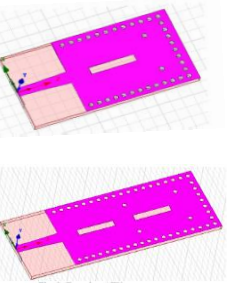
- **In 2019, Mariam El Ghrabi et al [23]** presented a cavity backed triangular slot antenna with SIW technology and two feeding transitions. This indicate that microstrip to SIW based on taper gives the best result. The antenna operates on K-band, its resonant frequency is 21 GHz and it is gain about 6 dBi.

- **In 2020, L. Liu et al [24]** presented antenna with SIW technology using odd mode spoofing for broadside radiation. This antenna resonates at 12.8 GHz. The bandwidth is about 700MHZ (5.5%) and the gain is about 5.66 dBi.
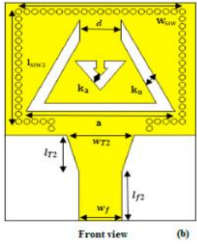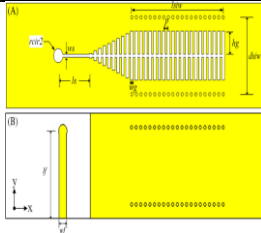
All the previous studies of the above-mentioned references have been cleared for some basic factors such as bandwidth and Fraction Bandwidth (FBW), gain, resonant frequency, design shape, and the type of the substrate material as shown in Table (1.1).

Table (1.1): Summary of literature survey.

No.	Ref.	year	Geometry	Resonant frequencies GHz	Substrate material type	Gain in dBi	B.W And/or FBW
1.	[7]	2008		10	Rogers RT5880 ε_r=2.2 δ=0.0009	5.4	1.7%
2.	[8]	2010		12.5	Rogers RT5880 ε_r=2.2 δ=0.0009	8	9 %
3.	[9]	2011		10	Rogers RT5880 ε_r=2.2 δ=0.0009	7.79	14.42% 2.06 GHz
4.	[10]	2012		9.84 10.27	Rogers RT5880 ε_r=2.2 δ=0.0009	6	6.3%
5.	[11]	2012		30.5	two layers ε_{r1} =10.2 ε_{r2} =2.33	3.5	8.6%

6.	[12]	2013		15.75 16.16 15.5	Dielectric material With dielectric constant of 3.2	3.7 5.7 6.3	---
7.	[13]	2014		9.98 10.6	Rogers RT5880 ε_r=2.2 δ=0.0009	3.7	9.4% 1.03GHz
8.	[14]	2014		8.3	Rogers RT5880 ε_r=2.2 δ=0.0009	7.5	9.6%
9.	[15]	2015		8.2	Rogers Duroid 5880 ε_r=2.2 δ=0.0009	8.93	---
10.	[16]	2016		25.4 29 35	Rogers RT5880 ε_r=2.2 δ=0.0009	---	---

11.	[17]	2016		1.30	acork ε_r =1.22, δ=0.0363	4.3	23.7%
12.	[18]	2017		11.8	Rogers RT5880 ε_r=2.2 δ=0.0009	4.29	2.9 % 342.7 MHz
13.	[19]	2017		2.2 3.8 5.8	FR4 ε_r =4.3 δ=0.025	1.2 1.5 2.3	---
14.	[20]	2018		4	Taconic TLX-9 ε_r = 2.5 δ =0.0022	3.24	120 MHz
15.	[21]	2018		14.6 15.7	Rogers RT5880 ε_r=2.2 δ=0.0009	4	13.53% 2.09GHz
16.	[22]	2018		10.2	FR4 ε_r =4.3 δ=0.025	6.35	345 MHz (3.38%)

| 17. | [23] | 2019 | | 21 | FR4 $\varepsilon_r = 4.3$ $\delta = 0.025$ | 6 | 0.9GHz |
| 18. | [24] | 2020 | | 12.8 | Rogers RT5880 $\varepsilon_r = 2.2$ $\delta = 0.0009$ | 5.66 | 700MHz 5.5% |

1.4   Thesis layout

Chapter One: as presented an introduction about the SIW antenna, aim of thesis, literature survey about several works of SIW antenna and thesis layout.

Chapter Two: It includes theory about SIW structure and it is important principles.

Chapter Three: It includes design configuration and total dimensions of the five proposed SIW antennas.

Chapter Four: It discusses the simulation and the results which are obtained from the proposed SIW antennas.

Chapter Five: It discusses the conclusion of the proposed SIW antennas and the recommendations for future scope.

Chapter Two

Theory

CHAPTER TWO

THEORY

2.1   Introduction

This chapter give an introduction to SIW technology, advantages, and disadvantages of SIW are examined and it is applications. The important design considerations used in the structure of SIW antennas are illustrated.

2.2   Substrate Integrated Waveguide

The traditional waveguide circuit has the minimum radiation loss as it is a closed structure and all the electromagnetic energy is bounded inside the waveguide. With frequency increasing, the physical dimensions of the waveguide decrease. However, the integration of many waveguide circuits is still not as easy as that for the microstrip or strip-line circuits [25].

Type of transmission line called substrate integrated waveguide or post-wall waveguide is invented. It is a low-cost realization of the traditional waveguide circuit for microwave and millimeter-wave applications. It inherits the merits of both the traditional microstrip for easy integration and the waveguide for low radiation loss. In such a circuit, metallic posts are embedded into a printed circuit board, covered with conducting sheets on both sides, to emulate the vertical walls of a traditional waveguide [25].

2.2.1 Advantages and disadvantages of SIW

SIW has the advantages of the traditional waveguide circuit, such as low radiation loss, high Q-factor, and high power capacity. Besides, the integration of many substrate integrated waveguide circuits into a single-board sub-system is also possible [25].

One possible drawback of SIW is that the loss of leakage can be significant. It has to do with the close spacing of the vias. This means that radiation losses is not zero. Another drawback is dielectric losses are incorporated, by adding a dielectric into the guide comparing to air on standard rectangular waveguide [26].

2.2.2 Applications of the SIW antenna

SIW antennas have several applications. Such as as radar, satellite, mobile network like Global System Mobile (GSM), Bluetooth, Wi-Fi, direct broadcasting, IoT and 5G, etc.[19],[21][22][23]. The applications of the five proposed antennas in this thesis are for wireless communication systems such as radar, satellite communications, direct broadcasting, astronomical observation and fifth generation (5G).

2.2.3 SIW Structure and Performance

The traditional waveguides are low loss structures but are expensive to be fabricated. The planar transmission lines have low Q-factor, but are lightweight and have cheap fabrication process.

Substrate Integrated Waveguide, as shown in Fig. (2.1) combines advantages from both technologies and hence it is put forward by the academics as described in [27,28].
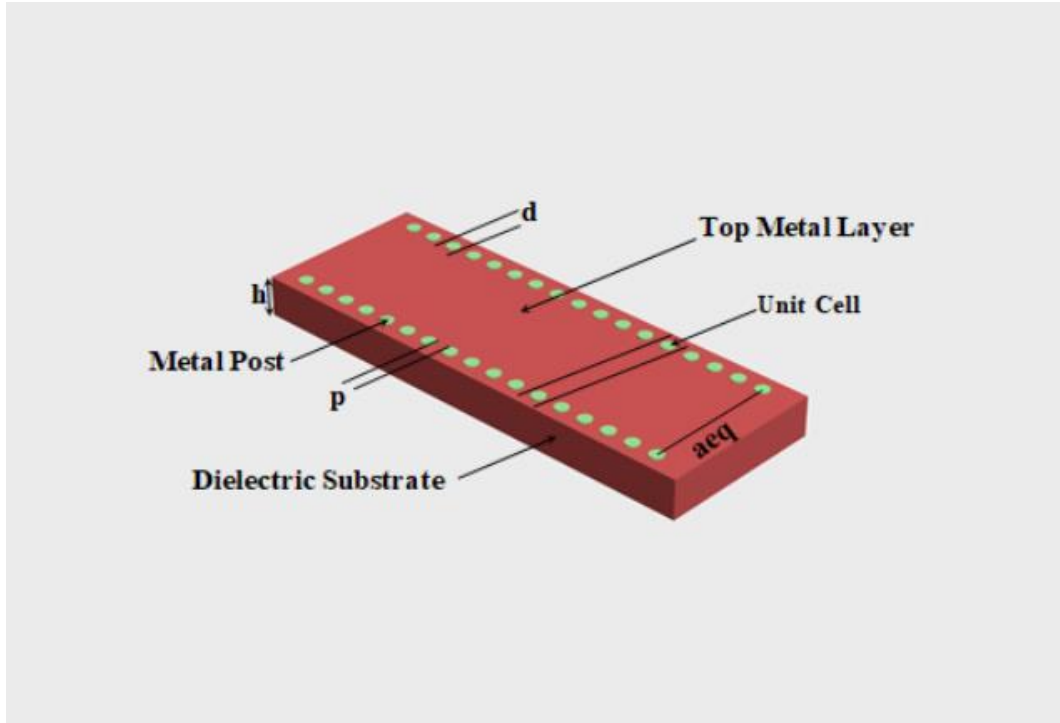
Fig. (2.1): Geometry of SIW.

The geometry of SIW is close to the rectangular dielectric waveguide. However, by adopting the Printed Circuit Board (PCB) fabrication process, the height is reduced drastically to the thickness of the PCB substrate.

The two metallic broad walls are substituted by two copper sheets and the narrow walls are replaced by two rows of plated vias that are drilled through the substrate. If the vias are close enough, the two rows become equivalent to two electrical walls for the electromagnetic waves. Hence, a pair of via in the cross-section can generate a current loop [28].

As SIW inherits largely properties from the metallic waveguide, a cut-off frequency shown below in which there is no propagation. Therefore, by adjusting correctly the space between vias, the diameter, and the width, the leakage loss from SIW structure are negligible and a design procedure is

proposed. It can be noticed that one of the major changes in the behavior of a SIW compared to a rectangular waveguide is the surface current [29].

In a conventional waveguide, the current surface circulates freely in any direction but in the case of SIW, due to via holes, the current flow is limited to the vertical direction. As the structure of via holes is periodically spaced, the sidewall current cannot circulate alongside the SIW across each regular interval. That is why there is only the Transverse Electric TEm0 mode that can propagate. As a result, the first mode called dominant mode is the TE10 mode as illustrated in Fig. (3.2) [29].
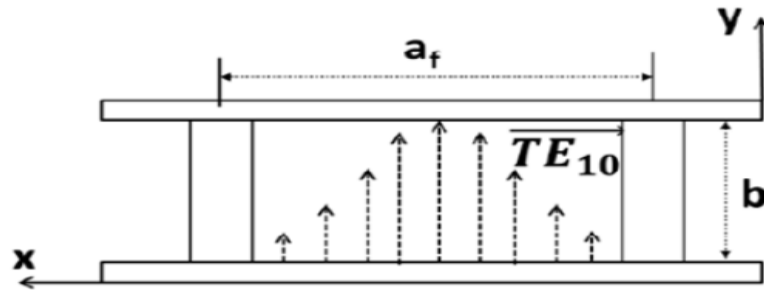
Fig. (2.2): The cross-section area of SIW view the fundamental of TE10 mode as electrical field representation[28].

2.2.4 SIW Technique and Basics Design

The SIW is a Rectangular Waveguide-like structure in an integrated planar form which can be synthesized and fabricated by using two rows of conducting cylinders. Vias embedded in a dielectric substrate that is electrically sandwiched by two parallel metal plates as shown in Fig. (2.1) [30].

The operating frequency range is defined by the monomode propagation of quasi-TE10 wave as its cut-off frequency is only related to

the equivalent width a_{eq} of the synthesized waveguide as long as the substrate thickness or waveguide height is smaller than this width. This equivalent width will be discussed in the following section [30].

2.2.5 Equivalent width

The SIW can be modeled by a conventional Rectangular Waveguide (RW) through the so-called equivalent width a_{eq}. This parameter is calculated the resulting dielectric-filled rectangular waveguide has the same cut-off frequency of the dominant mode TE10 as its corresponding SIW structure. This determines the propagation characteristics of the TE10 mode. Physical parameters of via-holes d and p are set to minimize the radiation (or leakage) loss as well as the return loss. The equivalent rectangular waveguide width can be approximated according to the geometrical parameters illustrated in Fig.(2.1) as follows [30]:

$$a_{eq} = asiw - \frac{d^2}{0.95\,p} \qquad (2.1)$$

where

$asiw$:width between two rows of vias.

p : pitch: distance between two vias.

d : diameter of hole.

The cut-off frequency (f_c) of the dominant mode is defined by [30]:

$$f_c\ (TE_{10}) = \frac{c}{2\,.\sqrt{\epsilon_r}} \,.\left(asiw - \frac{d^2}{0.95\,p}\right)^{-1} \qquad (2.2)$$

supposed that $a_{eq} \gg h$.

where

$\in_r$: dielectric constant of the substrate.

and for second mode by [30]:

$$f_c \ (TE_{20}) = \frac{c}{\sqrt{\in_r}} \cdot (asiw - \frac{d^2}{1.1 \, P} - \frac{d^3}{6.6 \, P^2}) \quad (2.3)$$

2.2.6 Losses in SIW

The energy in transmission may be lost or dissipated through different physical mechanisms including dielectric losses, conductor losses, and radiation losses. The main issue is to control and minimize the losses from the transmission line, especially for the SIW structure. There are three main loss mechanisms.

First, the dielectric loss is mainly generated by the dielectric from a chosen PCB board like in rectangular dielectric waveguide. It depends on the substrate height and the width of the structure as demonstrated in [31]. It can be explained by the dielectric area contained between two rows of vias and, the top and bottom copper sheet. If this area increases, which means that the height or the width is raised, then the dielectric stocks more energy. Indeed, the greatest part of this energy is transformed into heat [31]. Attenuation, because of the dielectric losses is related to the tanδ of the dielectric substrate [30]:

$$\alpha_{d=} \frac{k^2 \, tan\delta}{2\beta} \quad (2.4)$$

With

$$k = \frac{2\pi}{\lambda} \quad (2.5)$$

Where :

k: free space wave number

β: phase constant

$\tan\delta$: dielectric loss tangent

λ: wave length

The second losses are created by the conductor used in the SIW. The ohmic loss is subject to the height of the structure and the conductivity of the metal [43]. Attenuation because of the conductive loss [30]:

$$\alpha_c = \frac{R_s}{a^3 b \beta k \eta} (2b\pi^2 + a^3 k^2) \qquad (2.6)$$

With

$$R_s = \sqrt{\frac{\omega \mu_o}{2\sigma}} \qquad (2.7)$$

Where

Rs: surface resistance of the conductors

η: intrinsic impedance of the medium

σ: conductivity of the metal

μ_o: permeability of the free space ($4\pi \times 10^{-7}$) H/m

The radiation loss can occur if conditions are not fulfilled on the diameter and the space between two vias as expressed in (2.8)and (2.9) pulled out [27].

$$d < \frac{\lambda_g}{5} \qquad (2.8)$$

$$p \leq 2d \qquad (2.9)$$

Where

λ_g: the guided wavelength

with

$$\lambda_g = \frac{\lambda_o}{\sqrt{\epsilon_r}} \qquad (2.10)$$

Attenuation because of the radiation leakage [27] :

$$\alpha_R = \frac{\frac{1}{aSIW} \left(\frac{d}{aSIW}\right)^{2.84} \left(\frac{p}{d} - 1\right)^{6.28}}{4.85 \sqrt{\left(\frac{2aSIW}{\lambda g}\right)^2 - 1}} \qquad (2.11)$$

It is also particularly relevant to compare losses in SIW structures and other traditional planar structures, for example, microstrip or coplanar lines. A systematic comparison of SIW and microstrip components is not easy because SIW circuits are usually implemented on a thick substrate with low dielectric constant (which is not suitable for the implementation of microstrip circuits) to minimize conductor losses [31].

In principle, microstrip component losses could also be mitigated by increasing the substrate thickness. In practice, however, this cannot be exploited due to the unacceptable increase in radiation loss and excitation of surface waves. A detailed comparison of losses in SIW structures, microstrip lines, and coplanar waveguides are reported in [31]. SIW structures can guarantee comparable or lower losses as compared to traditional planar transmission lines.

2.3   Principal SIW Parameters

2.3.1 Substrate Materials

Low-loss material is the foundation for developing high-performance integrated circuits and systems. This becomes more critical for power budget as frequency increases to the millimeter-wave ranges and beyond. This is because it is relatively difficult to amplify over those ranges. The thermal effect, dielectric non-uniformity, and metallic surface roughness may have to be taken into account for better and accurate design. This is especially important for antenna developments [30].

The SIW can theoretically be constructed with any available substrate. The most used ones are Rogers RT/duroid®5880 glass microfiber reinforced PTFE composite and RT/duroid®6002 for conventional PCB processing. They which are easily sheared with laser and machined to the required shape.

The holes can easily be drilled mechanically into these machinable materials as compared to ceramics which can only be processed by the laser perforation and other special techniques. All these materials have excellent dimensional stability. Indeed, the good thermal stability of the material of choice should also be considered in the design. These selections will not just affect the performances but also defines power handling capabilities [30].

2.3.2 Characteristic Impedance

The impedance is an important characteristic especially when the SIW is connected to other planar and nonplanar structures. One definition of impedance in a rectangular waveguide is the wave impedance.

This impedance, however, does not take into account the geometry of the transmission line. Another impedance definition, more often employed in the design of matching networks, is the characteristic impedance [30].

2.3.3 SIW Transitions

The transitions between planar transmission lines and SIW structures represent another important element related to SIW components. Several broadband transitions between microstrip or coplanar waveguide and SIW have been developed [32,33] as in Fig.(2.3). In particular, microstrip-to-SIW transitions are typically based on a simple taper Fig.(2.3(a)), provided that the microstrip and the SIW structure are integrated on the same substrate [32].

Design equations have been proposed for the fast implementation of microstrip-to-SIW transitions. Microstrip-to-SIW transitions in a multi-layer substrate environment have been proposed to connect a microstrip implemented in a thin substrate with a thicker SIW structure. The use of thick substrates allows for reducing conductor losses in SIW structures [34,35].
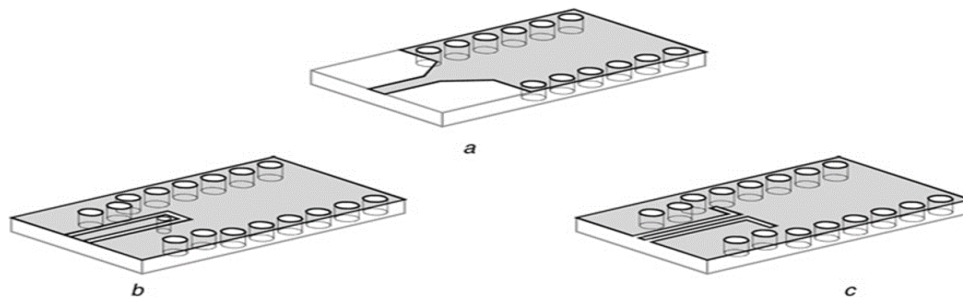
Fig. (2.3) : Transitions from SIW to typed transmission lines.(a) Transition from microstrip to SIW, based on a taper.(b) Transition from Coplanar to SIW, based on the current probe.(c) Transition from Coplanar to SIW, centered on a 90 ° bend.[32,33]

23

On the other hand, there are two solutions found for coplanar-to-SIW transitions. The first solution makes use of a current probe Fig.(2.3(b)): the current flowing through the probe generates a magnetic field which matches with the magnetic field inside the SIW structure [33].

Another possible configuration is found which consists of a coplanar waveguide with a 90° bend on each slot inside the SIW structure Fig.(2.3(c)). It has been noted that using coplanar waveguides may be convenient when thick substrates are adopted to reduce conductor losses. Consequently, the use of microstrip lines is not possible [36].

Finally, transitions between the air-filled waveguide and SIW structure have also been found. This transition is based on a radial probe inserted into a tapered metallic waveguide [37].

2.3.4 Configuration of SIW

In order to transform solid devices into planar structures, some derivative designs for SIW structure are developed see Fig. (2.4)[38].
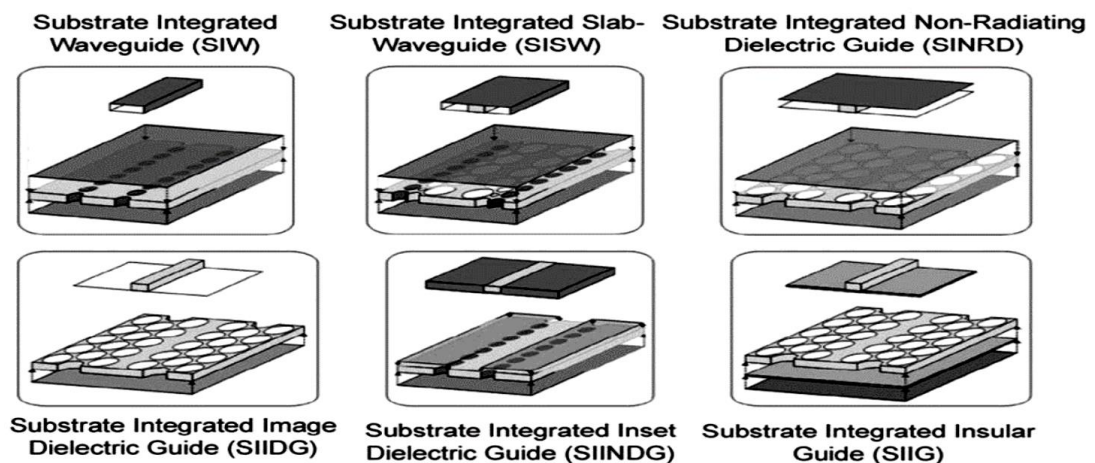
Fig. (2.4): Planar corresponding architectures of each 3-D prototype.[38]

Dielectric transmission lines in nonplanar forms are transformed into corresponding planar structures, as shown in Fig. (2.4), such as Substrate Integrated Non-Radiative Dielectric (SINRD) [39], Substrate Integrated Inset Dielectric Guide (SIINDG) [40], Substrate Integrated Slab Waveguide (SISW) [41], Substrate Integrated Insular Guide (SIIG) [42,43], Substrate Integrated Image Dielectric Guide (SIIDG) [44,27], and Substrate Integrated Ridge Waveguide (SIRW) [45,46]. A common characteristic of these new planar designs is that the large holes in the regular arrangement are not for via fence purpose.

The hollow nonmetal large holes in the substrate adjust the effective relative permittivity of the substrate between the dielectric permittivity and vacuum permittivity. All these planar designs can be fabricated in one circuit board as parts of a substrate by a one-step process. Using the same dielectric material, these new designs as transitions can efficiently connect different interfaces in a broad frequency range.

2.4   Analysis Formulation of the Microstrip SIW Structures.

The length and width of the microstrip can be calculated by the equations in [47]. To calculate the length and width by equations (2.12) and (2.13) and slightly manipulate the extracted values to suit our design.

$$wp = \frac{c}{2f_0 \sqrt{\frac{(\epsilon_r + 1)}{2}}} \quad (2.12)$$

Where

wp: Microstrip width.

c: Light speed within free space.

25

f_o: The frequency of resonance.

$$lp = \frac{c}{2f_o\sqrt{\in_{reff}}} - 2\Delta l \quad (2.13)$$

Where

lp: Microstrip length.

$\in_{reff}$: the efficient permittivity.

ΔL: the extended increase of patch length

The effective dielectric constant for microstrip antenna is given in [48] :

$$\in_{reff} = \frac{\in_r + 1}{2} + \frac{\in_r - 1}{2}[1 + 12\frac{h}{w}]^{-\frac{1}{2}} \quad (2.14)$$

h: dielectric substrate thickness.

w: the patch the width.

Chapter Three

Design

Configuration

CHAPTER THREE

DESIGNS CONFIGURATION

3.1   Introduction

This chapter presents the design of several SIW antennas with different geometrical shapes. The exciting ports of all proposed SIW antenna are named waveguide port. The effect of changing various shapes of the SIW is discussed to choose the optimum one.

3.2   Designs Configuration

In this part, five designs for antennas with millimeter dimensions will be proposed using SIW technology as all of them operate at frequencies above 10 GHz -20 GHz and support applications of X-band, Ku-band and K-band. All designs was structured on dielectric substrate from FR4 material which it is dielectric constant ε_r=4.3 and tangent loss is δ=0.025, this dilectric material coated by conducting on both sides this conducting matrial is copper with thikness t=0.035 mm.

3.2.1 The proposed model I: Curved Slot SIW Antenna (CSSIWA)

The first model CSSIWA is designed using a square geometry shape. This indicates that the substrate and the ground plane takes the square shape with suitable dimensions to achieve a good result. This SIW antenna is designed on the FR4 substrate (middle layer) with dimensions of (42 x 42) mm^2 W, L respectively with a thickness 1.6mm. To give more illustration, the diameter of via holes (d) and spacing (p) between them has been chosen according to equation (2.8) and (2.9).The CSSIWA is shown in Fig. (3.1).
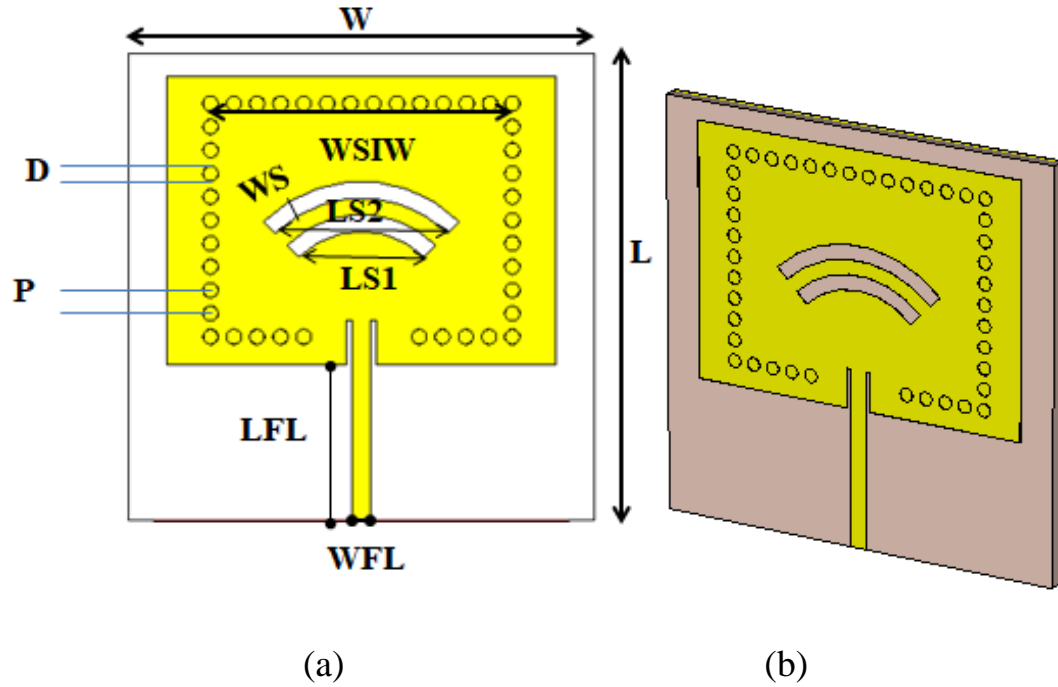
Fig. (3.1): CSSIWA geometry

The patch layer (upper layer) material composed from copper metal, the dimension of copper patch width Wp is 35mm and 26mm for length Lp chosen according to equation (2.12)and (2.13) with thickness 1.6 mm, while the equivalent width is 27.22mm. Feeding antenna directly by connecting it with the microstrip transmission line, additionally, two carved slots are etched on the patch's top of CSSIWA design to change the current distribution on the patch that leads to the enhancement of radiation pattern of CSSIWA.

The ground layer (lower layer) consists of copper with dimension (42 x 42) mm^2. The overall parameters of CSSIWS are shown in Table 3.1.

Table 3.1. CSSIWA dimensions.

Parameters	Symbol	Values (mm)
Substrate width	W	42
Substrate length	L	42
Thickness of Substrate	H	1.6
Diameter of via	d	1.35
Pitch between two vias	P	2.10
Length of feed line	LFL	16
Width of feed line	WFL	1.6
Patch width	Wp	35
Patch length	Lp	26
Thickness of patch	T	0.035
Equivalent width	W_{SIW} / a_{eq}	27.22
Width of slot	Ws	1.5
Length of slot1	Ls1	11.31
Length of slot2	Ls2	15.56

3.2.2 The proposed model II: SIW Patch Antenna with Offset Feeding (SIW-PAOF)

The second model SIW-PAOF is derived from the conventional square patch antenna is more adopted in antenna design as shown in Fig. (3.2). The feeding line was offset. This SIW antenna is designed on an FR4 substrate (middle layer) with the dimension of 21.72 x 26 mm^2 W, L respectively with the thickness h 1.5mm.

(a)   (b)
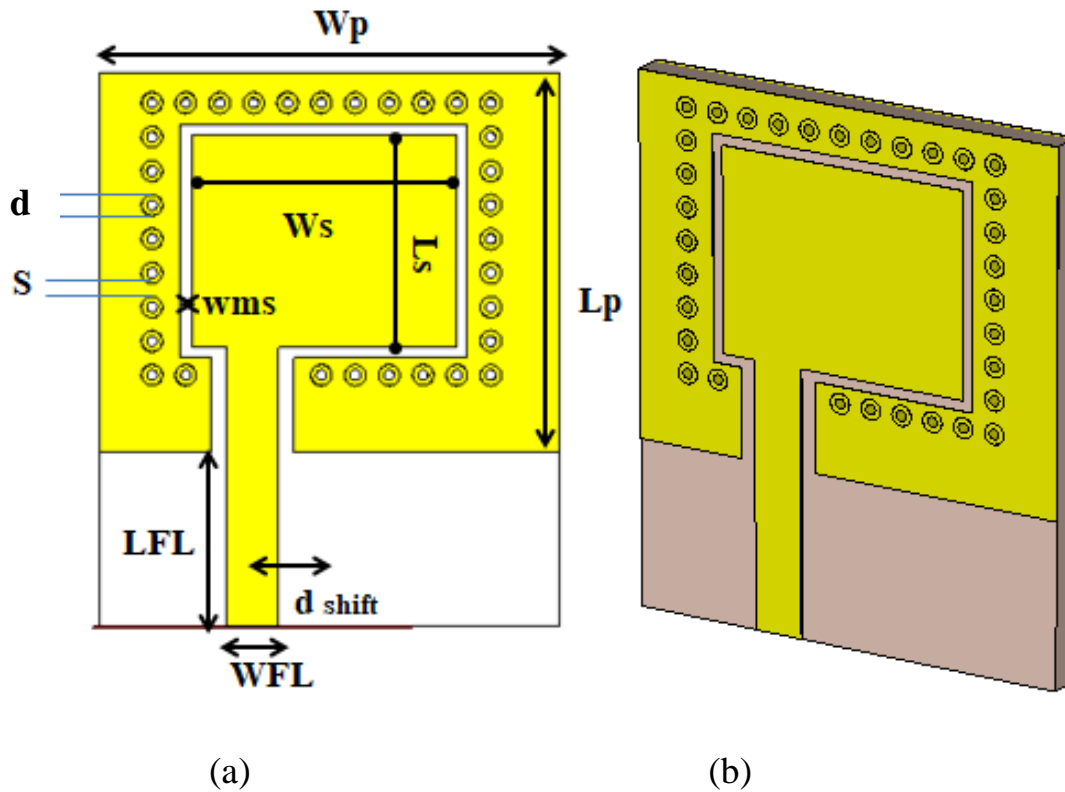
Fig. (3.2):The SIWPAOF geometry.

The patch layer (upper layer) material is composed from copper metal, the dimension of SIWPAOF patch antenna is 21.72mm for width Wp, and 17.80mm for length Lp. In this work, a square slot with a certain dimension is etched at the center of the square. This antenna is fed by grounded coplanar waveguide.

The ground layer (lower layer) consists of copper with dimensions 21.72x26mm^2. The overall parameters of SIWPAOF are shown in Table 3.2.

Table 3.2. SIW-PAOF dimensions**.**

Parameters	Symbol	Values (mm)
Total length	L	21.72
Total width	W	26
Patch width	Wp	26
Patch length	Lp	17.80
Thickness of patch	t	0.03
Substrate width	W	21.72
Substrate length	L	26
Thickness of Substrate	h	1.5
Diameter of via	d	1
Pitch between vias	p	1.6
Length of feed line	LFL	8.20
Width of feed line	WFL	2.42
Dimension of feed shift	d_{shift}	2
Width of slot	WS	12.5
Length of slot	LS	10
Space between slots	Wms	0.71

3.2.3 The proposed model III: Active - Parasitic Element SIW Antenna (APESIWA)

The proposed antenna mainly consists of two elements; lower (active) and upper (parasitic) these elements concentrated on the upper side of substrate. The lower element is directly connected to the feeding line, whereas the other element is connected by electromagnetic coupling with the lower element via a gap g between them with dimensions as indicated in Table (3.3), APESIWA is shown in Fig. (3.3).
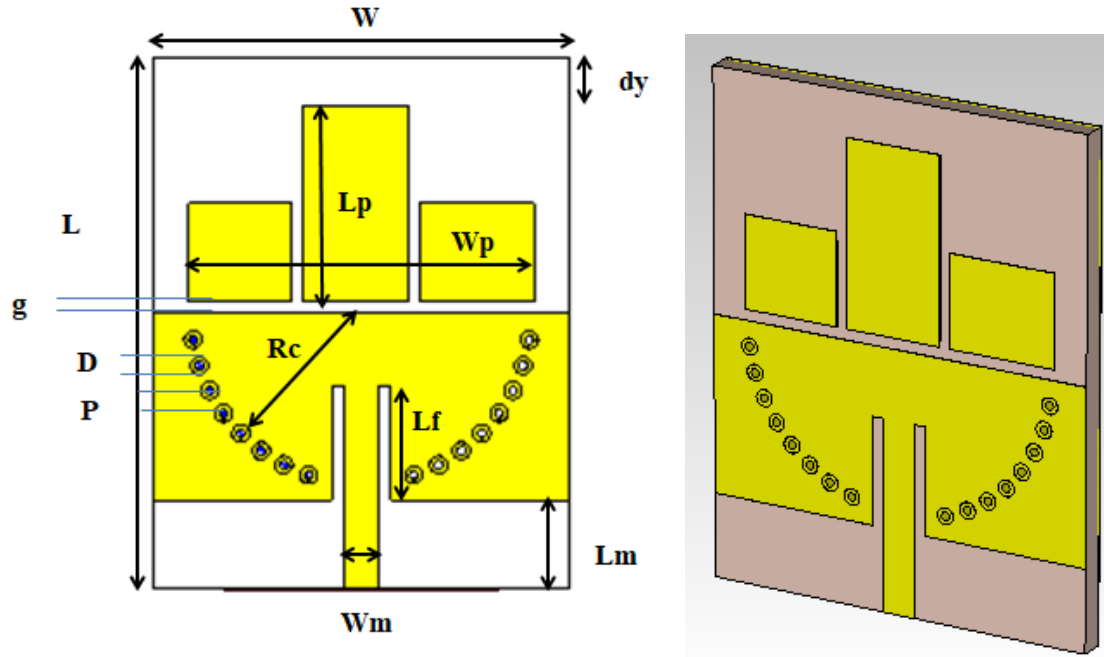
Fig. (3.3): APESIWA geometry.

The active element in this antenna is in the form of semi half circle through an arrangement of via holes which represent the SIW part. It can be said that the main idea of the design for this antenna is essentially taken from the popular antenna called the Yagi-Uda antenna [34]. So the active element in the proposed antenna represents the driven element, while the parasitic element represents the director element.

Moreover, the use of half semi-circle arrangement of SIW via holes is to reflect the radiated power in direction of parasitic element. This will ensure the minimization of backward direction and maximization of the front to back ratio (f/B).

Table 3.3: APESIWA dimensions.

Parameters	Symbol	Values (mm)
Total length	L	30
Total width	W	23.5
Patch width	Wp	19.5
Patch length	Lp	11.08
Thickness of patch	t	0.035
Substrate width	W	25.5
Substrate length	L	30
Thickness of Substrate	h	1.5
Diameter of via	d	1
Length of middle feed	Lm	5
Length of feed line	Lf	6.4
Width of feed line	Wm	2
Driven element	dy	2
Gap between element	g	o.65
Radius of semi half circle	Rc	9.6

3.2.4 The proposed model IV: Dual Circular Slots SIW Antenna (DCSSIWA)

Fourth model DCSSIWA is derived from the conventional rectangular patch antenna, as shown in Fig. (3.4). The feeding of the antenna is Microstrip-SIW-Transition type. This SIW antenna is designed on an FR4 substrate (middle layer) with the dimension of 18 x 27 mm^2 with the thickness h 1.5mm. The DCSSIWA geometry is shown in Fig. (3.4).
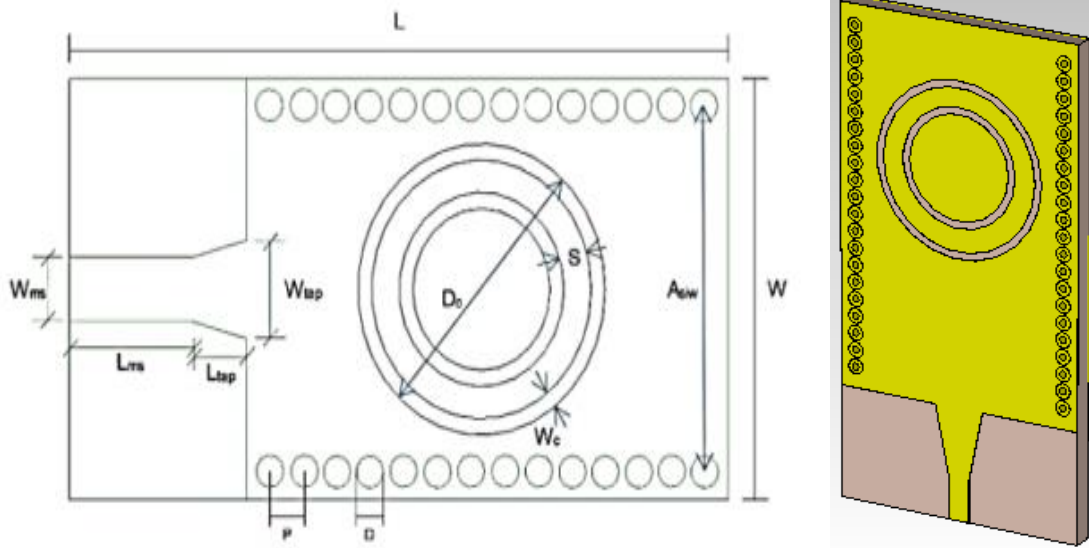
Fig. (3.4): Geometry of DCSSIWA.

The patch layer (upper layer) material is composed from copper metal dual circular slots was etched on it.

The ground layer (lower layer) consists of copper with dimensions 18 x 35mm^2. The overall parameters of DCSSIWA are shown in Table 3.4.

Table 3.4. DCSSIWA dimensions**.**

Parameters	Symbol	Values (mm)
Total length	L	35
Total width	W	18
Patch width	Wp	18
Patch length	Lp	27
Thickness of patch	t	0.035
Substrate width	W	18
Substrate length	L	35
Thickness of Substrate	h	1.5
Diameter of via	d	1.08
Pitch between vias	p	1.20
Equivalent width of SIW	Asiw	15.8
Microstrip Width	Wms	1.56
Microstrip Length	Lms	3.10
Taper 's width	Wtap	3.58
Taper's length	Ltap	4.90
Diameter of circular slot	Dc	12.5
Width of circular slot	Wc	0.5
Distance between slots	S	2

3.2.5 **The proposed model V: Circular SIW Antenna (CSIWA)**

This consists of a circular patch and circular slot etched at a rectangular patch fixed on the top layer of a substrate. The feeding is connected directly with a

microstrip transmission line and distributing via holes in a circular path to surround the circular patch. The proposed antenna is shown in Fig.(3.5).
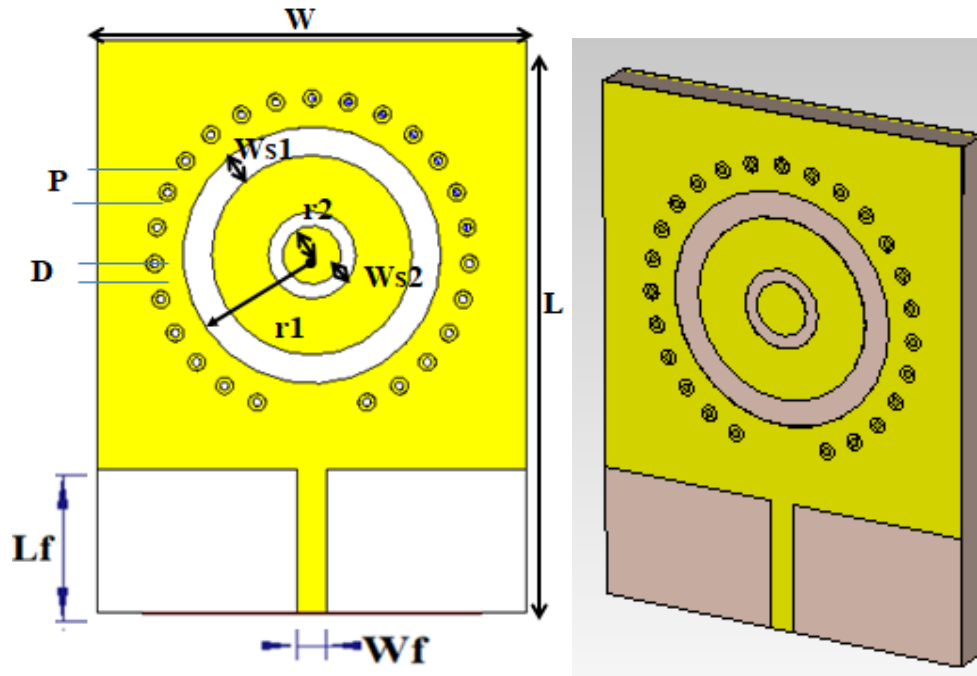

Fig.(3.5): Geometry of CSIWA.

The ground layer consists of copper with dimensions 15 x 20mm^2. The overall parameters of CSIWA are shown in Table 3.5.

Table 3.5. CSIWA dimensions**.**

Parameters	Symbol	Values (mm)
Total length	L	20
Total width	W	15
Patch width	Wp	15
Patch length	Lp	15
Thickness of patch	t	0.035
Substrate width	W	15
Substrate length	L	20
Thickness of Substrate	h	1.5
Diameter of via	d	0.6
Pitch between vias	p	1.2
Length feeding	Lf	5
Width feeding	Wf	1
Width of slot 1	Ws1	1
Width of slot 2	Ws2	0.5
Radius of a circular patch	r1	4.5
Radius of circular slot	r2	1.03

Chapter Four

Results

CHAPTER FOUR

RESULTS

4.1   Introduction

In this chapter, all design parameters of the proposed SIW antennas are to be discussed.

4.2   Characteristics of the Curved Slot SIW Antenna (CSSIWA) and Curved Slot Antenna Without SIW (CSAWSIW).

The simulation results of the first proposed antenna for various parameters are dealt with presented in the following sub sections:

4.2.1 Reflection coefficient of CSAWSIW.

For the CSAWSIW, the reflection coefficient is illustrated in Fig. (4.1). Reflection coefficient indicates that the first proposed Curved Slot SIW Antenna resonates at 11.34 GHz with reflection coefficient S_{11} -40.88 dB and 18.44 GHz with reflection coefficient S_{11} -43.31 dB. This is one of the properties of SIW that make the signal guided and radiated in one direction.
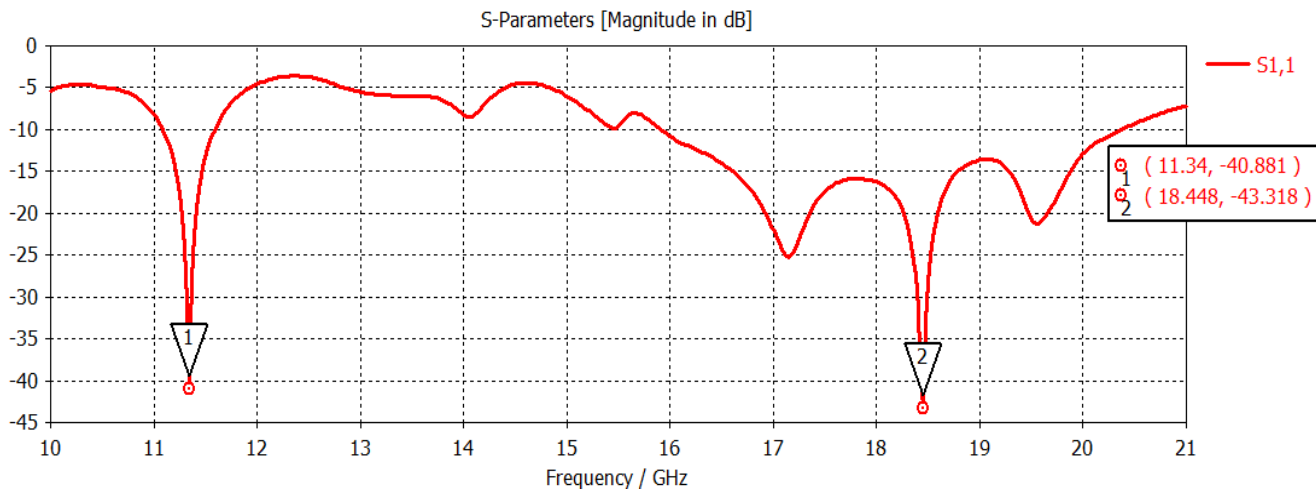

Fig.(4.1): S_{11} of CSAWSIW.

4.2.2 Directivity for CSAWSIW and CSSIWA.

The 3-D plot for directivity is illustrated in Fig. (4.2) for the CSAWSIW and Fig. (4.3) for CSSIWA. The value of directivity is 9.61dB at the resonant frequency of 11.62 GHz and 9.79 dB at the resonant frequency of 18. 23 GHz. The value of directivity at the resonant frequency 11.34 GHz is 10.6 dB and at the resonant frequency 18.42 GHz is 9.77 dB. notice that the CSSIWA design has more directivity than the CSAWSIW design due to the SIW technology because of the vias that operate as an electrical side to make the signal more directive and get enhancement.
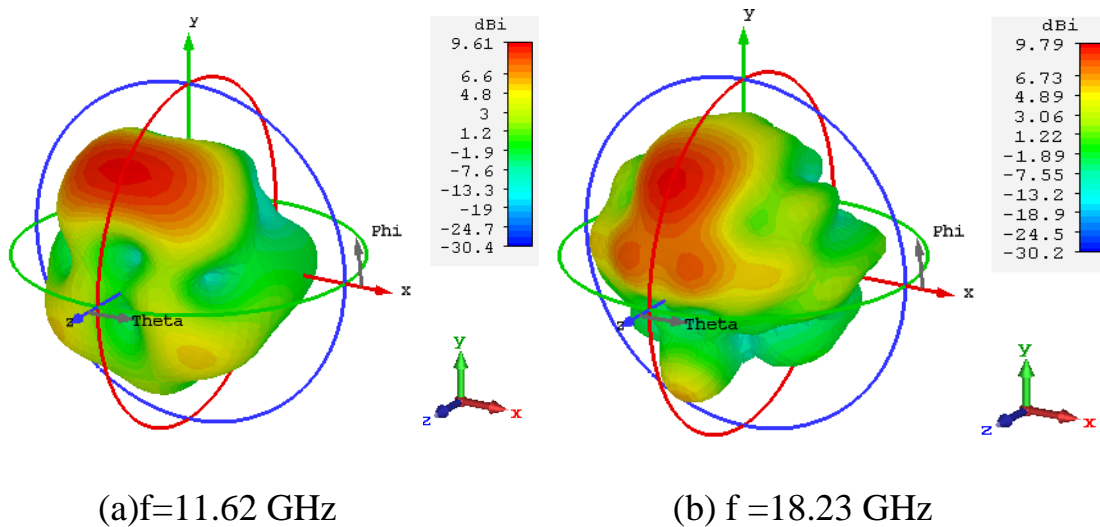

(a)f=11.62 GHz   (b) f =18.23 GHz

Fig. (4.2):Directivity of the CSAWSIW.

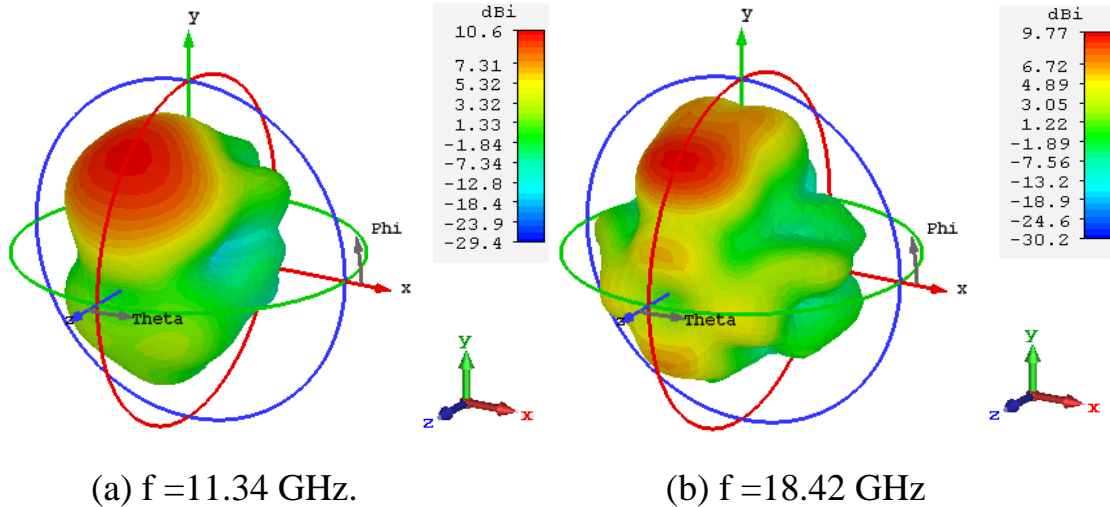(a) f =11.34 GHz.   (b) f =18.42 GHz

Fig. (4.3):Directivity for CSSIWA.

4.2.3 Gain for CSAWSIW and CSSIWA.

The 3-D plot for a gain of the CSAWSIW and CSSIWA is shown in Fig. (4.4) and Fig. (4.5) respectively. So, the largest value of the gain is 6.82 dB at the resonant frequency 11.34 GHz and gain is 3.9 dB at the resonant frequency of 18.42 GHz for the CSSIWA, while the gain of the CSAWSIW is 3.86 dB at the resonant frequency 11.62 GHz and gain is 3.4 dB at the resonant frequency 18.23 GHz. This gives us an indication that the gain of the design with SIW also increased.
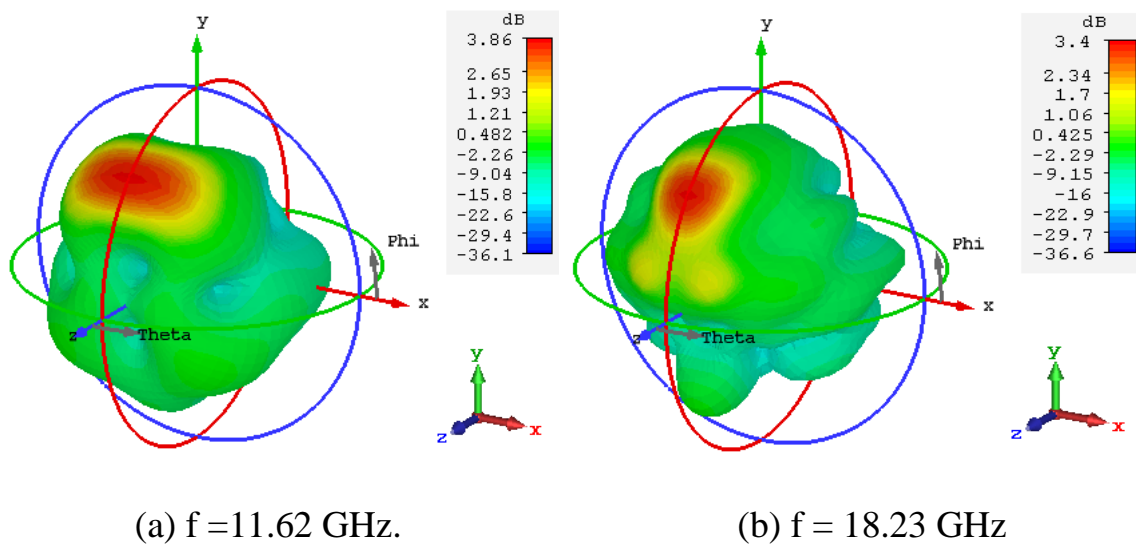

(a) f =11.62 GHz.   (b) f = 18.23 GHz

Fig. (4.4):Gain of CSAWSIW.

<div align="center">

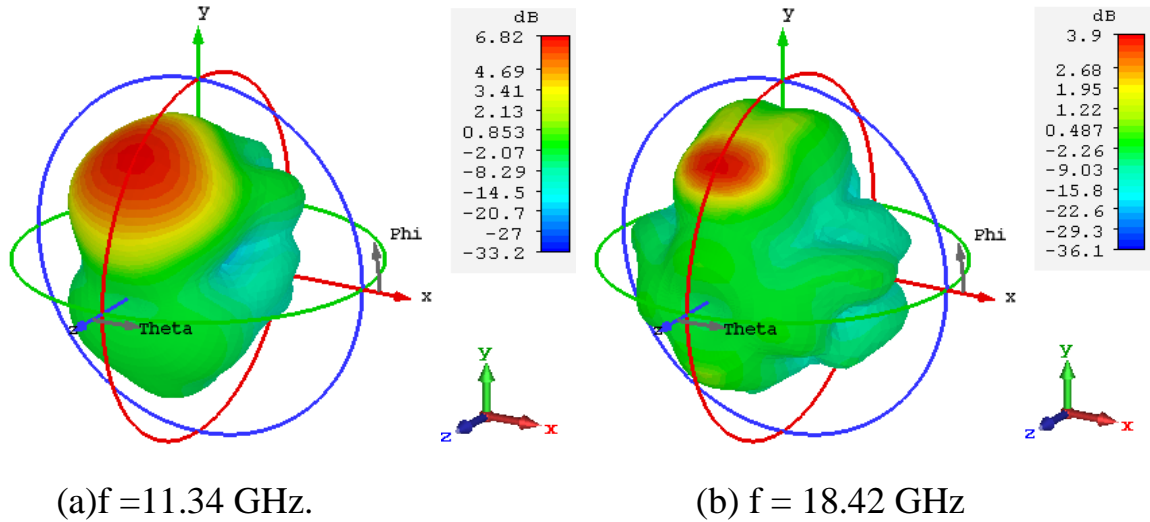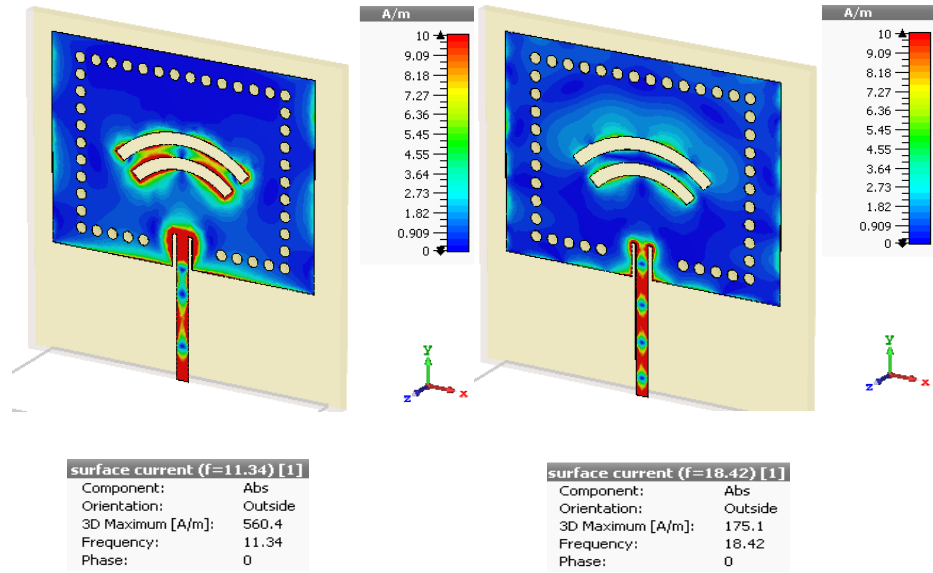(a)f =11.34 GHz.   (b) f = 18.42 GHz

Fig. (4.5):Gain of CSSIWA.

</div>

4.2.4 Current Distribution for CSSIWA.

The simulated current surface for the proposed design CSSIWA at resonant frequencies is shown in Fig. (4.6) where it is illustrates the current distribution on the patch surface and directions at first resonant frequency 11.34 GHz. It is obvious that most of the current concentration is in two regions of the antenna's surface. Fig. (4.6(b)) shows the current distribution on the patch surface and directions at the second resonant frequency 18.42 GHz. See that the maximum current focuses around the slot because the current in this region is maximum, and at the edge is evanesce.

(a): at 11.34 GHz.   (b): at 18.42 GHz.

Fig. (4.6):Simulated current surface distributions CSSIWA antenna.

4.2.5 Radiation Patterns of CSSIWA (Electric Field (E-field) and Magnetic Field (H-field) patterns).

Table 4.1 shows the simulation results of characteristic far-field power radiation at different resonant frequencies. Besides, Fig. (4.7) shows the results of polar radiation pattern for first resonant frequency 11.34 GHz. Fig. (4.8) shows the results of polar radiation pattern for the second resonant frequency of 18.42 GHz of CSSIWA.

Table 4.1:The characteristic of far field power radiation E-field of CSSIWA.

Design	Frequency In GHz	Parameter (E&H)field	x-y plane ($\theta=90$)	y- z plane ($\Phi=90$)	x-z plane ($\Phi=0$)
CSSIWA	11.34	Main lobe magnitude(dB) (E-field)	12.6 dBV/m	21.6 dBV/m	14.2 dBV/m
		Main lobe direction	88°	49°	19°
		Angular width (3dB)	44.3^o	47.2^o	79.6^o

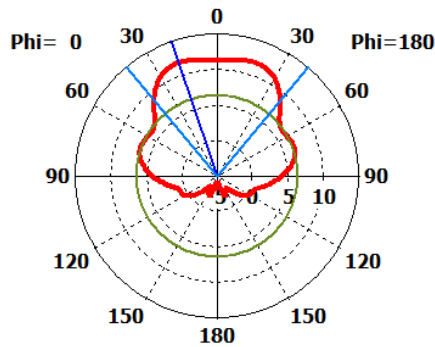|					
		Side lobe level (dB)	-4.6dB	-8.4dB	-5.3dB
	18.42	Main lobe magnitude(dB) (E-field)	14.2 dBV/m	18.7 dBV/m	13.6 dBV/m
		Main lobe direction	104º	47º	25º
		Angular width (3dB)	52.6º	34.4º	36.6º
		Side lobe level (dB)	-5.7dB	-3.2dB	-4dB

Farfield E-Field(r=1m) Abs (Theta=90)

Farfield E-Field(r=1m) Abs (Phi=90)
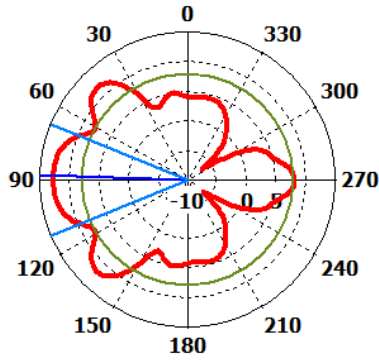
X-Y
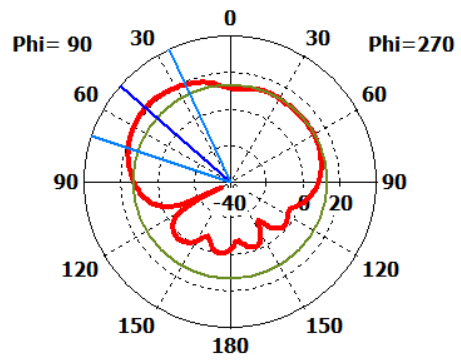
Y-Z

Farfield E-Pattern Abs (Phi=0)

X-Z

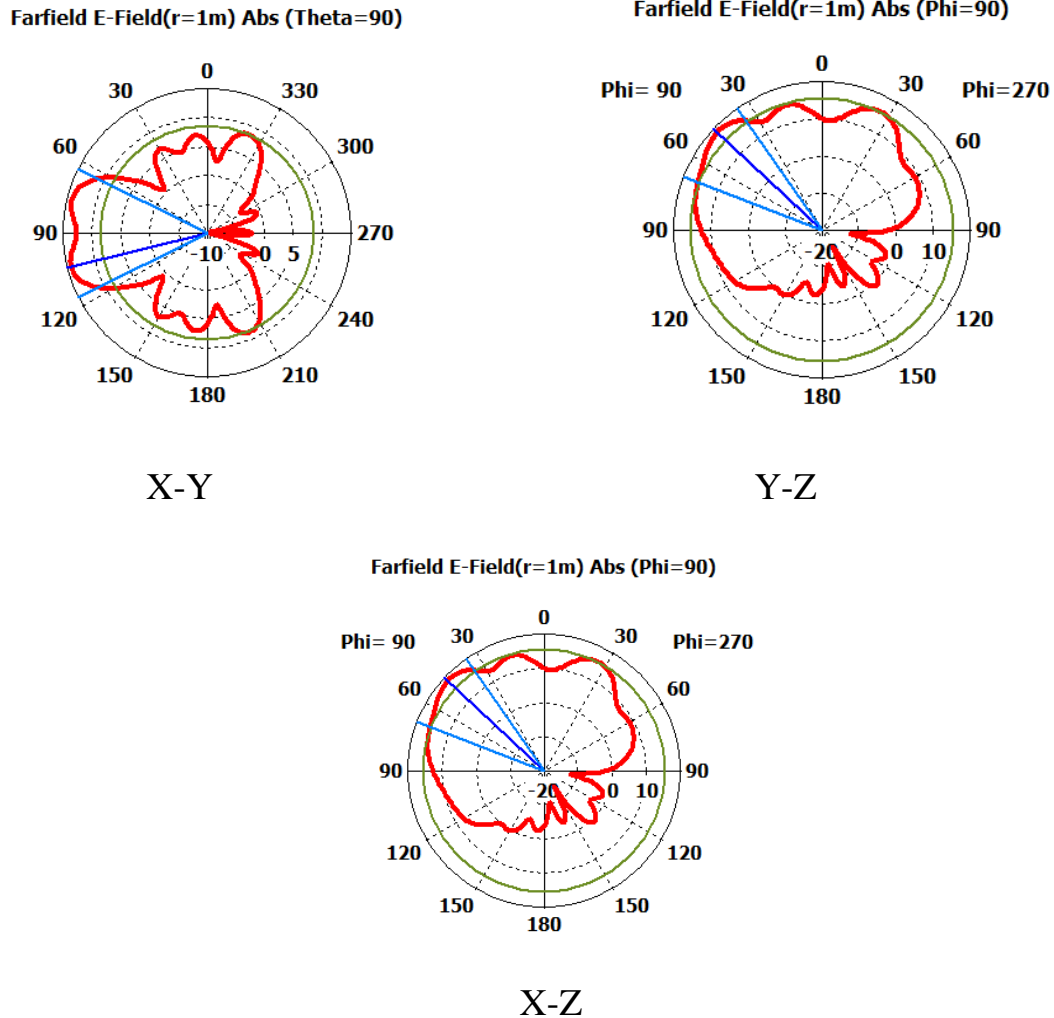Fig. (4.7): Polar plot of the radiation pattern in E-plane at 11.34 GHz.

Farfield E-Field(r=1m) Abs (Theta=90)

Farfield E-Field(r=1m) Abs (Phi=90)

X-Y   Y-Z

Farfield E-Field(r=1m) Abs (Phi=90)

X-Z

Fig. (4.8): Polar plot of the radiation pattern in E-plane at 18.42 GHz.

4.2.6 Efficiency for CSAWSIW and CSSIWA.

The efficiency of CSAWSIW is 40 %. It is calculated from the relationship between the gain and directivity .The efficiency of CSSIWA is 64 %. So, based on these values, can say that the CSSIWA design is more acceptable than the CSAWSIW design and also the SIW technology enhances the overall efficiency of the antenna.

4.2.7 Bandwidth of CSSIWA.

Figure (4.9(a)), shows CSSIWA bandwidth , CSSIWA have dual bands first band starts from frequency 11.08 GHz and ends at frequency

11.59 GHz, producing a bandwidth approximately 502 MHz about (4.49%) . However, Fig. (4.9 (b)),show the second bandwidth of CSSIWA starts from frequency 15.90 GHz and ends at frequency 20.38 GHz, producing a bandwidth approximately 4.475 GHz about (24.29%).
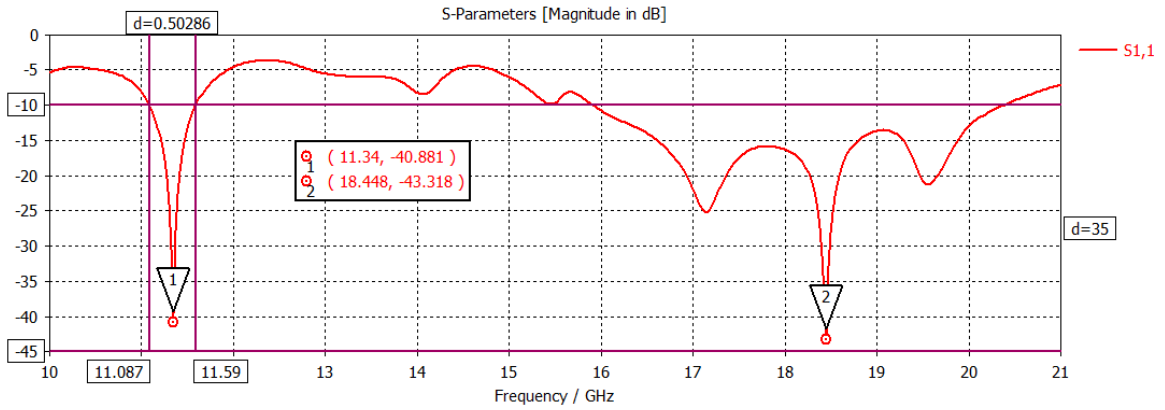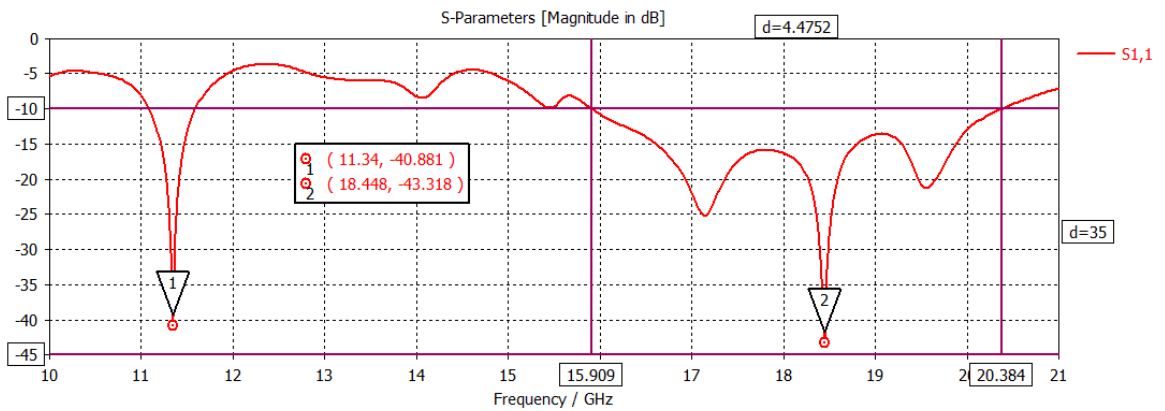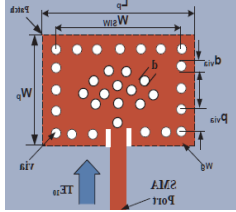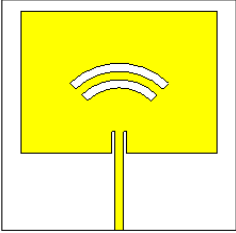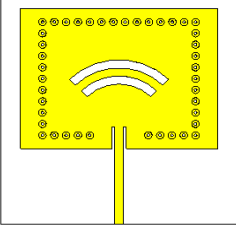

(a) at f=11.34 GHz

(b) at f=18.44 GHz

Fig. (4.9): CSSIWA bandwidth.

4.2.8 Comparisons between CSAWSIW and CSSIWA.

Comparisons between CSAWSIW , CSSIWA and reference are shown in Table 4.2 perform the enchantment on the antenna performance after add SIW technology.

Table 4.2 : Comparisons between CSAWSIW, CSSIWA and reference .

| Name & Material	Design & Dimensions	Freq. in GHz	Ref. Coff. In dB	Directivity in dBi	Gain in dB	B.W & FB.W	e %
Ref. [60] (Roger) With $\varepsilon_r = 2.2$	(42x42)mm^2	1.25 2.4 6.7	-25	---	6.24	12%	20-70%
CSAWSIW FR4	(42x42)mm^2	11.62	-25	9.61	3.86	359 MHz 3.09%	40 %
		18.23	-19	9.79	3.4	3.464 GHz 18.97%	
CSSIWA FR4	(42x42)mm^2	11.34	-40	10.6	6.82	502 MHz 4.49%	64 %
		18.42	-43	9.77	3.9	4.475 GHz 24.29%	

4.3   Characteristics of Patch Antenna With Offset Feeding (PAWOF) and SIW Patch Antenna With Offset Feeding (SIW-PAOF).

The simulation results of the second proposed antenna for various parameters are dealt with presented in the following sub sections:

4.3.1 Reflection Coefficient of PAWOF and SIW-PAWOF.

At the beginning the antenna is structured by using a microstrip patch antenna with a feeding line in the middle with SIW technology.

The performance of the antenna is enhanced by offset feeding line by 0.6 mm to the left. Also, offset feeding line by 3.6 mm the antenna performance is enhanced and gives better result because it allows transferring of maximum power. This is the final structure of the antenna SIW-PAWOF. The antennas structure and S_{11} parameter for all of the antenna are shown in Fig. (4.10).
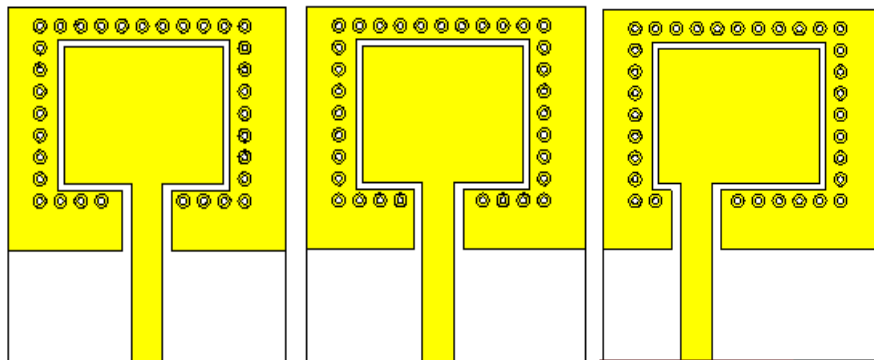
(a) Middle feeding line. (b) 0.6mm Offset   (c) SIW-PAWOF
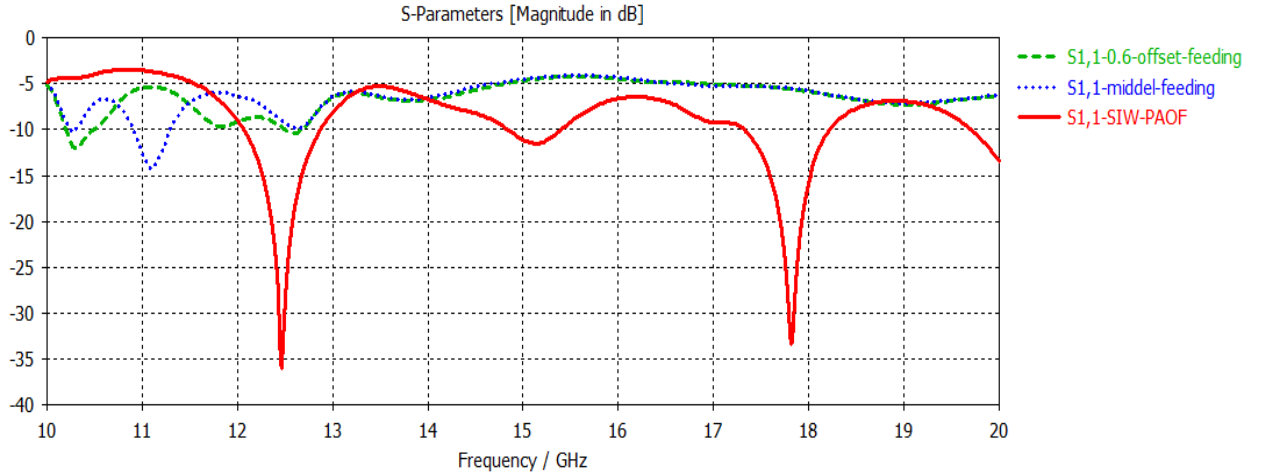
Fig. (4.10): Antennas structure and S_{11} parameter for the three
proposed antenna.

4.3.2 Directivity of PAWOF and SIW-PAWOF.

The result of the PAWOF and SIW-PAWOF in Table 4.3

Table 4.3: Directivity of the PAWOF and SIW-PAWOF.

Name	Frequency in GHz	Directivity in dBi
PAWOF	12.51	4.96
	17.15	6.42
SIW-PAWOF	12.47	7.67
	17.82	8.54

The 3-D plot for Directivity of the PAWOF and SIW-PAWOF is
shown in Fig. (4.11) and Fig. (4.12) respectively. So, the value of the
directivity is 7.67 dBi at the resonant frequency 12.47 GHz and directivity is
8.54 dBi at the resonant frequency 17.82 GHz for the SIW-PAWOF.

(a)12.51 GHz   (b)17.15 GHz
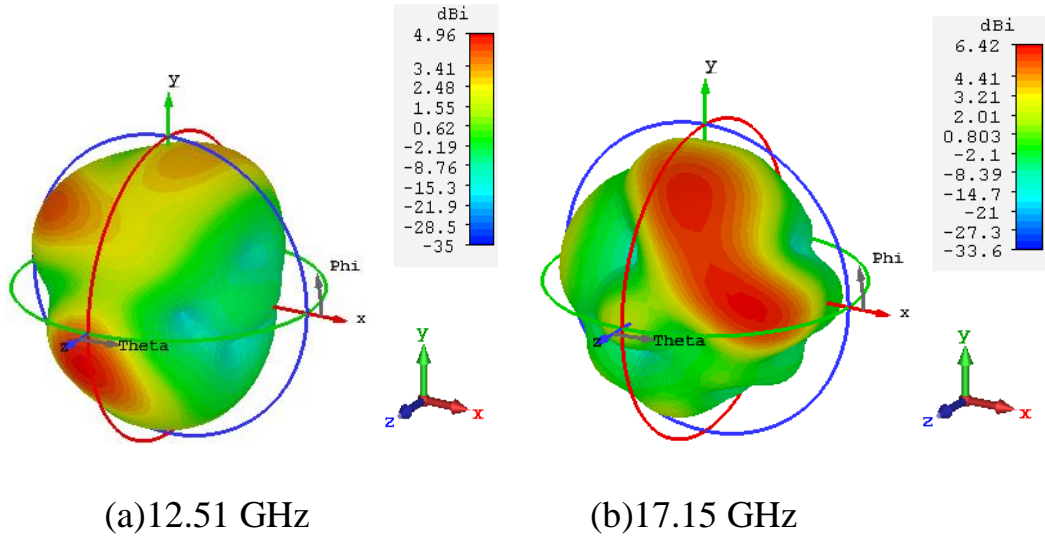
Fig. (4.11): directivity of PAWOF

(a)12.47 GHz   (b)17.82 GHz
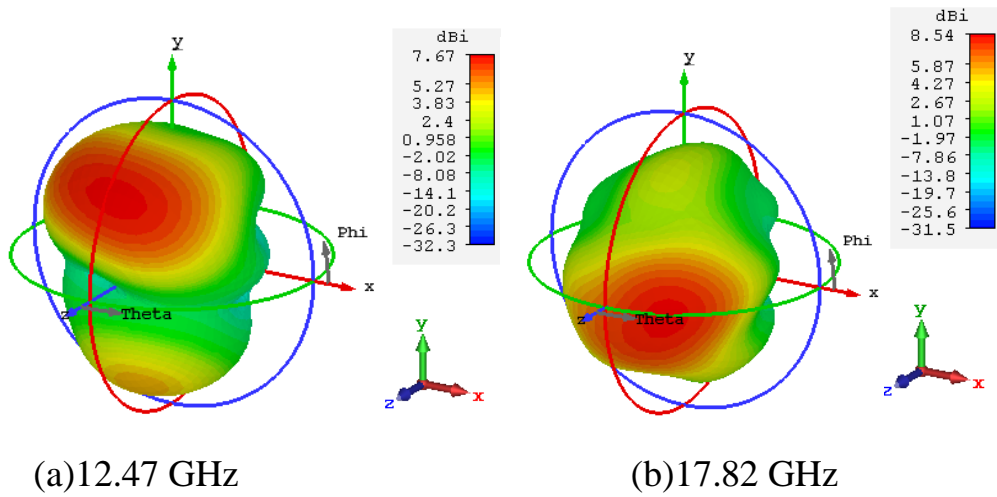
Fig. (4.12): directivity of SIW-PAWOF.

4.3.3 Gain for PAWOF and SIW-PAWOF.

The result of the PAWOF and SIW-PAWOF are shown in Table 4.4

Table 4.4: Gain of the PAWOF and SIW-PAWOF.

Name	Frequency in GHz	Gain in dB
PAWOF	12.51	0.682
	17.15	1.79
SIW-PAWOF	12.47	4.89
	17.82	3.15

The 3-D plot for gain of the PAWOF and SIW-PAWOF is shown in Fig. (4.13) and Fig. (4.14). The value of the gain is 4.89 dB at the resonant frequency 12.47 GHz and gain is 3.15 dB at the resonant frequency 17.82 GHz.

(a)12.51 GHz   (b)17.15 GHz
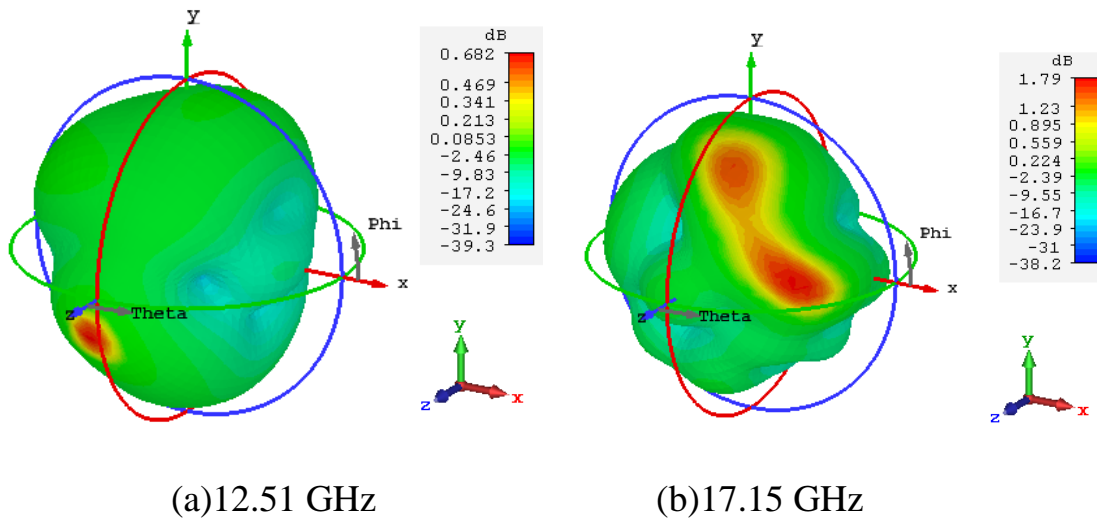
Fig. (4.13): Gain of PAWOF.

(a)12.47 GHz   (b)17.82 GHz
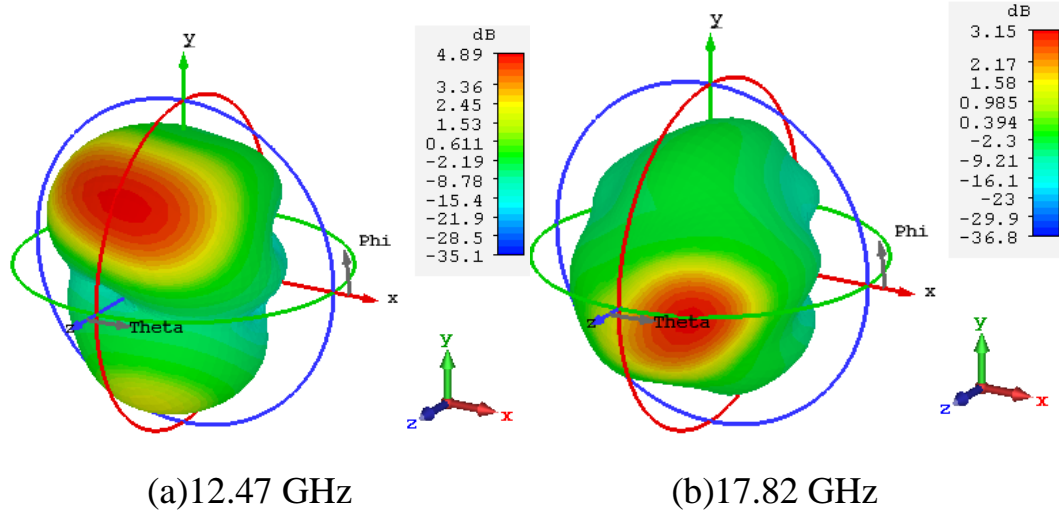
Fig. (4.14): Gain of SIW-PAWOF.

4.3.4 Current Distribution of SIW-PAWOF.

The simulated current surface for the proposed SIW-PAWOF at different resonant frequency is shown in Fig. (4.15). Fig (4.15 (a)) illustrates the current distribution on the patch surface at first resonant frequency 12.47 GHz. Fig. (4.15(b)) shows the current distribution on the patch surface and at the second resonant frequency 17.82 GHz. By testing the distribution of surface current, it has been noticed that the current is highly gathered along the created square slot.
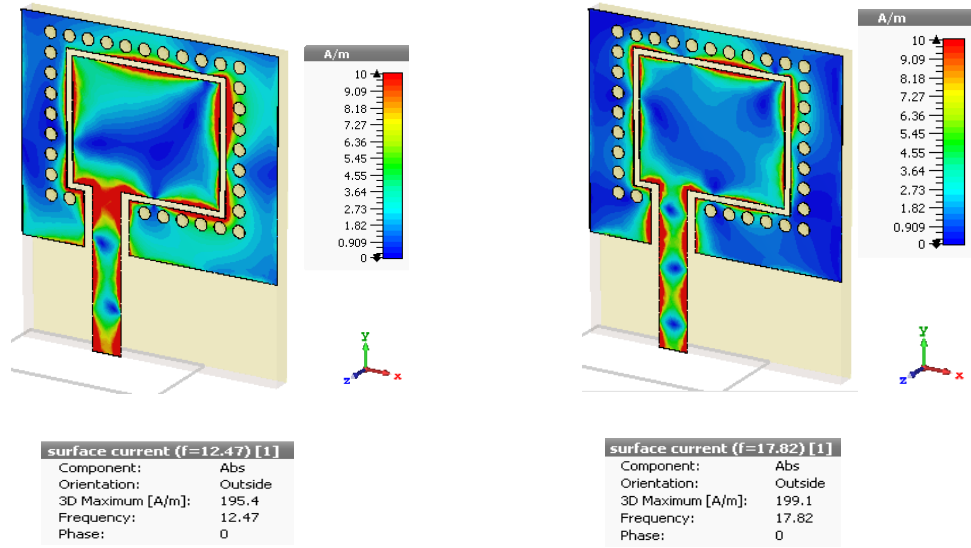
(a) 12.47 GHz.   (b) 17.82 GHz.

Fig. (4.15): Simulated current surface distributions of SIW-PAWOF antenna.

4.3.5 Radiation Patterns of SIW-PAWOF (Electric Field (E-field) .patterns

Table 4.5 shows the simulation result of characteristic far-field power radiation for different resonant frequencies. Fig. (4.16) shows the results in polar of radiation pattern for first resonant frequency 12.47 GHz. Fig. (4.17) shows the results in polar of radiation pattern for the second resonant frequency of 17.82 GHz of SIW-PAWOFA.

Table 4.5: The characteristic of far field power radiation E-field of SIW-PAWOF.

Design	Frequency In GHz	Parameter (E&H)field	x-y plane (θ=90)	y- z plane (Φ=90)	x-z plane (Φ=0)
SIW-PAWOF	12.47	Main lobe magnitude(dB) (E-field)	14.4 dBV/m	19.5 dBV/m	9.33 dBV/m
		Main lobe direction	125º	39º	41º
		Angular width (3dB)	102º	47.9º	76.1º
		Side lobe level (dB)	-3.3dB	-2.9dB	-2.5dB
	17.82	Main lobe magnitude(dB) (E-field)	10.4 dBV/m	16.7 dBV/m	17.7 dBV/m
		Main lobe direction	75º	11º	23º
		Angular width (3dB)	40.4º	50.6º	68.4º
		Side lobe level (dB)	-2.3dB	-5.3dB	-16.5dB

X-Y

Y-Z
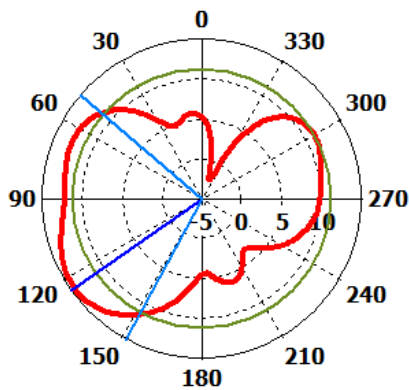
Farfield E-Field(r=1m) Abs (Phi=0)
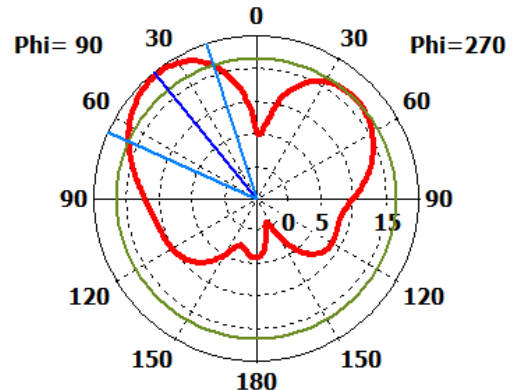
X-Z

Fig. (4.16): Polar plot of the radiation pattern for E-field plane at 12.47 GHz.

Farfield E-Field(r=1m) Abs (Theta=90)

X-Y

Farfield E-Field(r=1m) Abs (Phi=90)

Y-Z

Farfield E-Field(r=1m) Abs (Phi=0)

X-Z

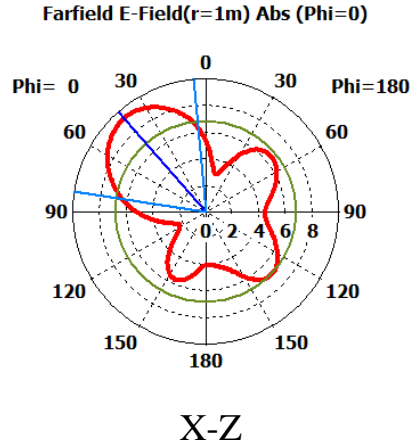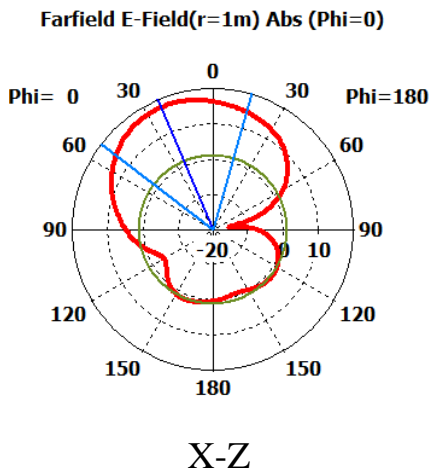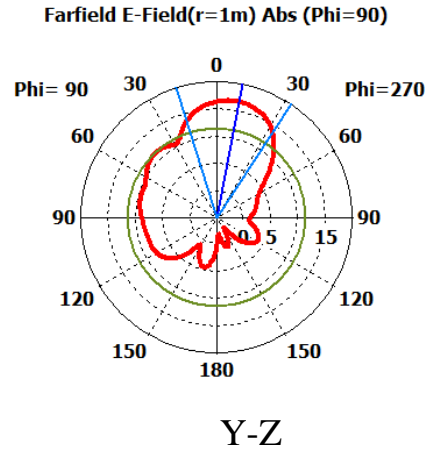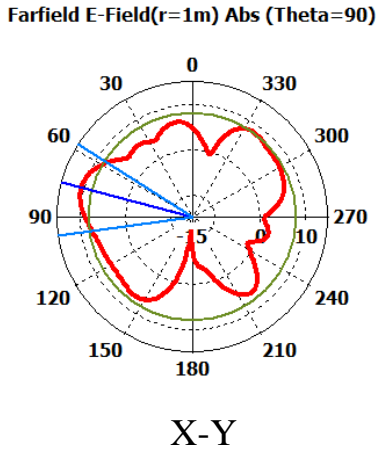Fig. (4.17): Polar plot of the radiation pattern in E- field plane at 17.82 GHz.

4.3.6 Efficiency for PAWOF and SIW-PAWOF.

The efficiency of PAWOF antenna is 14 %. It is calculated from the relationship between the gain and directivity. The efficiency of SIW-PAWOF antenna is 64 %. So, based on these values, the SIW technology enhanced the overall efficiency of the antenna.

4.3.7 Bandwidth of PAWOF and SIW-PAWOF.

Fig. (4.18 (a)) shows SIW-PAWOF bandwidth. SIW-PAWOF has dual bands; the first band starts from frequency 12.06 GHz and ends at frequency 12.87 GHz, producing a bandwidth approximately 805.74 MHz about (6.49%). However, Fig. (4.18 (b)) shows the second bandwidth of SIW-PAWOF which starts from frequency 17.30 GHz and ends at frequency 18.22 GHz, producing a bandwidth approximately 921.81 MHz about (5.16%).
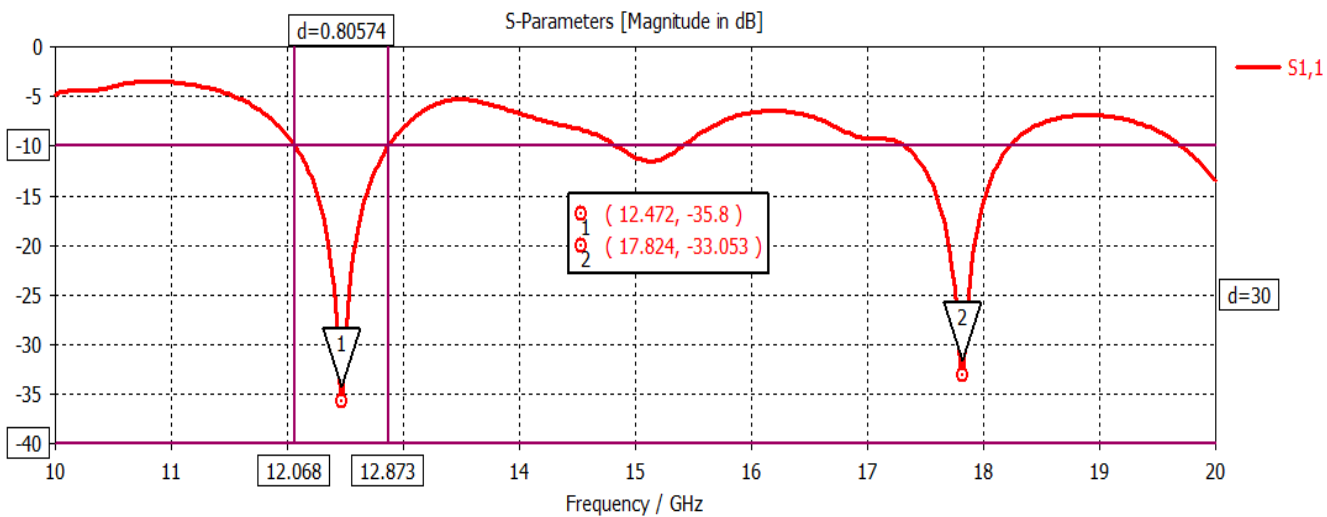
(a) at f=12.47 GHz
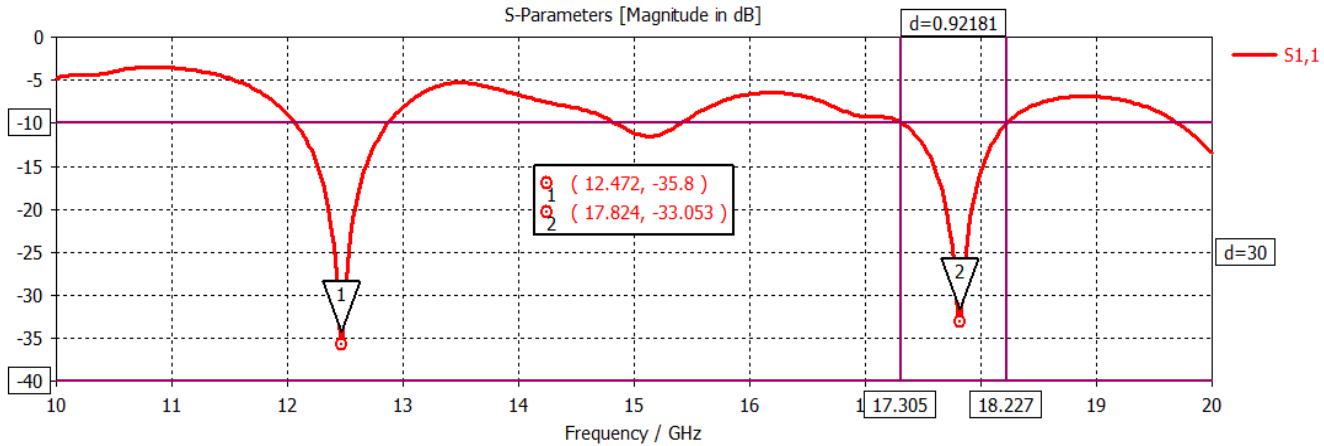
(b) at f=17.82 GHz
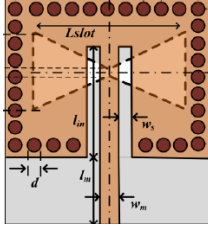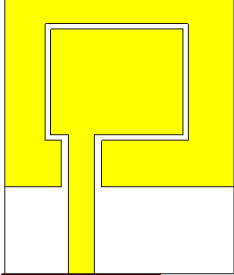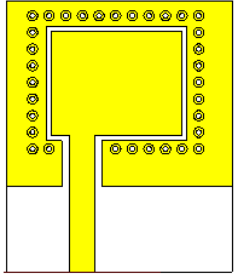
Fig. (4.18): shows SIW-PAWOF bandwidth.

Indeed, the microstrip patch antenna gives narrow bands but the SIW technique keeps the bandwidth and enhances the directivity, gain and efficiency of these bands, so as to serve our applications in these bands.

4.3.8 Comparisons between PAWOF and SIW-PAWOF.

Comparisons between PAWOF and SIW-PAWOF are shown in Table 4.6 perform the enchantment on the antenna performance after add SIW technology.

Table 4.6 : Comparisons between PAWOF, SIW-PAWOF and reference.

Name & Material	Design & Dimensions	Freq. in GHz	Ref. Coff. dB	Directivity in dBi	Gain in dB	B.W & FB.W	e %
Ref. [14] (Roger)	(21.27x26)mm^2	10.6	-30	----	3.7	9.4% 1.03GHz	---
PAWOF (FR4)	(21.27x26)mm^2	12.51	-23	4.96	0.682	585.26 MHz 4.63%	14 %
		17.15	-12	6.42	1.79	1.775 GHz 10.32%	
SIW-PAWOF (FR4)	(21.27x26)mm^2	12.47	-35	7.67	4.89	805.74 MHz 6.49%	64 %
		17.82	-33	8.54	3.15	921.81 MHz 5.16%	

4.4 Characteristics of Active - Parasitic Element SIW Antenna (APESIWA).

APESIWA consists of two elements The active element is directly connected to the feeding line while the other element is excited by coupling with the active element via a gap. Further study has been considered by dividing the parasitic element into some segments (three-segment), such that each one has a dimension of 8.85 x 11.08mm^2 and spaced by a distance (0.65 mm). In order to study the effect of change the size of segments by reducing the size of two segment gradually. The obtained structure and S$_{11}$ parameter results of the previously mentioned operation is illustrated in Fig. (4.19).
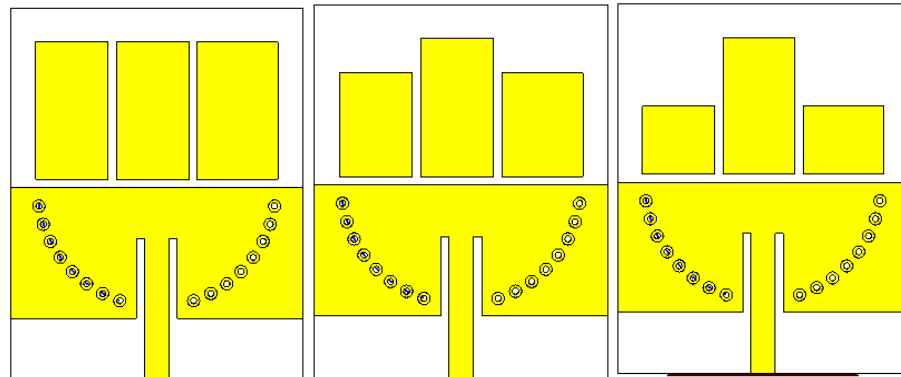
(a) first   (b) second   (c) third
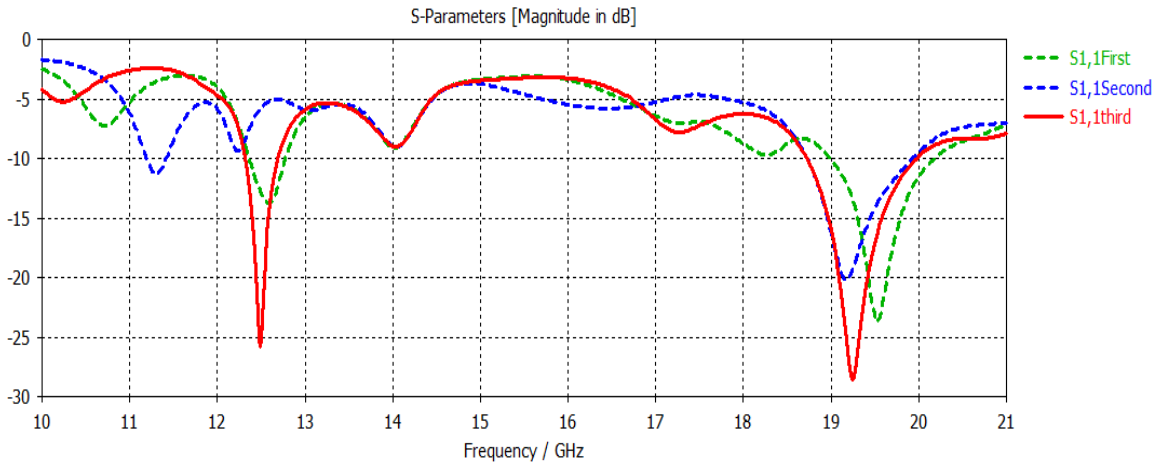
Fig. (4.19): Antennas structure and simulation result S_{11} of the proposed antenna in three cases.

Table 4.7: summarized result in three cases.

Antenna Design	First		Second		Third	
Frequency(GHZ)	12.58	19.53	12.21	19.17	12.49	19.24
Directivity(dBi)	6.52	6.9	---	8.64	8.5	8.63
Gain (dB)	2.3	1.04	---	3.49	3.5	4.01
B.W	460 MHz	1.18 GHZ	---	1.19 GHz	373 MHz	1.25 GHz
Reflection coefficient	-13	-23	-9	-20	-25	-28

The simulation results of the third proposed antenna for various parameters are dealt with in the following sub sections:

61

4.4.1 Reflection Coefficient of APESIWA.

APESIWA concentrate on FR4 dielectric material with thickness h 1.5mm and εr=4.3. Fig.(4.20) shows the S_{11} parameter of APESIWA antenna when using Roger as a dielectric material with thickness h (0.787mm) and εr=2.2.
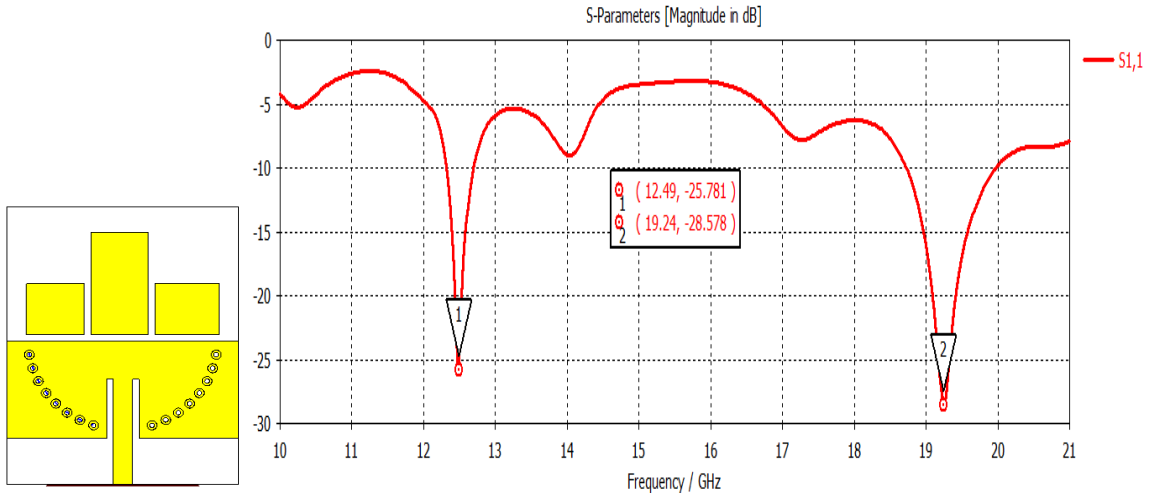
(a) FR4
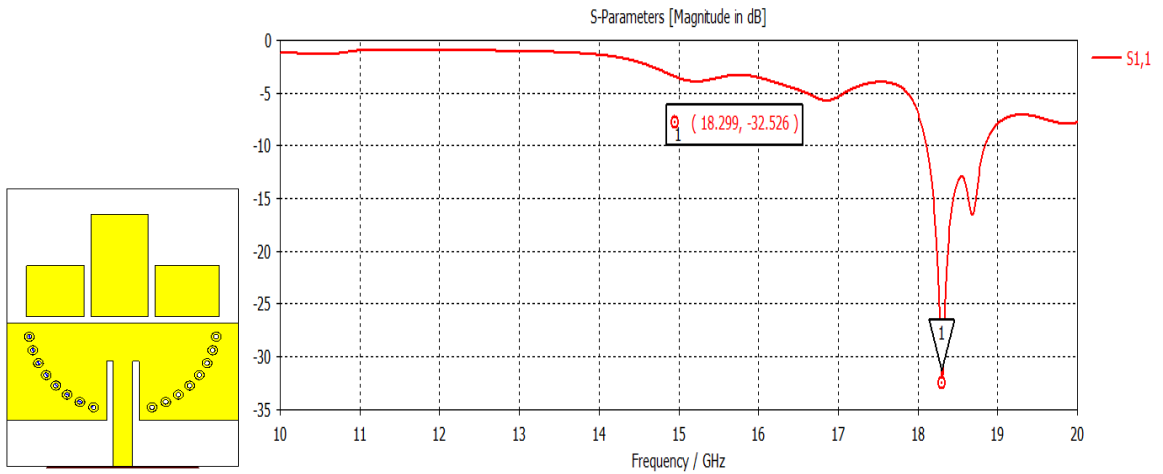
(b) Roger

Fig. (4.20): (a) APESIWA structure and S_{11} parameter with FR4.

(b) APESIWA structure and S_{11} parameter with Roger.

4.4.2 Directivity of APESIWA.

The result of antenna by using Roger and FR4 dielectric marital are shown in Table 4.8.

Table 4.8: Directivity of APESIWA.

Name	Frequency in GHz	Directivity in dBi
Antenna with SIW using FR4	12.49	8.5
	19.24	8.63
Antenna with SIW using Roger	18.3	7.96

The 3-D plot for directivity of APESIWA antenna is shown in Fig. (4.21). So, the largest value of the directivity is 8.63 dBi at the resonant frequency 19.24 GHz and directivity is 8.5 dBi at the resonant frequency 12.49 GHz with FR4 as a substrate. However, the directivity of antenna when using Roger as a substrate is 7.96 dBi at frequency 18.29 GHz as shown in Fig. (4.21).

(a)12.47 GHz at (FR4)   (b)17.82 GHz at (FR4)
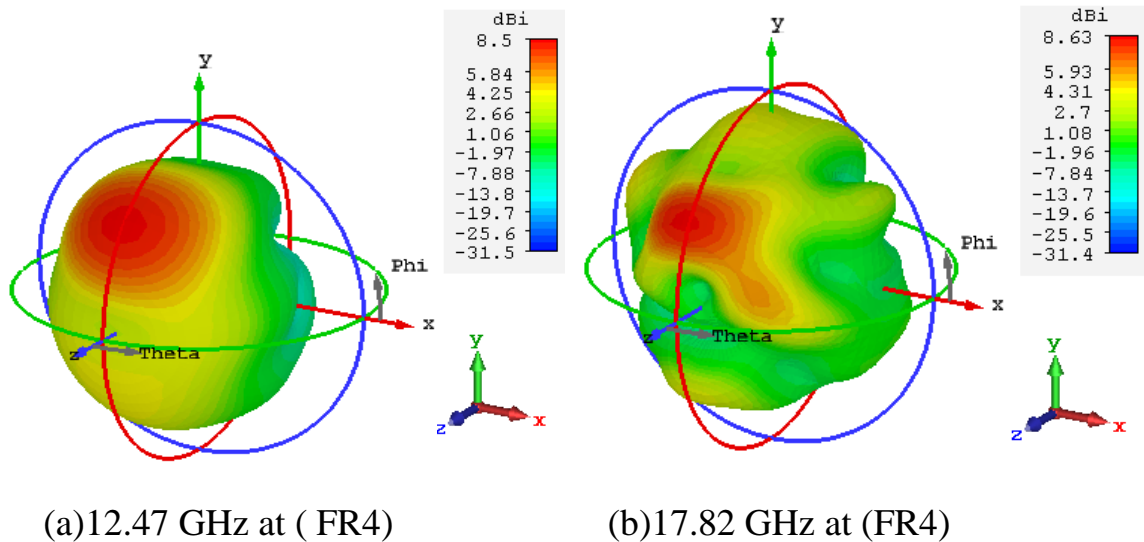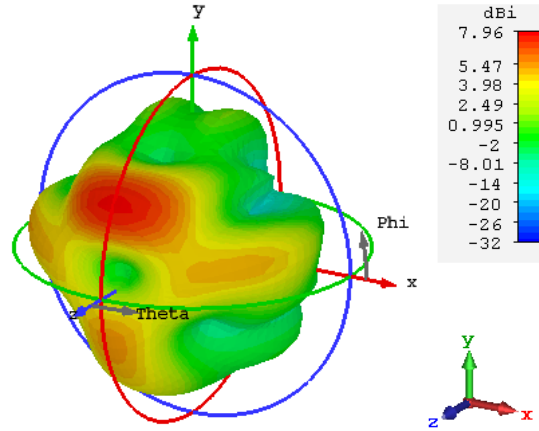
(c)18.3 GHz at (Roger)

Fig. (4.21): Directivity of APESIWA.

4.4.3 Gain of APESIWA.

The gain of APESIWA antenna are shown in Table 4.9.

Table 4.9: Gain of APESIWA.

Name	Frequency in GHz	Gain in dB
APESIWA	12.49	3.5
FR4	19.24	4.01
APESIWA	18.3	7.86
Roger		

The 3-D plot for the gain of APESIWA antenna is shown in Fig. (4.22) and. So, the largest value of the gain is 7.86 dB at 18.3 GHz frequency when using Roger as a substrate as shown in Fig. (4.22). This gives us an indication that the gain of the design with Roger have a better performance for an antenna.

(a)12.49 GHz - FR4   (b)19.24 GHz - FR4

(c)18.3 GHz - Roger
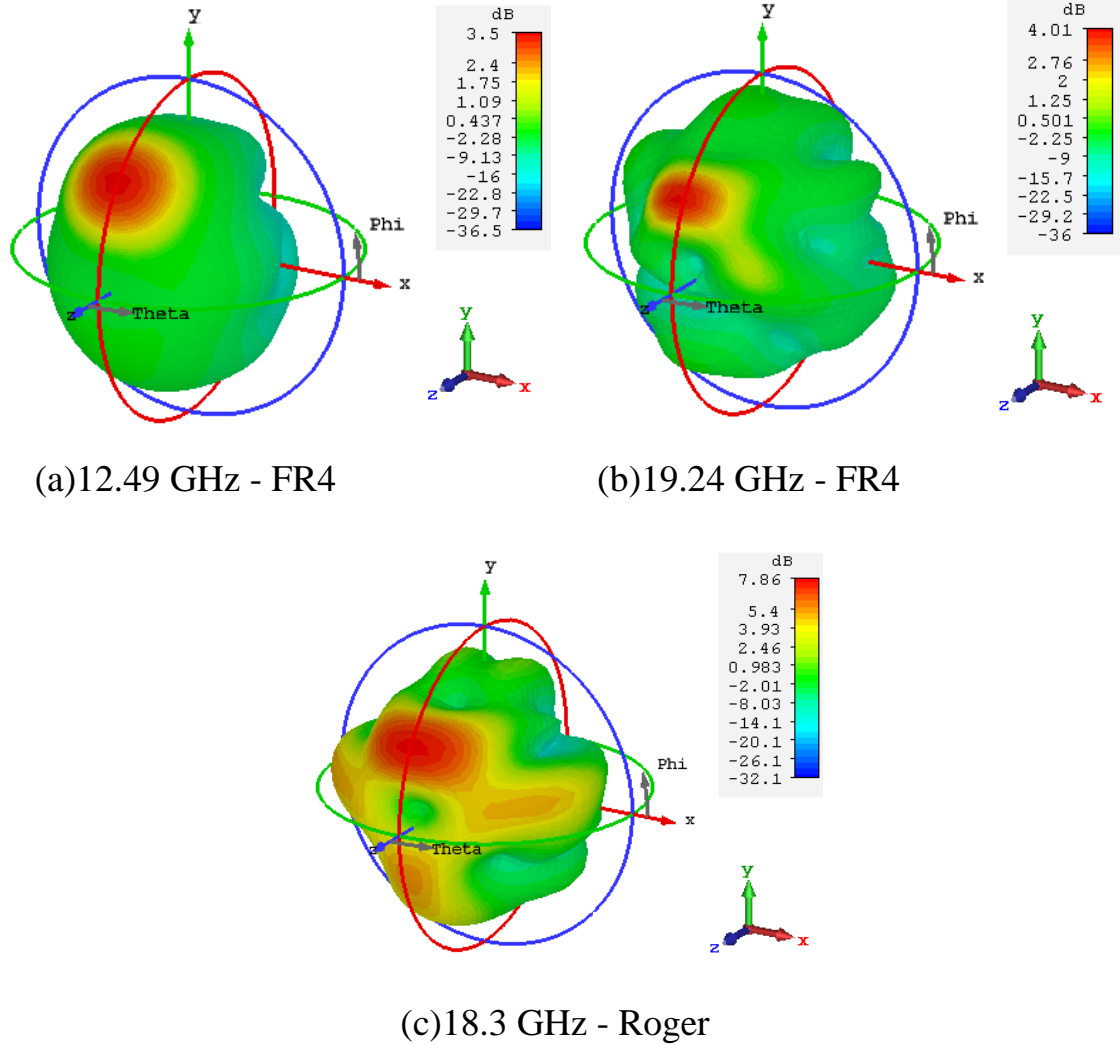
Fig. (4.22): Gain of APESIWA.

4.4.4 Current Distribution of APESIWA.

The simulated current surface for APESIWA antenna is shown in Fig. (4.23). It illustrates the current distribution on the patch surface at first resonant frequency at 12.49 GHz. It is obvious that most of the current concentration is in two regions of the antenna's surface. Also, Fig. (4.23(b)) shows the current distribution on the patch surface at the second resonant frequency 19.24 GHz and 18.3 GHz.

It is clear that the distribution of the surface current at the resonant frequencies has gathered at the inset slot beside the upper edge of the active element as shown in Fig. (4.23). Furthermore, there is a large number of current concentrates in the segments near the active segment. This is due to the high coupling with the active element, while a slight amount of current at the far edges of the parasitic segment, because of the poor coupling with the ends and the current distributions, decreases.

(a) 12.49 GHz.-FR4.   (b) 19.24 GHz.-FR4.   (C)18.3GHz-Roger.
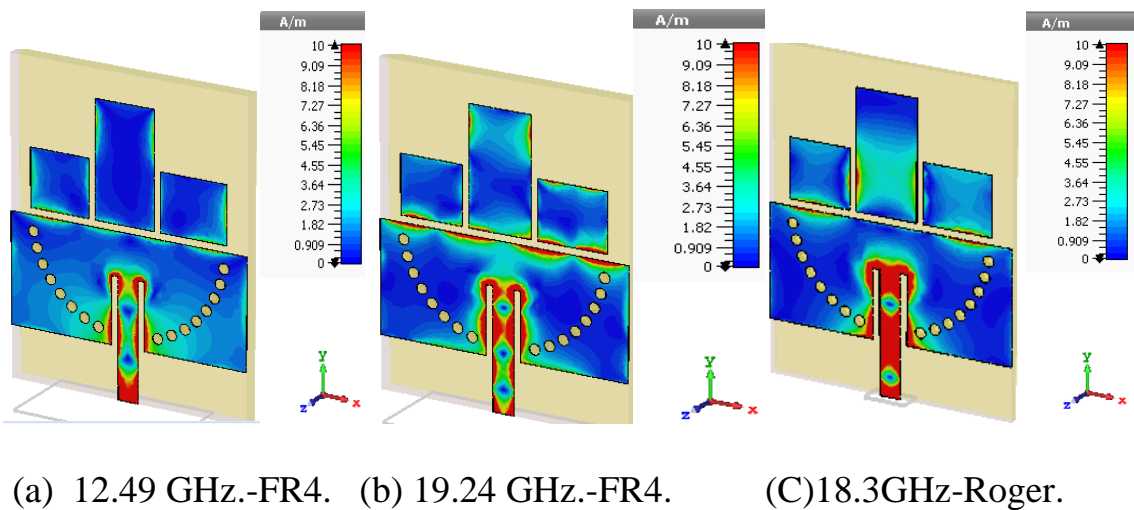
Fig. (4.23): Simulated current surface distributions of APESIWA.

4.4.5 Radiation Patterns of APESIWA Electric Field (E-field) pattern

Table 4.10 shows the simulation result of characteristic far field power radiation for different resonant frequencies. Fig. (4.24(a)) shows the results in polar of radiation pattern for first resonant frequency 12.49 GHz. and Fig. (4.24(b) shows the results in polar of radiation pattern for the second resonant frequency 19.24 GHz of APESIWA antenna. Fig(4.24 (c)) shows the results in polar of radiation pattern for the resonant frequency 18.3 GHz.

Table 4.10: The characteristic of far field power radiation (E-field) of

APESIWA.

Design	Frequency in GHz	Parameter (E-field)	x-y plane (θ=90)	y- z plane (Φ=90)	x-z plane (Φ=0)
APESIWA FR4	12.49	Main lobe magnitude(dB) (E-field)	9.14 dBV/m	18.3dBV/m	13.1 dBV/m
		Main lobe direction	109°	38°	25°
		Angular width (3dB)	76.8^o	45.5^o	107.2^o
		Side lobe level (dB)	-1.4dB	-4.1dB	-8.6dB
	19.24	Main lobe magnitude(dB) (E-field)	14 dBV/m	18.8 dBV/m	14.8 dBV/m
		Main lobe direction	97°	31°	32°
		Angular width (3dB)	46°	24.6^o	40.3^o
		Side lobe level (dB)	-1.6dB	-4.6dB	-3.8dB
APESIWA Roger	18.3	Main lobe magnitude(dB) (E-field)	16.2 dBV/m	22.6 dBV/m	19 dBV/m
		Main lobe direction	105°	31°	25°
		Angular width (3dB)	49.9^o	25.6^o	71.3^o
		Side lobe level (dB)	-1.6dB	-2.4dB	-6.3dB

Farfield E-Field(r=1m) Abs (Theta=90)

Farfield E-Field(r=1m) Abs (Phi=90)

X-Y   Y-Z
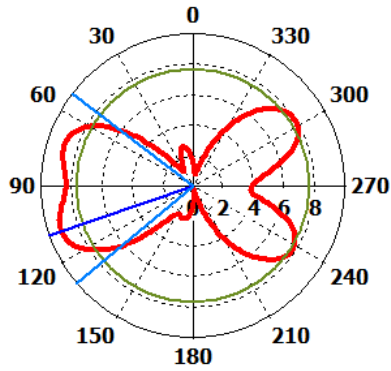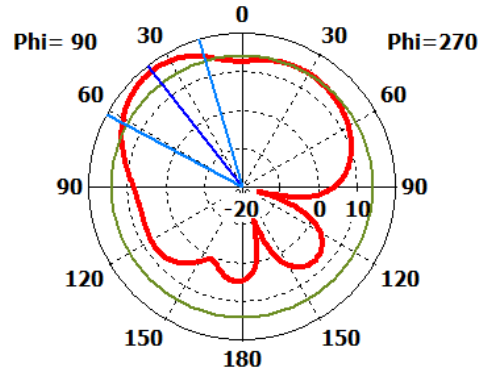
Farfield E-Field(r=1m) Abs (Phi=0)

X-Z

(a) At 12.49 GHz-FR4.

Farfield E-Field(r=1m) Abs (Theta=90)

Farfield E-Field(r=1m) Abs (Phi=90)

X-Y   Y-Z

Farfield E-Field(r=1m) Abs (Phi=0)

X-Z

(b) At 19.24 GHz-FR4

Farfield E-Field(r=1m) Abs (Theta=90)

Farfield E-Field(r=1m) Abs (Phi=90)

X-Y

Y-Z

Farfield E-Field(r=1m) Abs (Phi=0)

X-Z

(c) At 18.3 GHz- Roger
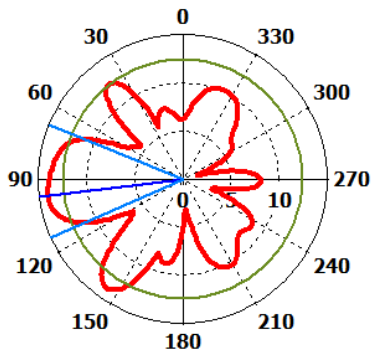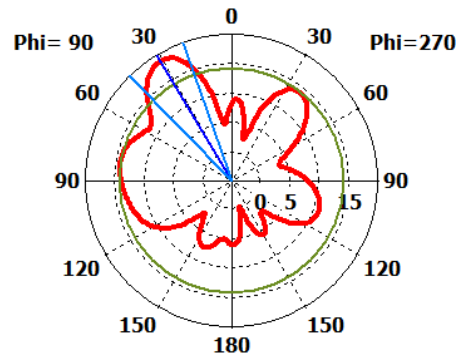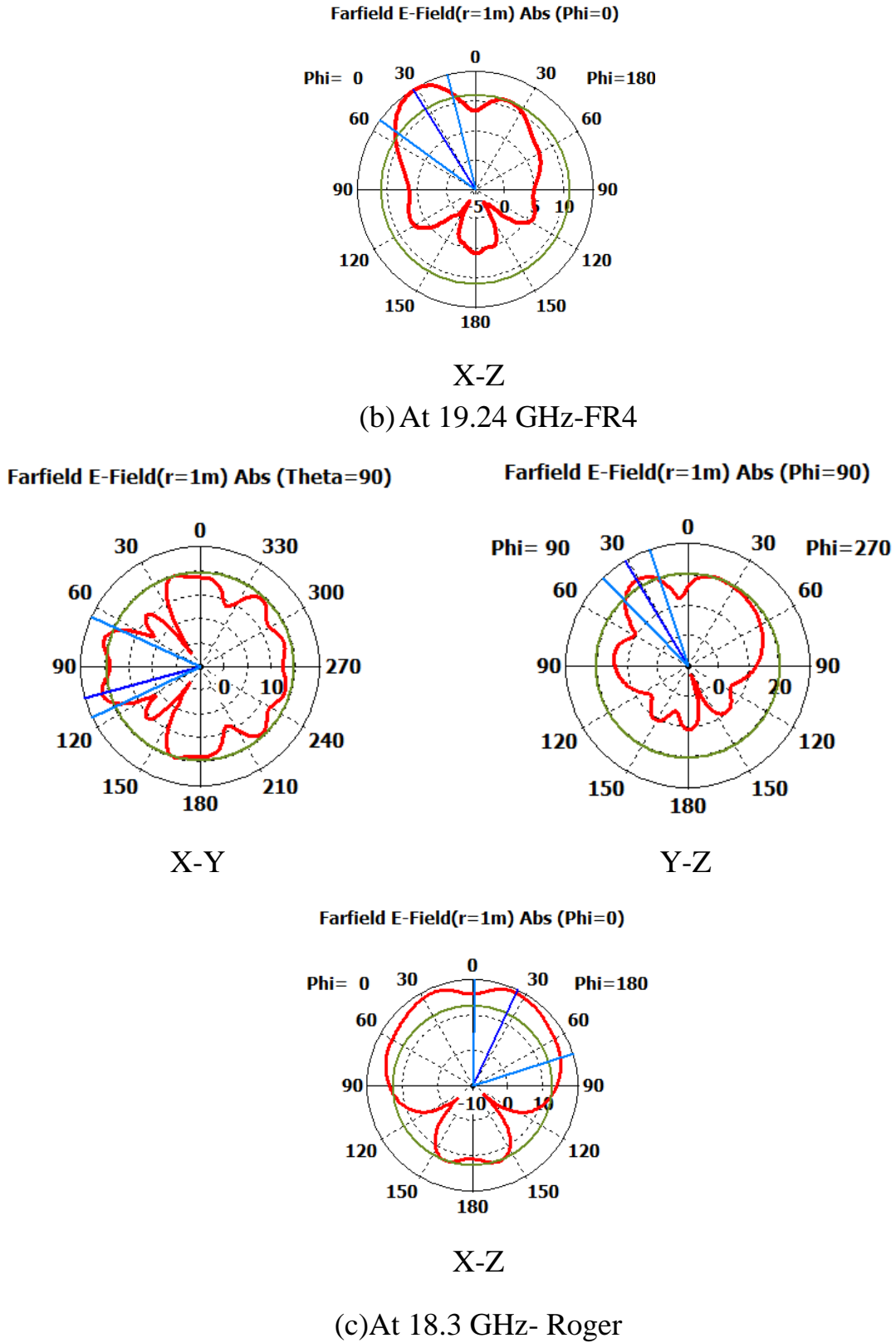
Fig. (4.24): Polar plot of the radiation pattern in E-plane.

4.4.6 Efficiency of APESIWA.
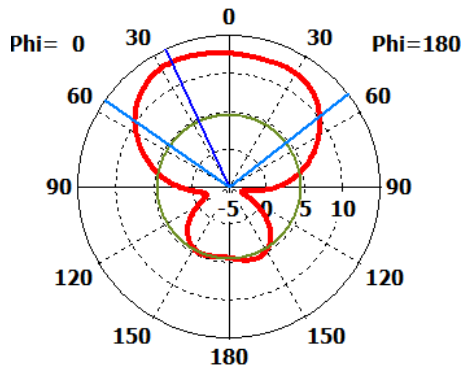
The efficiency of APESIWA is 46 % when using FR4 dielectric material as a substrate and the efficiency of APESIWA is 98% when using Roger dielectric material as a substrate. Roger makes the antenna more efficient because of its low tangent loss material.

4.4.7 Bandwidth for APESIWA.

Fig. (4.25 (a)) shows APESIWA bandwidth. APESIWA has dual bands first band which starts from frequency 12.31 GHz and ends at frequency 12.69 GHz, producing a bandwidth approximately 374 MHz . However, Fig. (4.25 (b)),show the second bandwidth of APESIWA which starts from frequency 18.72 GHz and ends at frequency 19.97GHz, producing a bandwidth approximately 1.251 GHz when using FR4.

Fig. (4.26) shows APESIWA bandwidth. YUSSIWA has single band which starts from frequency 18.10 GHz and ends at frequency 18.84 GHz, producing a bandwidth approximately 736.9 MHz.
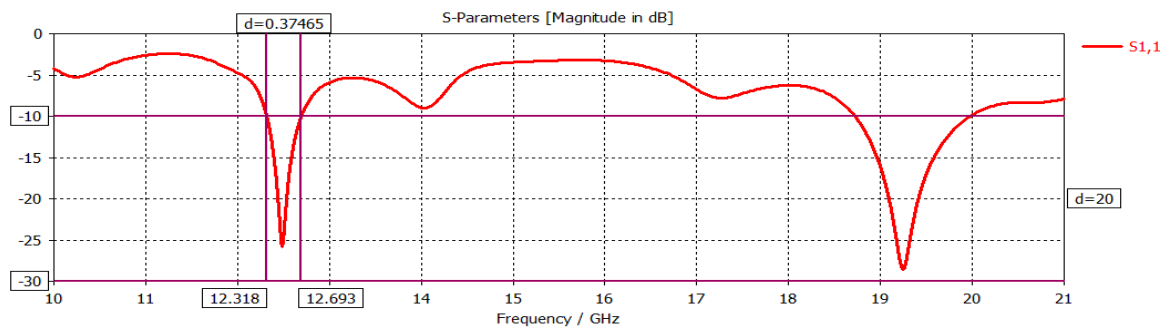
(a) at f=12.49 GHz
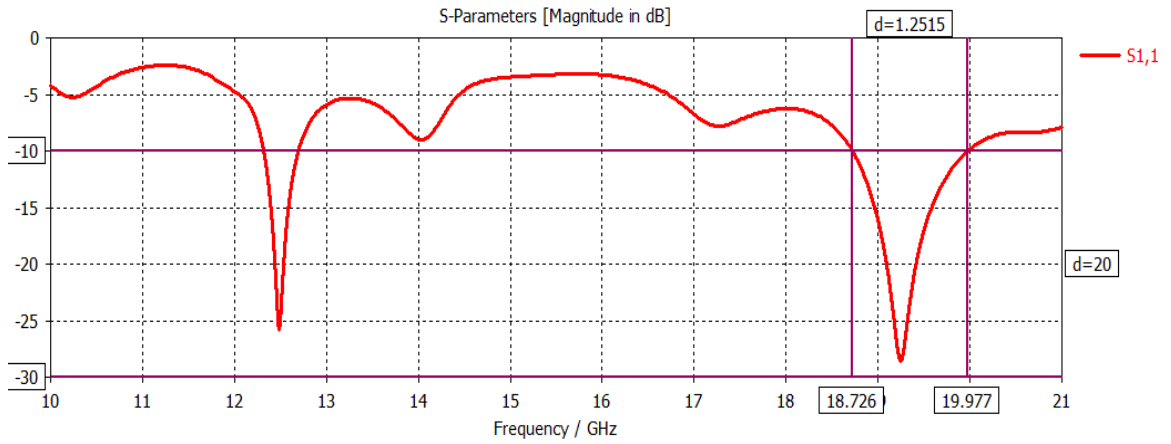
(b) at f=19.24 GHz

Fig. (4.25): APESIWA bandwidth at FR4.
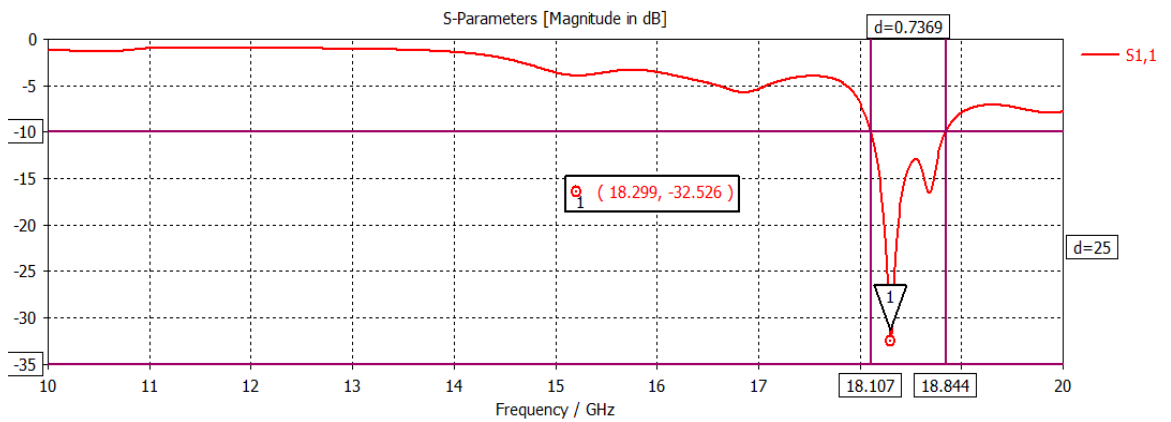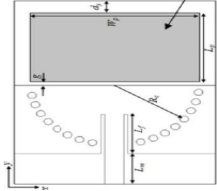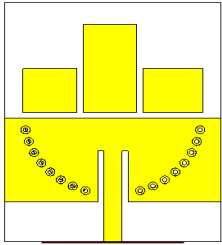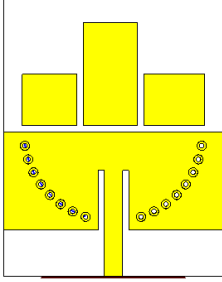
Fig. (4.26): APESIWA bandwidth at Roger.

4.4.8 Comparisons between APESIWA Type and Reference.

Comparisons between APESIWA and references are shown in Table 4.11.

Table 4.11 : Comparisons between APESIWA type and references.

Name & Material	Design & Dimensions	Freq. in GHz	Ref. Coff. in dB	Directivity in dBi	Gain in dB	B.W & FB.W	e %
Ref . [15] (Roger)	(30x23.5)mm^2	8	-30	----	7.5	780 MHz 9.6 %	95 %
APESIWA (Roger)	(30x23.5)mm^2	18.3	-33	7.96	7.86	736.9 MHz 4.04%	98 %
YUSSIWA (FR4)	(30x23.5)mm^2	12.49	-25	8.5	3.5	374 MHz 3.04%	46%
		19.24	-28	8.63	4.01	1.25 GHz 6.49%	

4.5   Characteristics of Dual Circular Slots Antenna (DCSA) and Dual Circular Slots SIW Antenna (DCSSIWA).

Initially proposed antenna has been designed without SIW and slot as shown in Fig. (4.27 (a)) to evaluate and compare our results. The antenna

has been modeled with a prescribed substrate. Simulation results reveal that the antenna offers a single band resonance within the a frequency range of (9-20) GHz with resonant frequency at about 10 GHz as shown in Fig. (4.27 (b)) and Table 4.12. This behavior does not prevent the possibility of the existence of other resonances outside this frequency range.

(a)   (b)
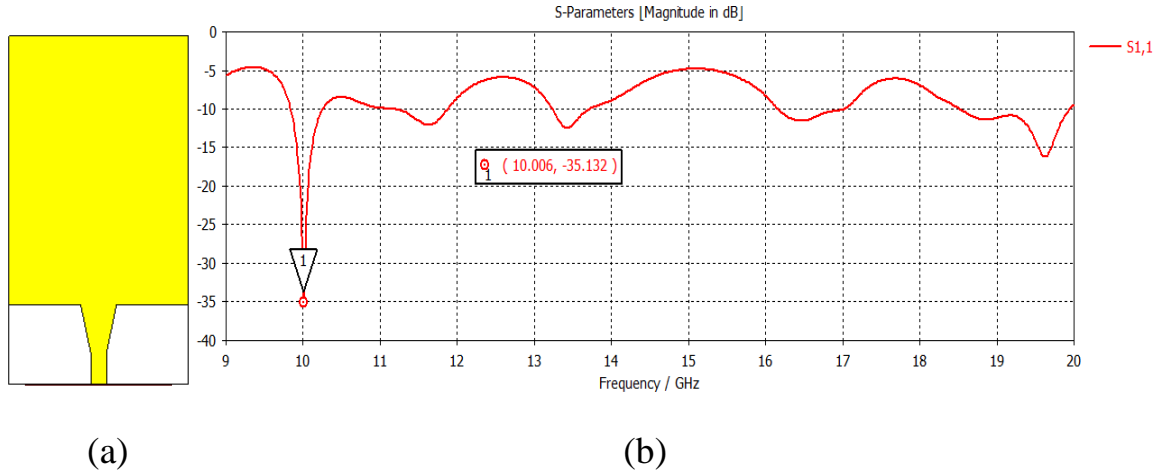
Fig. (4.27) : (a) Geometry of first proposed antenna (b) Simulated reflection coefficient S_{11} parameter of antenna without SIW.

Table 4.12: Result of initially proposed antenna.

Design	Frequency GHz	Directivity dBi	Gain dB	B.W
	10	8.81	2.03	4.1 MHz

Than SIW technique is applied with prescribed calculated dimensions of via and the equivalent distance between vias to enhance the bandwidth and gain. The circular slot is added to increase the bandwidth, directivity,

gain, and enhance the antenna matching. After the executed above procedure, the proposed SIW antenna for one, two, and three circular slots have been done as shown in Fig. (4.28 (a, b, c, d)).

(a)   (b)   (c)   (d)
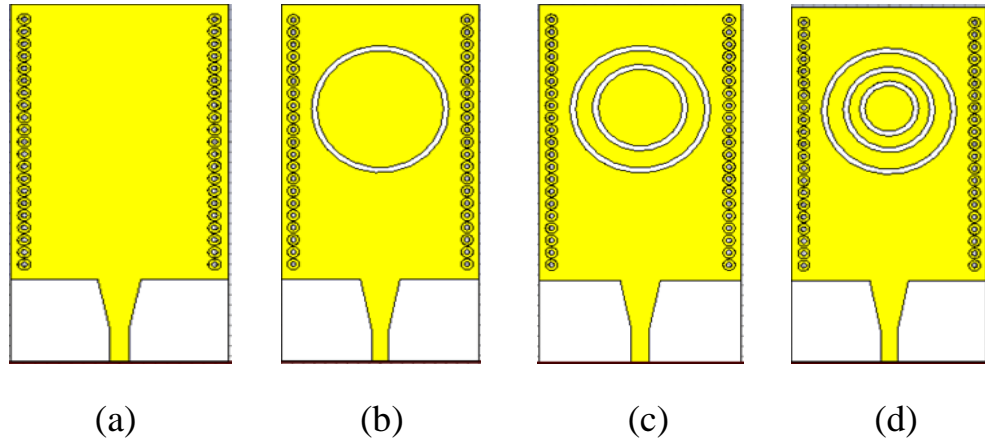
Fig. (4.28): (a) SIW antenna without slots. (b) SIW antenna with one circular slot. (c) SIW antenna with two circular slot. (d) SIW antenna with three circular slot.

The result of the antenna in Fig. (4.28 (a)) shows that, when SIW applied to the conventional microstrip antenna, the antenna gives two resonant frequencies 14.8 GHz and 19.22 GHz. While the results of the antenna in Fig. (4.28(b)) gives three resonant frequencies which are (11.20,13.18,19.53) GHz. The results of the SIW antenna Fig. (4.28 (d)) with two slots show that etched two circular slots on the one top of the antenna give one resonant frequency about 13.2 GHz. Finally, when the third slot etched on the one top of the antenna the frequency there is still about 13.2 GHz as shown in Fig. (4.28 (d)). The results of the S_{11} parameter of all the proposed antennas are shown in Fig. (4.29). Table 4.13 shows the results of the antenna mentioned in Fig. (4.40).
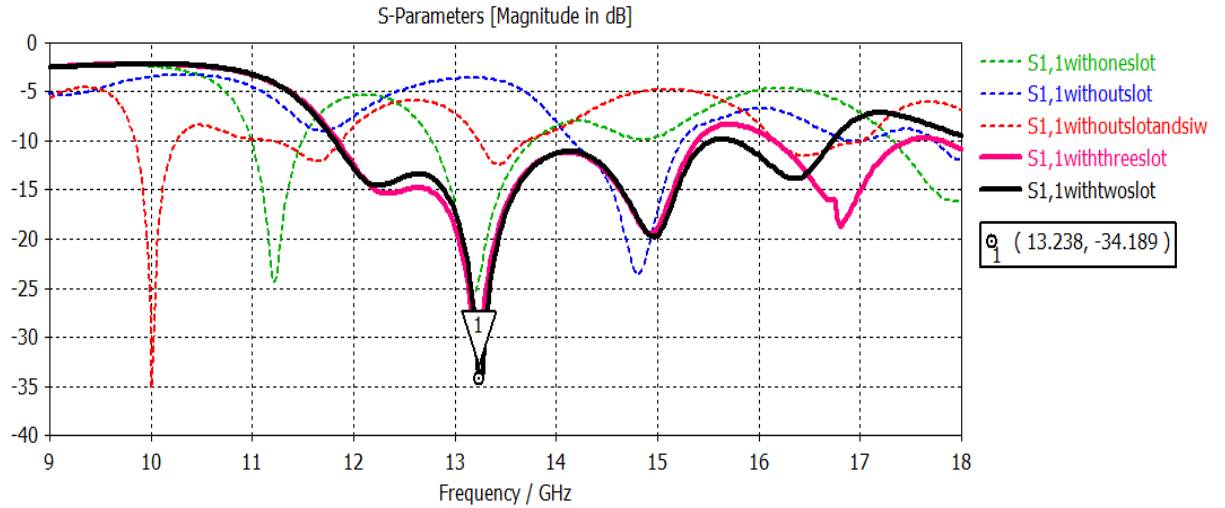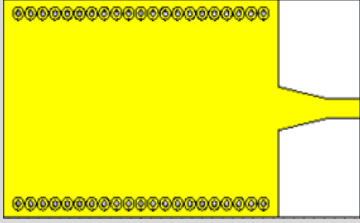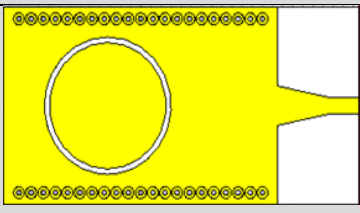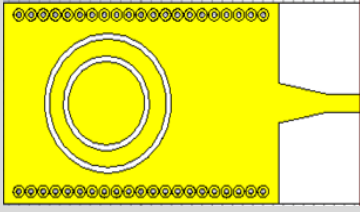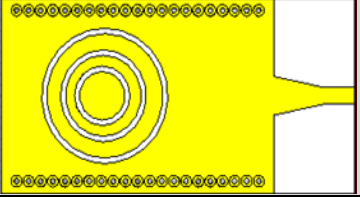
Fig. (4.29): The results of S_{11} parameter of all the proposed antennas.

Table 4.13: Results of all the proposed antennas.

Design	Frequency GHz	Directivity dBi	Gain dB	B.W & FB.W
	14.8	8.41	2.97	1.086 GHz
	19.22	9.65	2.17	1.349 GHz
	11.20	7.65	4.73	502 MHz
	13.18	8.32	5.5	1 GHz
	19.53	10.1	3.44	3 GHz
	13.32	8.54	6.05	4.913 GHz

	13.32	8.78	6.28	3.568 GHz

4.5.1 Reflection Coefficient of DCSSIWA.

DCSSIWA antenna is structured by using a conventional rectangular patch antenna with dual circular slots etched on the one metallic top of the DCSSIWA antenna structure and S_{11} parameter is shown in Fig. (4.30). Microstrip to SIW transition feeding is used.
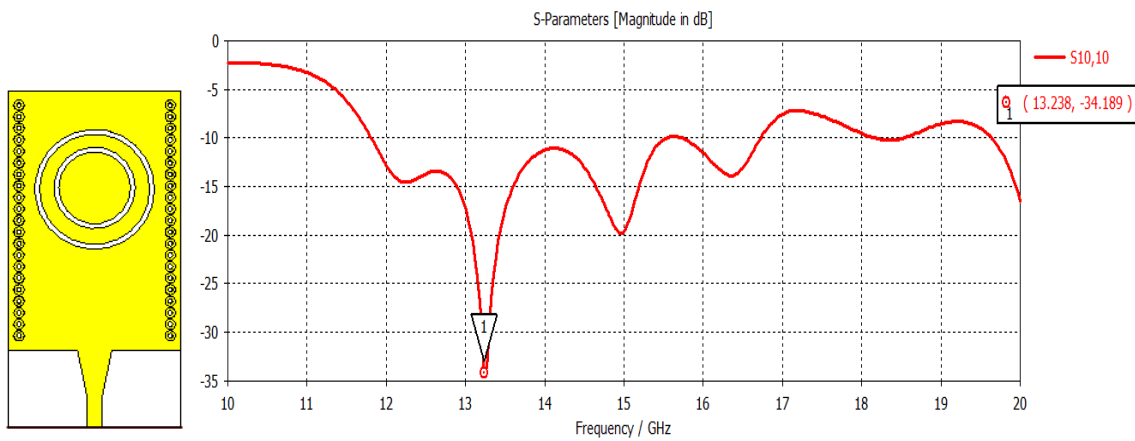
Fig. (4.30): DCSSIWA structure and S_{11} parameter.

4.5.2 Directivity of DCSSIWA.

The result of DCSSIWA are shown in Table 4.14

Table 4.14: Directivity of DCSSIWA.

Name	Frequency in GHz	Directivity in dBi
DCSSIWA	13.2	8.54

The 3-D plot for Directivity of DCSSIWA is shown in Fig. (4.31). Directivity is 8.54 dBi at the resonant frequency of 13.2 GHz.
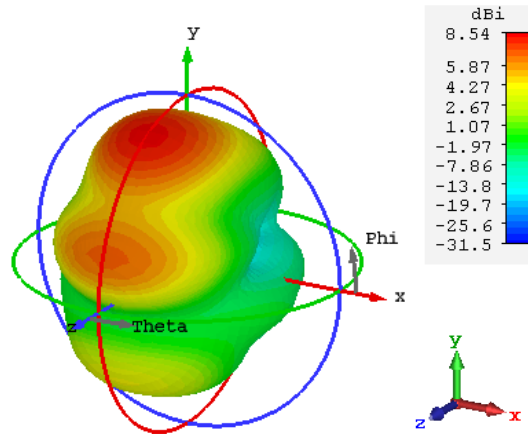
(b) f =13.2 GHz

Fig. (4.31): Directivity of DCSSIWA antenna.

4.5.3 Gain of DCSSIWA.

The result of DCSSIWA at frequency 13.2 GHz is shown in Table below.

Table 4.15: Gain of DCSSIWA.

Name	Frequency in GHz	Gain in dB
DCSSIWA	13.2	6.05

The 3-D plot for the gain DCSSIWA is shown in Fig. (4.32). So, the gain is 6.05 dB at the resonant frequency of 13.2 GHz.
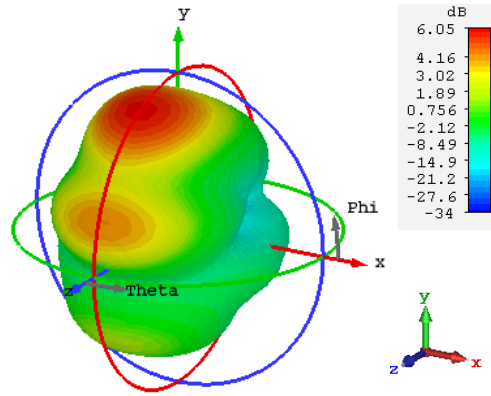
(b) f =13.2 GHz

Fig. (4.32): Gain of DCSSIWA antenna.

4.5.4 Current Distribution for DCSSIWA.

The simulated current surface for DCSSIWA at the resonant frequency 13.2 GHz is shown in Fig. (4.33). It is obvious that most of the current concentration are in two regions of the antenna's surface.
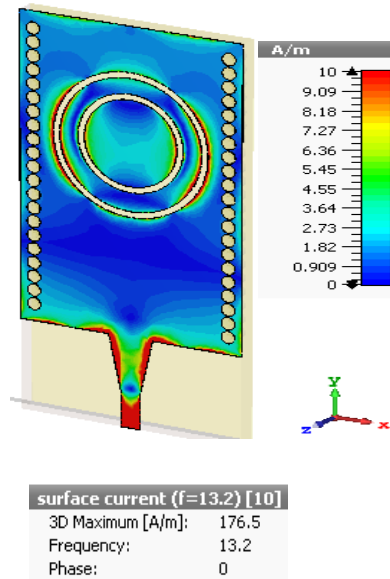
Fig. (4.33): Simulated current surface distributions of DCSSIWA antenna.

4.5.5 **Radiation Patterns of DCSSIWA (Electric Field (E-field).**

Table 4.16 shows the simulation result of characteristic far field power radiation for the resonant frequency. Fig. (4.34) shows the results in polar of radiation pattern for resonant frequency 13.2 GHz of DCSSIWA.

Table 4.16: The characteristic of far field power radiation E - field of DCSSIWA.

Design	Frequency GHz	Parameter (E&H)field	x-y plane (θ=90)	y- z plane (Φ=90)	x-z plane (Φ=0)
DCSSIWA	13.2	Main lobe magnitude(dB) (E-field)	17 dBV/m	20.8 dBV/m	14.4 dBV/m
		Main lobe direction	91°	63°	0°
		Angular width (3dB)	63.4^{o}	45.5^{o}	61.9^{o}
		Side lobe level (dB)	-9.2dB	-1.7dB	-6.2dB

X-Y   Y-Z
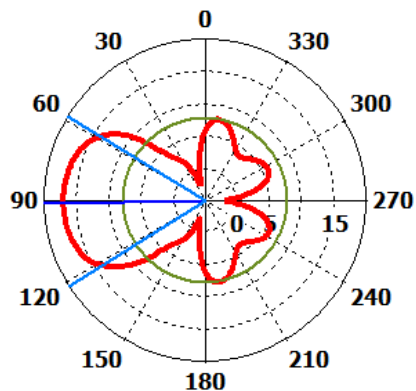
Farfield E-Field(r=1m) Abs (Phi=0)
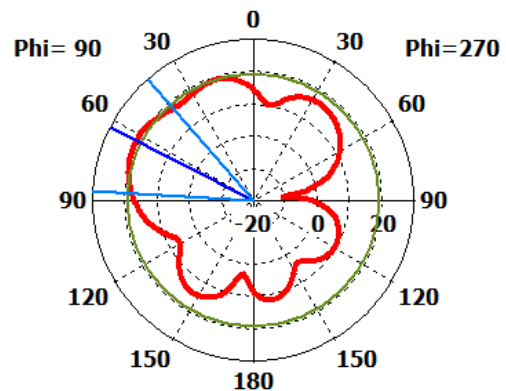
X-Z
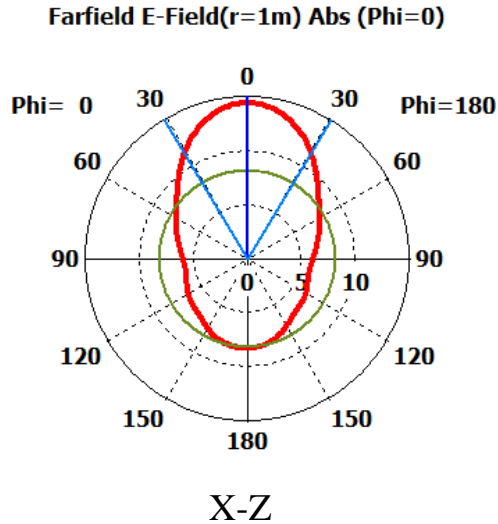
Fig. (4.34): Polar plot of the radiation pattern in E –plane.

4.5.6 THE Efficiency of DCSSIWA.

The efficiency of DCSSIWA is 71%. the SIW technology enhances the overall efficiency of the antenna.

4.5.7 Bandwidth for DCSSIWA.

Fig. (4.35) shows the bandwidth of DCSIWSA at resonant frequency 13.2 GHz. This band starts from frequency 11.81 GHz and ends at frequency 16.73 GHz, producing a bandwidth approximately 4.918 GHz.
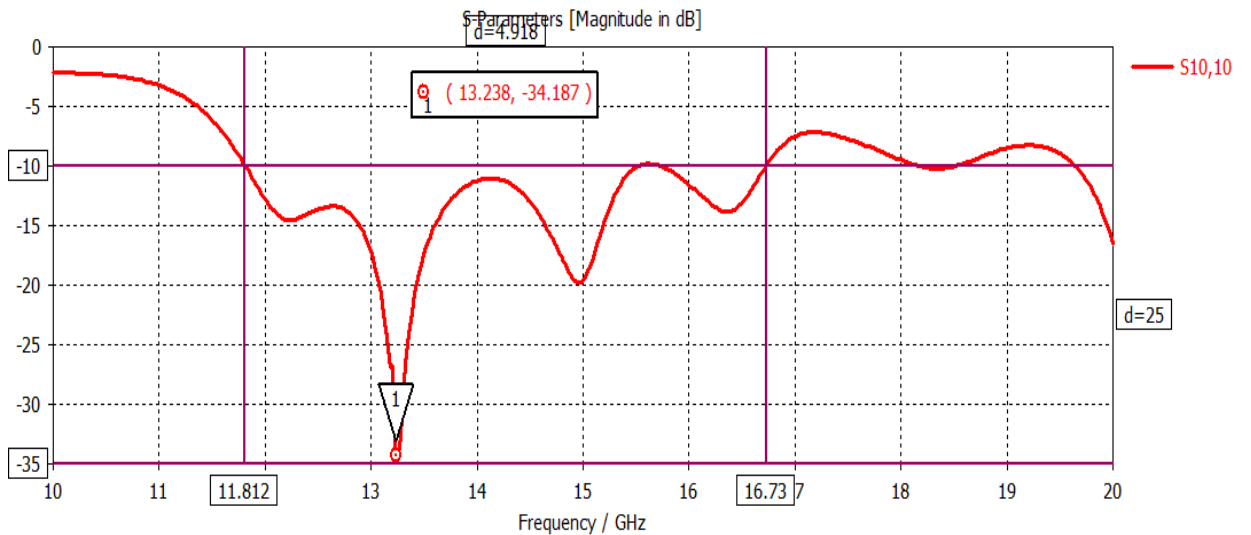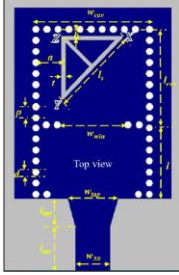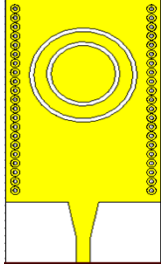
Fig. (4.35): DCSSIWA bandwidth at resonant frequency f =13.2 GHz.

SIW concentrates the power between vias and the two slots make the band wider to make the antenna cover much application with high efficiency in this band.

4.5.8 Comparisons between DCSSIWA and Reference.

Comparisons between DCSSIWA and reference are shown in Table below.

Table 4.17 : Comparisons between DCSSIWA and reference.

Name & Material	Design & Dimensions	Freq. GHz	Ref. Coff. dB	Directivity dBi	Gain dB	B.W & FB.W	e %
Ref .[23] (Roger)	(15.5x32.7) mm^2	(14.43-16.49)	-19	----	4	2.09 GHz (13.53%)	---
DCSSIWA (FR4)	(18x35) mm^2	13.32 (11.8-16.7)	-34	8.54	6.05	4.913 GHz 37.18%	71 %

4.6   Characteristic of Circular SIW Antenna (CSIWA).

The simulation results CSIWA antenna will be presented in the following subsections:

4.6.1 Reflection Coefficient of CSIWA.

The antenna is structured by using a circular patch and circular slot etched at a rectangular patch fixed on the top layer of a substrate with feeding line in the middle. The antenna structure and its result are shown in Fig. (4.36).
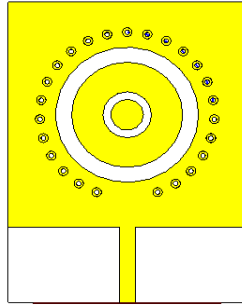
(a)
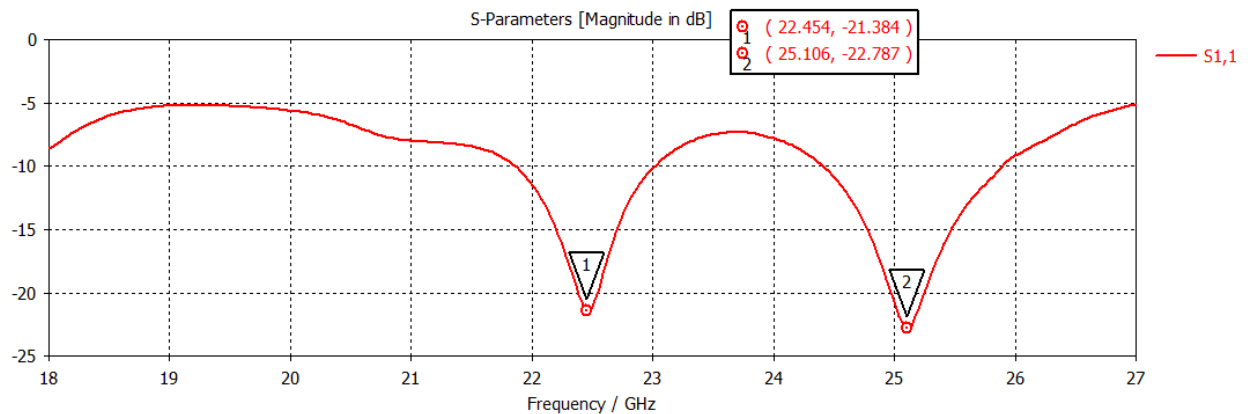
(b)

Fig. (4.36): (a) CSIWA antenna structure. (b):S_{11} parameter for the CSIWA antenna.

4.6.2 Directivity of CSIWA.

The result of CSIWA is shown in Table below.

Table 4.18: Directivity of CSIWA.

Name	Frequency in GHz	Directivity in dBi
CSIWA	22.4	9.26
	25.1	8.19

The 3-D plot for directivity of CSIWA is shown in Fig. (4.37) . The value of the directivity is 9.26 dBi at the resonant frequency 22.4 GHz and Directivity is 8.19 dBi at the resonant frequency 25.1 GHz for the CSIWA.

(a) 22.4 GHz   (b) 25.1 GHz
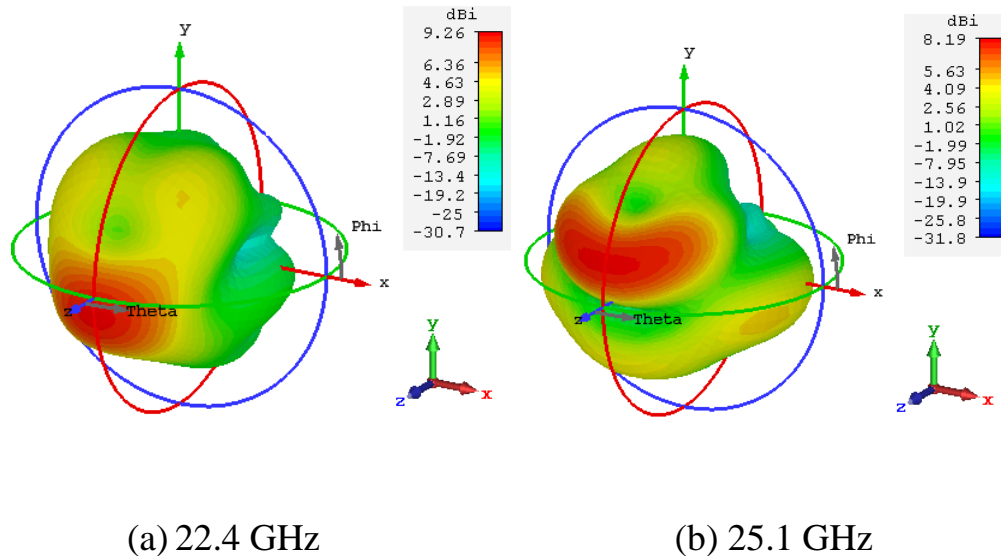
Fig. (4.37): Directivity of CSIWA.

4.6.3 Gain for CSIWA.

The results of CSIWA are shown in Table below.

Table 4.19: Gain of CSIWA.

Name	Frequency in GHz	Gain in dB
CSIWA	22.4	6.14
	25.1	4.72

The 3-D plot for the gain of CSIWA is shown in Fig. (4.38) the value of the gain is 6.14 dB at the resonant frequency 22.4 GHz and gain is 4.72 dB at the resonant frequency 25.1.

(a) 22.4 GHz   (b) 25.1 GHz
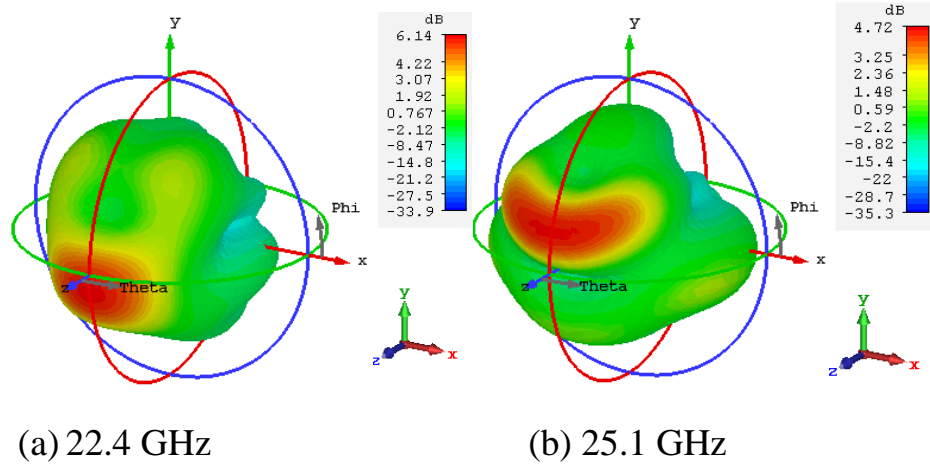
Fig. (4.38) : Gain of CSIWA.

4.6.4 Current Distribution for CSIWA.

The simulated current surface for the CSIWA is shown in Fig. (4.39) , which illustrates the current distribution on the patch surface at the resonant frequencies 22.4 GHz and 25.1 GHz for CSIWA antenna.
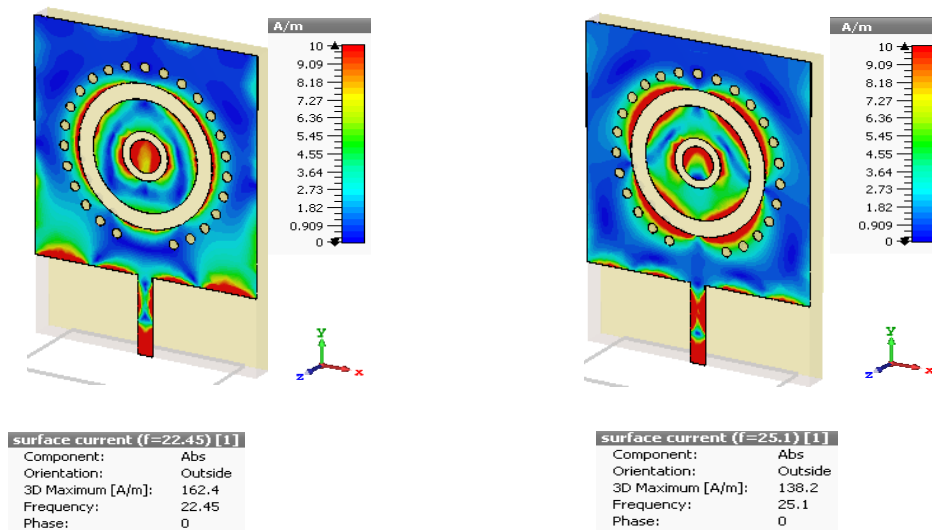
Fig. (4.39): Simulated current surface distributions CSIWA.

It is clear that the current is highly concentrated in the area related to the feed line as well as right and left sides. But, it is noticed that the surface current gradually begins to decrease as moving up.

4.6.5 Radiation Patterns of CSIWA (Electric Field (E-field.

Table 4.20 shows the simulation result of characteristic far-field power radiation for different resonant frequencies. Fig. (4.40) shows the results in polar of radiation pattern for first resonant frequency 22.4 GHz. Fig. (4.41) shows the results in polar of radiation pattern for second resonant frequency 25.1 GHz of CSIWA.

Table 4.20: The characteristic of far field power radiation (E – field) of CSIWA.

Design	Frequency In GHz	Parameter (E&H)field	x-y plane (θ=90)	y- z plane (Φ=90)	x-z plane (Φ=0)
CSIWA	22.4	Main lobe magnitude(dB) (E-field)	10.7 dBV/m	20.9 dBV/m	20.4 dBV/m
		Main lobe direction	245°	7°	0°
		Angular width (3dB)	27.7^o	34.2^o	42.3^o
		Side lobe level (dB)	-1dB	-5.9dB	-12.5dB
	25.1	Main lobe magnitude(dB) (E-field)	14.9 dBV/m	19.5 dBV/m	19.4 dBV/m
		Main lobe direction	353°	16°	0°
		Angular width (3dB)	32.6^o	26.9^o	47.5^o
		Side lobe level (dB)	-2.4dB	-3.9dB	-5.2dB

Farfield E-Field(r=1m) Abs (Theta=90)

X-Y

Farfield E-Field(r=1m) Abs (Phi=90)

Y-Z

Farfield E-Field(r=1m) Abs (Phi=0)

X-Z
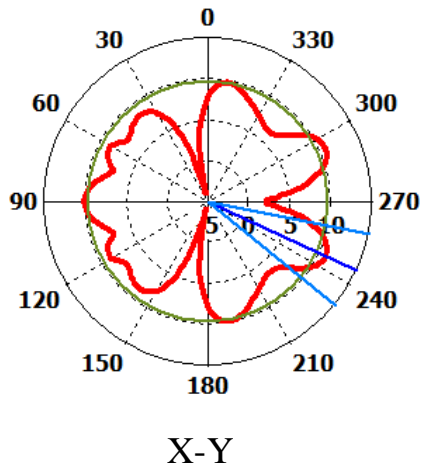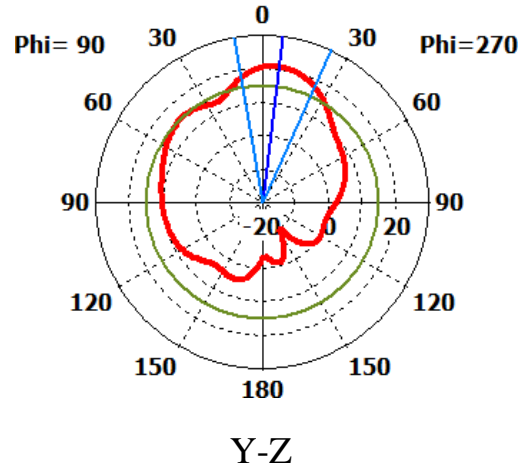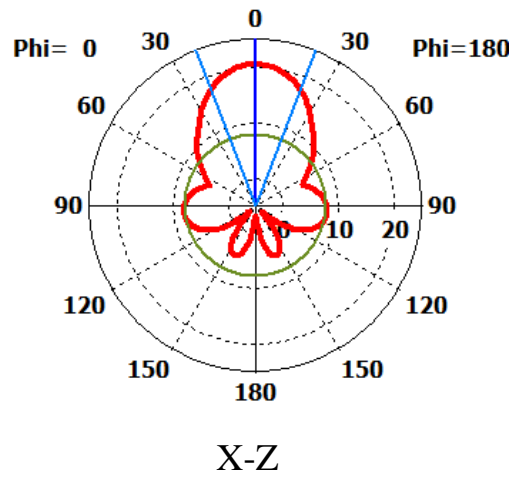
Fig. (4.40): Polar plot of the radiation pattern in E -plane at 22.4 GHz

.

Farfield E-Field(r=1m) Abs (Theta=90)

Farfield E-Field(r=1m) Abs (Phi=90)

X-Y

Y-Z

Farfield E-Field(r=1m) Abs (Phi=0)

X-Z
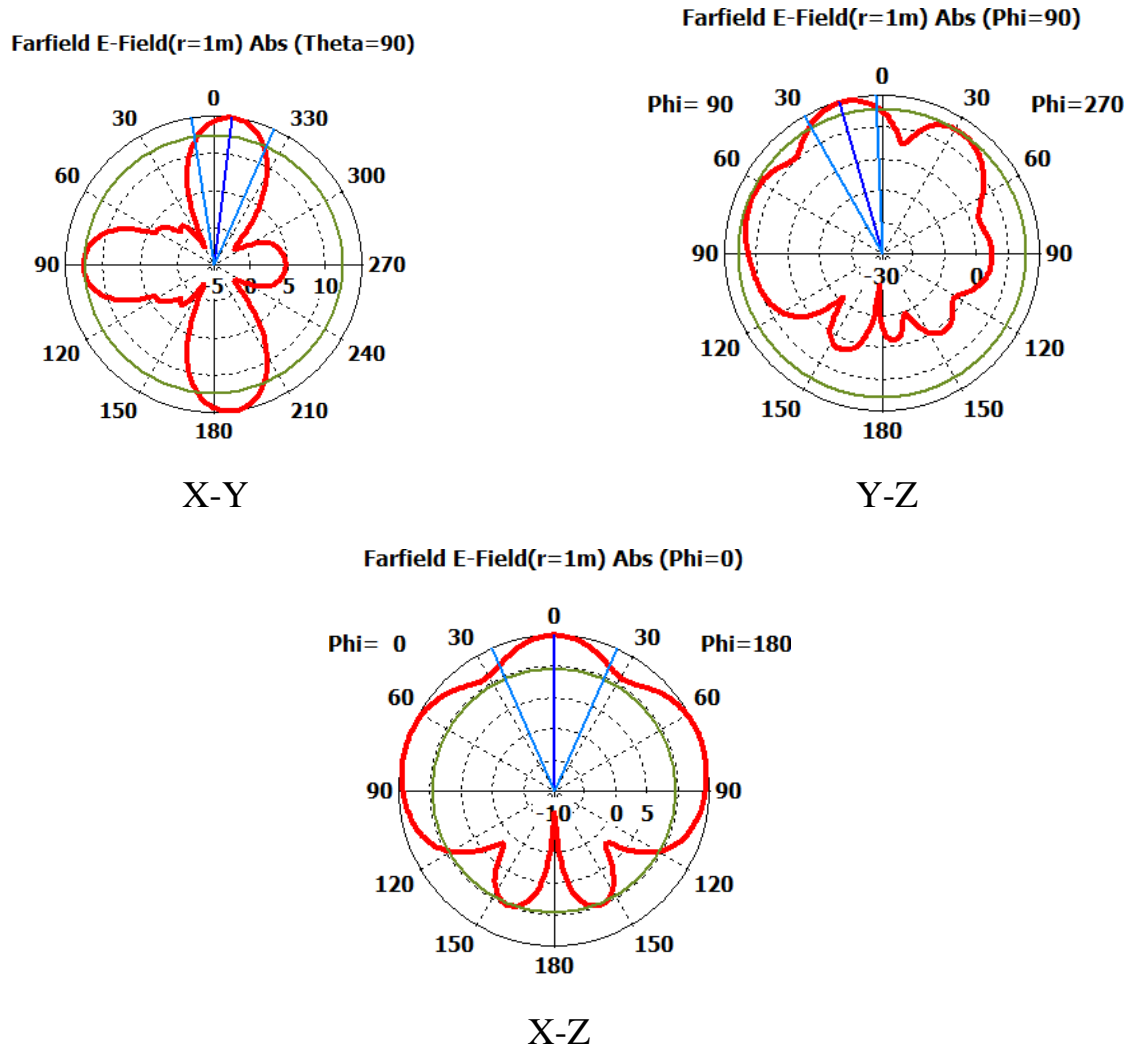
Fig. (4.41) : Polar plot of the radiation pattern in E-plane at 25.1 GHz.

4.6.6 The Efficiency of CSIWA.

The efficiency of CSIWA is 66 %.

4.6.7 Bandwidth of CSIWA.

Fig. (4.42), shows CSIWA bandwidth. CSIWA have dual bands first band starts from frequency 21.86 GHz and ends at frequency 23.01 GHz, producing a bandwidth approximately 1.146 GHz. However, Fig. (4.42 (b)), shows the second bandwidth of CSIWA which starts from frequency 24.41

GHz and ends at frequency 25.89 GHz, producing a bandwidth approximately 1.482 GHz.
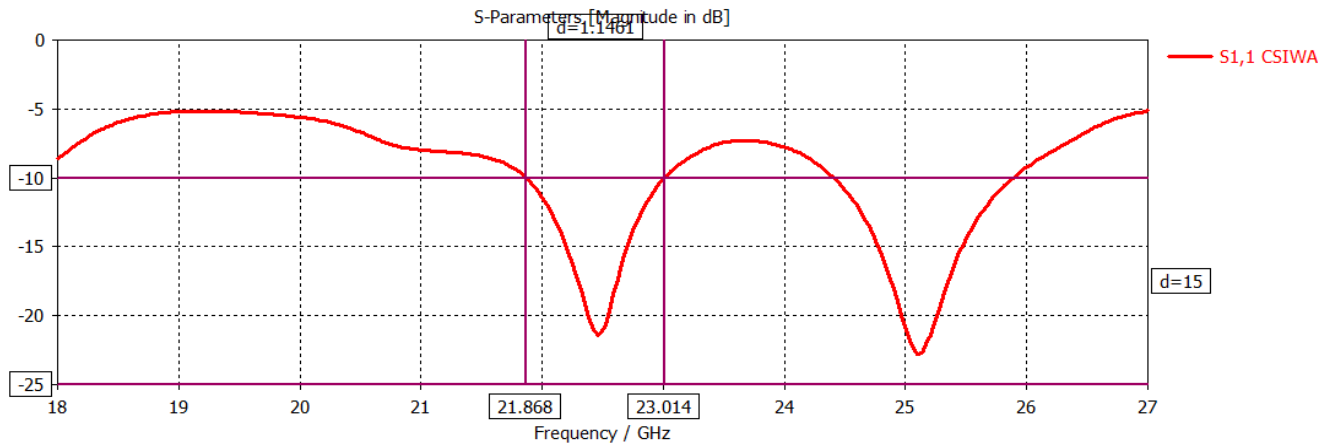
(a) at f=22.4 GHz.
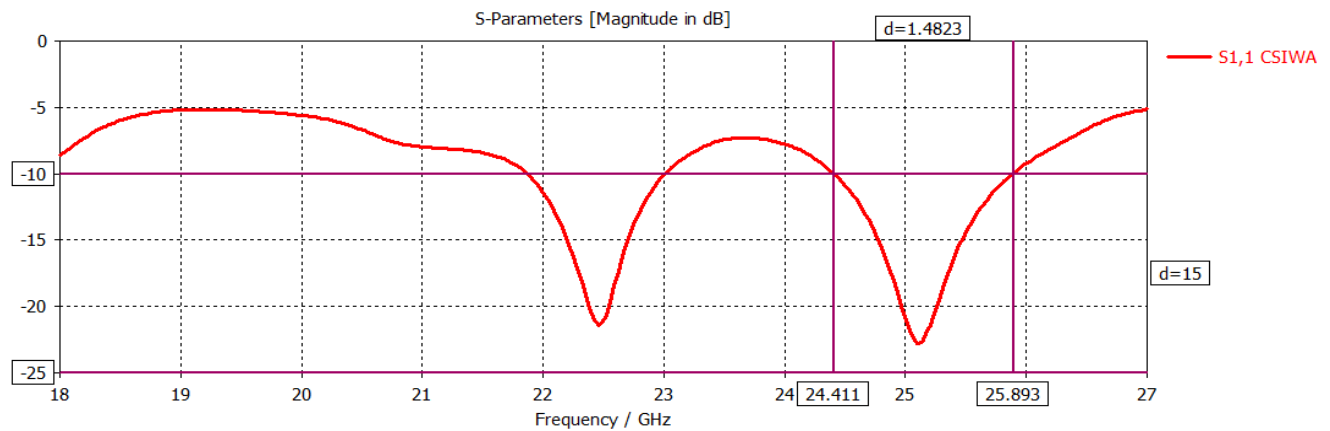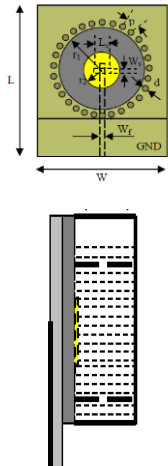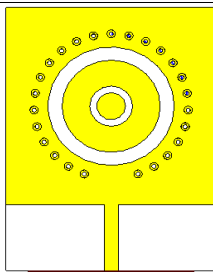
(b) at f=25.1 GHz

Fig. (4.42): CSIWA bandwidth.

4.6.8 Comparisons between CSIWA and Reference.

Comparisons between CSIWA and reference are shown in Table below.

Table 4.21 : Comparisons between CSIWA and reference.

Name & Material	Design & Dimensions	Freq. GHz	Ref. Coff. dB	Directivity dBi	Gain dB	B.W & FB.W	e %
Ref.[12] (Double layer)	(15x20)mm^2	30.5	---	----	3.5	8.6%	---
CSIWA (Single layer)	(15x20)mm^2	22.4	-21	9.26	6.14	1.146 GHz 5.13%	66 %
		25.1	-22	8.19	4.72	1.482 GHz 5.89%	

4.7   Comparison between overall five proposed designs.

Table 4.22, comparisons of five proposed SIW antenna in terms of parameters: reflection coefficient S_{11}, resonant frequency, gain, directivity, efficiency, bandwidth. We observe the S_{11} varying from -10 dB to -45 dB depending on the frequency band. All values are considered acceptable because they exceed the -10 dB. The resonant frequencies bands vary from (10 -30) GHz.

Table 4.22: Comparison between the five proposed SIW antennas.

Name	Best Result	S_{11}	f(GHz)	D(dB)	G(dB)	Eff.%	FB.W	Applications
CSSIWA	larger dimensions	-40 -43	11.34 18.42	10.6 9.77	6.82 3.9	64	4.49% 24.2%	X-band & Ku-band (radar, satellite communications, direct broad casting) & 5G systems.[15][21][26]
SIW-PAWOF	Higher reflection coefficient	-35 -33	12.47 17.82	7.67 8.54	4.89 3.15	64	6.49% 5.16%	Ku-band (satellite communications, direct broad casting) & 5G systems.[21][26]
APESIWA-Roger	Higher gain & efficiency	-33	18.3	7.96	7.86	98	4.04%	Ku-band & K-band (radar, satellite communications, direct broad casting) & 5G systems.[21][23][26]
DCSSIWA	Wider B.W	-34	13.32	8.54	6.05	71	37.18 %	Ku-band (satellite-direct broad casting) & 5G systems. [21][26]
CSIWA	Smaller dimensions	-21 -22	22.4 25.1	9.26 8.19	6.14 4.72	66	5.13% 5.89%	K-band (satellite communications, astronomical observations, and radars) & 5G systems. [23] 26]

Chapter Five

Conclusions and

Suggestions for

Future Scope

CHAPTER FIVE

CONCLUSION and SUGGESTIONS for FUTURE SCOPE

5.1 Introduction

This chapter is a review of the most important aims of thesis work, as well as the conclusions drawn from the proposed designs. Also shed light on the recommendations for the future scope.

5.2 Conclusions

SIW which is a member of substrate integrated circuits SICs family is the best candidate to overcome issues of the traditional waveguide, because it is Lightweight, compact size, low cost, and easy fabrication using cheap PCB technology are the key advantages of the SIW. In this thesis, the proposal of various innovative single antennas is extended utilizing the SIW as the main transmission line.

Five different proposed antennas using the SIW and each individual proposed antenna has features allowing it to work in different applications. All proposed antennas are simulated using the FR4 substrate with a dielectric constant of 4.3, a thickness of 1.5mm, and a tangent loss of 0.02 and only one design used Roger as a substrate with a dielectric constant of 2.2, a thickness of 1.5mm, and a tangent loss of 0.0009 . The FR4 substrate is used because it is widely available in markets and affordable. All antennas are excited using either the microstrip or the CPW where the transition junctions are required to transfer from the TEM into TE modes which are the fundamental modes in waveguides. The proposed antennas are evaluated using the computer simulation technology CST software.

The first proposed design is a square SIW cavity with two-curved slots having different lengths to make the design working at dual frequency bands. Both slots are etched out from a center of the cavity to excite slots with the highest electric fields. The first band is obtained at a resonant frequency of 11.34GHz with a bandwidth of 502MHz gain of 6.28dB, while the 18.42GHz is the resonant frequency of the second band with a bandwidth of 4.48GHz and a gain of 3.9dB. As can be seen, the second band is wider and maybe the reason behind that is the electrical size of the structure which becomes larger at the high frequencies, permitting signals to leave freely.

Next, a square slot surrounded by rows of vias working as a SIW cavity is presented. This design is similar to a square microstrip patch but it is inside the SIW cavity. The benefit of the cavity here is to mitigate the surface waves which consider the main cause of the gain reduction. Also, the feedline was shifted from the center, offset-fed, in order to enhance the matching. As compared to a design without the SIW cavity, the gain enhancement is salient.

The third design is different from other previous works because it has both active and parasitic elements. The parasitic elements are excited by electromagnetic coupling means. The distance between the parasitic and active (driver) elements plays a vital role in determining the overall performance. A variety of numbers of parasitic elements are employed to widen the bandwidth of the targeted design. Also, two bands are obtained in this design working at frequencies of 12.49GHz and 19.24GHz, respectively. The gain at the first band is 3.5dB and the second band is 4dB.

Eventually, two other designs are introduced where the first design is a rectangular patch antenna shielded by two rows of vias and it is a rectangular SIW which is open-ended two concentric circular slots are carved from the top wall of the SIW. This antenna resonate at 13.2 with bandwidth approximately 4.918 GHz with very good and gain.

The fifth antenna consists of a circular patch and circular slot etched at a rectangular patch fixed on the top layer of a substrate with one substrate and feeding antenna directly by connecting it with a microstrip transmission line. Distributing via holes in a circular path to surround the circular patch. It has dual bands because of the dual slots carved on patch. Also have wideband with very good gain.

5.3   Suggestion for Future Scope

- Distribute vias in other way to increase the directivity of antenna.
- Use the rectangle or triangle vias in same design to obtain another frequency band also work in wireless communication systems.
- Design SIW slot array to modify the gain to be suitable for applications that need higher gain and wideband.
- Modify the slot in the proposed designs so as to give another bands to be used in other applications

References

[1] T. S. Rappaport, R. Mayzus, Y. Azar, K. Wang, G. N. Wong, J. K. Schulz, M. Samimi and F. Gutierrez, "Millimeter Wave Mobile Communications for 5G Cellular: It Will Work" IEEE, Access, vol. 1, pp. 335–349, 2013.

[2] Letaief, R. D. Murch and K. B., "Antenna Systems for Broadband Wireless Access," IEEE Communications Magazine, vol. 2, pp. 76-83, April 2002.

[3] G. Ramesh, "Microstrip Antenna Design Handbook" Artech House, Inc., 2001.

[4] M. M. Siddiqui "Vision of 5G Communication" Springer-Verlag Berlin Heidelberg, pp. 252-–256, 2011.

[5] Nokia Siemens Networks, "2020: Beyond 4G Radio Evolution for The Gigabit Experience", White Paper, 2011.

[6] Ericsson, "More than 50 billion connected devices," White Paper, 2011.

[7] G. Q. Luo, Z. F. Hu, L.X. Dong, L. L. Sun," Planar Slot Antenna Backed by Substrate Integrated Waveguide Cavity", IEEE Antennas and Wireless Propagation Letters, Vol.7, 2008.

[8] Mohamed H. Awida et al., " Low-Cost High-Efficiency Substrate-Integrated Cavity-Backed Single Element Antenna ",IEEE ,2010 .

[9] D. Y. Kim, J. W. Lee, T. K. Lee, and C. S. Cho, "Design of SIW Cavity-Backed Circular-Polarized Antennas Using Two Different Feeding Transitions," IEEE Transactions on Antennas and Propagation, vol. 59, no. 4. pp. 1398–1403, doi: 10.1109/TAP.2011.2109675, 2011.

[10] G. Q. Luo, Z. F. Hu, W. J. Li, X. H. Zhang, L. L. Sun, and J. F. Zheng, "Bandwidth-Enhanced Low-Profile Cavity-Backed Slot Antenna by Using Hybrid SIW Cavity Modes, " *IEEE Trans. Antennas Propag.*, vol. 60, no. 4, pp. 1698–1704, doi: 10.1109/TAP.2012.2186226, 2012.

[11] A. Elboushi and A. Sebak, " High Gain MMW Hybrid antenna Using SIW Technology" 25th IEEE Canadian Conference on Electrical and Computer Engineering (CCECE), pp978-1-4673-1433-6/12, IEEE,2012.

[12] S. Moitra, A. K. Mukhopadhyay, and A. K. Bhattacharjee, "Ku-Band Substrate Integrated Waveguide (SIW) Slot Array Antenna for Next Generation Networks, " Glob. J. Comput. Sci. Technol., vol. 13, no. 5, 2013.

[13] S. Mukherjee, A. Biswas, and K. V. Srivastava, "Broadband Substrate Integrated Waveguide Cavity-Backed Bow-tie Slot Antenna" IEEE Antennas Wirel. Propag. Lett., vol. 13, no. c, pp. 1152–1155, doi: 10.1109/LAWP.2014.2330743, 2014.

[14] H. Dashti and M. H. Neshati, "New Hybrid Microstrip Patch Antenna Fed by Half- Mode Substrate Integrated Waveguide Cavity", 2nd Iranian Conference on Engineering Electromagnetics (ICEEM 2014), Jan. 8-9, 2014.

[15] C. Zhang, J. Wang, M. Chen, Z. Zhang, and Z. Li, "A New Kind of Circular Polarization Leaky-Wave Antenna Based on Substrate Integrated Waveguide," Int. J. Antennas Propag., , pp. 1–7, 2015, doi: 10.1155/2015/397960 vol. 2015.

[16] K. Nouri, T. H. C. Bouazza, B. S. Bouazza, M. Damou, K. Becharef, and S. Seghier" Design of Substrate Integrated Waveguide Multi-band

Slots Array Antennas", International Journal of Information and Electronics Engineering, vol. 6, no. 4, July 2016.

[17] O. Caytan *et al.*, "Half-Mode Substrate-Integrated-Waveguide Cavity-Backed Slot Antenna on Cork Substrate," IEEE Antennas Wirel. Propag. Lett., vol. 15, pp. 162–165 , doi: 10.1109/LAWP.2015.2435891, 2016.

[18] P. Chaurasia, R. Nigam, M. Bhowmik," SIW Based Slot Antenna in X-Band Using Rogers/RT duroid 5880 As Substrate", International Journal of Materials Science vol. 12, no. 1,2017.

[19] Hanumanthappa and I. Rosaline, "SIW Based Mono-Pole Antenna for WLAN and WIMAX Applications," RTEICT 2017 - 2nd IEEE Int. Conf. Recent Trends Electron. Inf. Commun. Technol. Proc., vol. - Janua,no.1,pp.1010–1013,2017,doi:
10.1109/RTEICT.2017.8256751,2018.

[20] H. A. Ali, E. Massoni, L. Silvestri, M. Bozzi, L. Perregrini, and A. Gharsallah, "Increasing the Bandwidth of Cavity-Backed SIW Antennas by Using Stacked Cavities," Int. J. Microw. Wirel. Technol., vol. 10, no. 8, pp. 956–967, doi: 10.1017/S1759078718000478, Oct. 2018.

[21] A. Kumar and S. Raghavan, "Broadband SIW cavity-backed triangular-ring-slotted antenna for Ku-band Applications, " AEU - Int. J. Electron. Commun., vol. 87, pp. 60–64, doi: 10.1016/j.aeue.2018.02.016, Apr. 2018.

[22] H. Amer and M. A., "Design of Substrate Integrated Waveguide (SIW) Antenna, " Commun. Appl. Electron., vol. 7, no. 17, pp. 14–20, doi: 10.5120/cae2018652774, 2018.

[23] Mariam El Ghrabi et al."Design of SIW Cavity Backed Tringular Slot

Antenna Using Two Different Feeding Transitions .", Procedia Manufacturing 32, 687–693,2019,2019.

[24] L. Liu et al., "An SIW Antenna Utilizing Odd-mode Spoof Surface Plasmon Polaritons for Broadside Radiation," Int. J. RF Microw. Comput. Eng., no. December 2019, pp. 1–7, doi: 10.1002/mmce.22177, 2020.

[25] X. Hui Wu and A. A. Kishk," Analysis and Design of Substrate Integrated Waveguide Using Efficient 2D Hybrid Method", Morgan& Claypool publishers, Constantine A. Balanis, Series Editor.

[26] J. M. Hasen, G. Saridakis, and V. Benson, "Kent Academic Repository," , PhD,Comput. Human Behav., pp. 197–206, doi: 10.1002/cb.1444/abstract,2018.

[27] K. Wu, D. Deslandes, and Y. Cassivi, "The Substrate Integrated Circuits - a New Concept for High-Frequency Electronics and Optoelectronics", pp. p-3 -, Yugoslavia, Oct. 1-3. 74, 2003

[28] M. Bozzi, L. Perrigrini, K. Wu, and P. Arcioni, "Current and Future Research Trends in Substrate Integrated Waveguide Technology", Radio Engineering, vol. 18, no. 2, June 2009.

[29] D. Deslandes and K. Wu, "Accurate Modeling, Wave Mechanism, and Design Consideration of A Substrate Integrated Waveguide", IEEE Trans. Microw. Theory Tech., vol. 54, no. 6, pp. 2516-2526, Jun. 2006.

[30] T. Djerafi, A. Doghri and K. Wu "Substrate Integrated Waveguide Antennas", Handbook of Antenna Technologies, Springer Science and Business Media Singapore, DOI 10.1007/978-981-4560-75-7_57-1, 2015.

[31] M. Bozzi, L. Perregrini, and K. Wu, "Modeling of Conductor, Dielectric and Radiation Losses in Substrate Integrated Waveguide by the Boundary Integral-Resonant Mode Expansion Method", IEEE Transactions on Microwave Theory and Techniques, vol. MTT-56, no. 12, pp. 3153-3161, Dec. 2008.

[32] D. Deslandes, K. Wu, "Integrated Microstrip and Rectangular Waveguide in Planar Form", IEEE Microw. Wirel. Compon. Lett., (2), pp. 68–70, 11, 2001.

[33] D. Deslandes, K. Wu, "Analysis and Design of Current Probe Transition From Grounded Coplanar to Substrate Integrated Rectangular Waveguides", IEEE Trans. Microw. Theory Tech., 53, (8), pp. 2487–2494, 2005.

[34] D. Deslandes, "Design Equations for Tapered Microstrip-to-Substrate Integrated Waveguide Transitions", IEEE. Microwave Symp. Digest, Anaheim, CA, USA, , pp. 704–707,23–28 May 2010

[35] Y. Ding, K. Wu, "Substrate Integrated Waveguide-to-Microstrip Transition in Multilayer Substrate", IEEE Trans. Microw. Theory Tech., pp. 2839–2844,2007, 55, (12)

[36] D. Deslandes, K. Wu, "Integrated Transition of Coplanar to Rectangular Waveguides", IEEE. Microwave Symp. Digest, Phoenix, Arizona, pp. 619–622, 20–25 May 2001,.

[37] L. Xia, R. Xu, B. Yan, J. Li, Y. Guo, J. Wang, "Broadband Transition Between Air-Filled Waveguide and Substrate Integrated Waveguide", Electron. Lett. pp. 1403–1405 , 42, (24), 2006.

[38] K. Wu, Y. J. Cheng, T. Djerafi, W. Hong, "Substrate-Integrated Millimeter-Wave and Terahertz Antenna Technology", IEEE Proc.

Vol.100 No.7, pp. 2219-2232, 2012.

[39] Y. Cassivi and Ke Wu, "Substrate Integrated NRD (SINRD) guide in High Dielectric Constant Substrate for Millimeter Wave Circuits and Systems", Microwave Symposium Digest, 2004 IEEE MTT-S International, Vol. 3, pp. 1639 -1642, 2004.

[40] K. R. Jha, G. Singh, "Terahertz Planar Antennas for Next Generation Communication, Switzerland": Springer, 2014.

[41] M. Bozzi, D. Deslandes, P. Arcioni, L. Perregrini, Ke Wu, G. Conciauro, "Efficient Analysis and Experimental Verification of Substrate-Integrated Slab Waveguides for Wideband Microwave Applications", International Journal of RF and Microwave Computer-Aided Engineering, Vol. 15, No. 3, pp. 296-306, 2005.

[42] A. Patrovsky and K. Wu, "Substrate Integrated Image Guide (SIIG) - A Planar Dielectric Waveguide Technology for Millimeter-Wave Applications", IEEE Trans. Microw. Theory Tech., vol. 54, no. 6, pt. 2, pp. 2872–2879, Jun. 2006.

[43] A. Patrovsky and K. Wu, "λ4-GHz Broadband Transition from Coplanar Waveguide to Substrate Integrated Image Guide (SIIG)", Proc. IEEE Int. Microw. Symp., pp. 1551-1554.35, 2007.

[44] A. Petosa. A. lttipiboon and S. Thirakoune. "Perforated Dielectric Resonator Antennas", Electronics Letters, Vol. 38, No. 24. 21", pp. 1493-1495, Nov. 2002.

[45] W. Li Che, C. Zhang, Y.L. D. Chow, "Investigations on Propagation and The Band Broadening Effect of Ridged Rectangular Waveguide Integrated in a Multilayer Dielectric Substrate", Microwaves, Antennas & Propagation, IET, Vol. 4, No. 6, pp. 674-684, 2010.

[46] M. W. Bozzi, K. S.A. Wu, "Broadband and Compact Ridge Substrate-Integrated Waveguides", Microwaves, Antennas & Propagation, IET, Vol. 4, No.11, pp. 1965-1973, 2010.

[47] C. A. Balanis, "Antenna Theory: Analysis and Design", Published by John Wiley & Sons, Inc., Hoboken, New Jersey, 4th edition,2016.

[48] David M. Pozar , Microwave Engineering, United Stateso f America: John Wiley & Sons,Inc, 3rd, 2005.

[49] R. Arora, S. B. Rana, and S. Arya, "Performance Analysis of Wi-Fi Shaped SIW Antennas," AEU - Int. J. Electron. Commun., vol. 94, no. July, pp. 168–178, doi: 10.1016/j.aeue.2018.07.002, 2018.

تصميم هوائيات الدليل الموجي للركيزة المتكاملة لأنظمة الاتصالات اللاسلكية

رسالة مقدمة الى

قسم هندسة تقنيات الاتصالات في الكلية التقنية الهندسية ـ نجف

وهي جزء من متطلبات نيل درجة ماجستير تقني في هندسة الاتصالات

تقدم بها

رند موفق هادي عبد الصاحب حنوش

بكالوريوس في هندسة تقنيات الاتصالات

إشراف

الاستاذ المساعد الدكتور فارس محمد علي الجعيفري

أيلول/ 2020

خلاصـــه

تقدم هذه الرسالة خمس هوائيات مختلفة باستخدام تقنية (SIW) ولكل هوائي مقترح مميزات تسمح له بالعمل في تطبيقات مختلفة. تمت محاكاة جميع الهوائيات المقترحة باستخدام ركيزة من مادة عازله تسمى (FR4) ذات ثابت عزل قدره 4.3, وسمك 1.5 ملمتر , وخسائر فقد قدرها 0.025.وتم استخدام ركيزة ال (FR4) لأنها متوفرة في الاسواق وبأسعار مناسبة. جميع الهوائيات تم تغذيتها باستخدام اما (Microstrip) او (Coplanar Waveguide CPW) حيث ان هذه التحويلات الانتقالية تكون مطلوبة لتحويل النمط الكهرومغناطيسي المستعرض (TEM Mode) الى النمط الكهربائي (TE Mode) والذي يعد النمط الاساسي في دليل الموجة المستطيل (RW) تم تصميم جميع الهوائيات في هذه الرسالة باستخدام برنامج المحاكاة (CST Software Program).

التصميم الاول المقدم هو عبارة عن تجويف مربع بداخل (SIW) ويحتوي على شقيين منحنيين بأطوال مختلفة وذلك لجعل الهوائي يعمل بحزمتين ترددتين مختلفتين. حيث تم الحصول الحزمة الاولى عند تردد رنين مقداره 11.34 كيكا هرتز وبعرض حزمة مقداره 502 ميجاهرتز وبكسب مقداره 6.28 ديسيبل ,بينما تم الحصول على الحزمة الترددية الثانية عند تردد الرنين 18.42 كيكا هرتز وعرض نطاق الحزمة مقداره 4.48 كيكا هرتز وبكسب مقداره 3.9 ديسيبل.

بعد ذلك, تم تصميم هوائي مربع الشكل ومحاط بصفوف من التجاويف الاسطوانية حيث انها تعمل كتجويف (SIW) يحتوي هذا الهوائي ايضا على حزمتين ترددتين , الحرمة الاولى عند تردد رنين مقداره 12.47 كيكا هرتز والحزمة الثانية عند التردد 17.82 كيكا هرتز وبأعلى كسب مقداره 4.89 ديسيبل ,وبعرض حزمة مقداره 805.7 ميكا هرتز للأولى و921.8 ميكا هرتز للثانية.

يختلف التصميم الثالث عن التصاميم السابقة لأنه يحتوي على جزئيين احدهما بأسفل الهوائي يسمى الجزء النشط لأنه متصل بخط التغذية مباشرة والاخر يكون الجزء العلوي ويسمى الجزء الحر والذي يرتبط بالجزء النشط عن طريق الحث الكهرومغناطيسي, حيث تم استخدام مادة (Roger) كمادة عازلة ذات ثابت عزل مقداره 2.2 وخسائر فقد مقدارها 0.0009 وبسمك 1.5 ملمتر حيث تم الحصول على حزمة ترددية واحدة عند تردد الرنين 18.3كيكا هرتز وكسب مقداره 7.8 وبأعلى كفائة مقدارها 98 %.

واخيرا, تم تصميم هوائيين اخرين احدهما ذو شكل مستطيل وتم توزيع الأسطوانات المعدنية على جوانب المستطيل وتم حفر شقوق دائرية لغرض تعزيز عمل الهوائي حيث تم الحصول على حزمة ترددية واسعة جدا عند تردد الرنين 13.2 كيكا هرتز وبكسب عالي . اما التصميم الاخير فتم توزيع الاسطوانات المعدنية بصورة دائريه حول شقوق دائرية ,حيث تم الحصول على حزمتين ترددتين واسعتين وبكسب عالي.